FINAL REPORT

Contract No. DSS 25ST.23440-3-9114

# INVESTIGATION OF THE SEMICONDUCTOR CATALYSTS FOR THE PRODUCTION OF LIQUID FUELS

CONTRACT SERIAL NUMBER OST83-00155
CONTRACTOR: SIMON FRASER UNIVERSITY

Prepared by:

S. Roy Morrison, L. Funt, K. Colbow
Simon Fraser Energy Research Institute
Simon Fraser University
Burnaby, B.C. V5A 1S6

Prepared for:

Dr. S.M. Ahmed
Department of Energy Mines and Resources
CANMET
Mineral Sciences Labs
555 Booth Street
Ottawa, Ont. K1A 0G1

This work was supported (in part) by the
Federal Panel on Energy R&D (PERD).

11CPP

MICROMEDIA

TABLE OF CONTENTS


| | | Page |
|---|---|---|
| | Summary | 1 |
| A. | Introduction | 3 |
| B. | Carbon Dioxide Reduction to Methanol | 5 |
| C. | Polymeric Coatings for the Enhancement of Carrier Transfer from Semiconductors | 5 |
| D. | The Effect of Crystal Damage on Selectivity in Anodic and Cathodic Electrode Reactions | 10 |
| E. | Studies of Cation Radical Formation by Hole Oxidation of Alkanes | 12 |
| F. | Recommendations | 14 |
| | Publications | 15 |
| | APPENDIX A | |
| | APPENDIX B | |
| | APPENDIX C | |
| | APPENDIX D | |
| | APPENDIX E | |

SUMMARY:

The objective of the research program was to use the unique advantages of semiconductor electrodes to generate radicals, and to apply this to the oligomerization of low molecular weight hydrocarbons, in particular methane, to higher weight (liquid fuel range) hydrocarbons. Substantial progress was made in that direction with the discovery that stable cation radicals can be formed in triflic acid by hole reactions with low molecular weight alkanes. Specifically propane, butane and ethane were oxidized to stable cation radicals, with possibly some radical formation from methane. Other solvents were being investigated as the program drew to a close that would support more easily the activation of methane.

At the beginning of the program the objectives were more general and the reduction of $CO_2$ to methanol was investigated. It was found that a competing reaction involving the corrosion of the semiconductor electrode confused the results.

Most of our studies have been of oxidation, primarily using the "current doubling" technique to study radical formation and radical reactions. A substantial background regarding the behaviour of radicals at the $TiO_2$ electrode has been amassed that will in future studies lead to rapid development of methods of oligomerization.

Studies of polymer coatings to protect the electrodes and to carry catalysts were made. Also, studies of the behaviour of bulk defects in the semiconductor electrodes were made because it was considered possible that such defects would destroy the unique selectivity of semiconductor electrodes in radical formation and other electrode processes.

It was found that such degradation of selectivity did occur and conditions for electrode preparation were laid down.

Finally, under "Recommendations" we discuss how we hope to take advantage of the great potential uncovered by this work, the possibility of oligomerization in a potentially practical room temperature system.

In the Appendices we include the more important publications resulting from this work (not including presentations and review papers) resulting from the support of CANMET.

# INVESTIGATION OF THE SEMICONDUCTOR CATALYSTS FOR THE PRODUCTION OF LIQUID FUELS

## A. INTRODUCTION:

The objective of this research program was to take advantage of the unique characteristics of semiconductor electrodes in inducing useful electrochemical reactions that are not possible on metal electrodes. There are many examples of such reactions in the literature. The most common example studied is the reduction of $CO_2$ to methanol; with metal electrodes $CO_2$ simply gets reduced to formic acid. We have studied this reaction in the early parts of the program, and in the more recent parts of the program we have emphasized the generation of stable cation radicals by oxidation of alkanes, the objective here being the oligomerization of low molecular weight alkenes and alkanes to produce higher hydrocarbons. The justification for the program was based partly on the possibility of converting solar energy into liquid fuels, but primarily on the opportunity for room temperature conversion of methane to liquid fuels.

There are two reasons why semiconductors show such potential in developing unusual reactions. One is the fact that the carriers from the semiconductor enter the solution at energies far from the Fermi energy (as opposed to metal electrodes where the carriers always enter the solution at the Fermi energy) and, thus, different reaction steps are preferred, compared to the high activity reaction steps on the metal. The second advantage is the stability of the radicals at the surface of

the semiconductor electrode. A radical at the surface of the metal electrode can inject or capture electrons from the metal electrode and be immediately oxidized or reduced to a stable product. On a semiconductor electrode carriers are not available so readily and the lifetime of the radical can be extended many orders of magnitude over that on the metal electrode. This permits radical reactions in solution on a semiconductor electrode that would not occur on a metal electrode.

Initially, the program was designed to study both reduction and oxidation reactions, emphasizing both the reduction of $CO_2$ to methanol as a fuel and the oxidation of alkanes (leading to stable radicals) for the purpose of oligomerization. In the last months of the contract the latter (oxidation) was the sole objective of the research. In addition to studies toward the primary research objectives several supporting studies were carried out to better understand the use of the semiconductor electrode for these purposes. These included studies of the use of polymers to support catalysts, and of the need for perfect crystal structure to control the selectivity of the reactions. In the following discussion we will first discuss the studies on $CO_2$ reduction, polymers, and crystal structure, with much of the discussion relegated to appendices containing published descripting. Then we will describe our studies of the oxidation of alkanes to form free radicals and the studies of the reactions of the free radicals. Finally, there will be a section outlining recommendations for future studies to take advantage of the new approach.

B. CARBON DIOXIDE REDUCTION TO METHANOL:

At the time we began our studies, reports in the literature suggested that the high conduction band energy of gallium arsenide would be particularly favorable for the reduction of CO to methanol. Thus, our study emphasized the arsenic face of heavily doped p-type gallium arsenide, where the electrons in the conduction band were produced by optical excitation of the gallium arsenide. This way of generating the electrons provided a better control of the electron density than available on n-type material. Also, of course, n-type material was studied itself. We concluded that a great part of the methanol formed from gallium arsenide was associated with the dissolution of the gallium arsenide in the somewhat acidic solution. The extra methanol formed associated with cathodic currents was negligible.

This work was reported in reference 5 below, a copy of which is attached to this final report as Appendix A. This research was concluded at this point because the sponsor suggested that we emphasize oxidation reactions more strongly.

C. POLYMERIC COATINGS FOR THE ENHANCEMENT OF CARRIER TRANSFER FROM SEMICONDUCTORS

A polymeric coating on a semiconductor can provide two important beneficial functions. First, an increase in stability of the semiconductor to photocorrosion is generally obtained. This is particularly important when the semiconductor is highly unstable in aqueous or oxygenated media, as is the case with silicon.

Secondly, the incorporation of appropriate electroactive groups in a polymer film produces electrocatalytic properties which can enhance the formation of a desired product. In other instances a better matching of conduction or valence band energies to the redox potential of the substrate can be attained.

The candidate coatings were selected from two classes of polymers. Redox polymers with pendant electroactive groups were investigated. These were based on the anthraquinone or benzoquinone structures, and were selected because of the proven electrocatalytic activity of the molecular parent compounds. The work with these coatings focussed on the stability, reversibility and electrocatylytic properties which were attainable. In order to systematize the study, the properties of these films were first studied as coatings on metal electrodes.

PAQ COATINGS

Coatings of poly-(p-(9,10-anthraquinone-z-carbon 1)styrene)-co-styrene (PAQ) were deposited by solvent evaporation. Good films were obtained which were free from imperfections. However, these coatings desorbed rapidly and the peak currents observed by cyclic voltammetry diminished in a short time.

A new technique was developed to stabilize these films. Exposure of the coating to ultraviolet radiation resulted in cross linking reactions which insolubilized the film. Conditions for obtaining optimum radiation with minimal deterioration of electrochemical properties were determined empirically. Generally, about 1% crosslinking produced the desired results.

The films were reversibly oxidized and reduced on successive redox cycles and the electrochemical behavior of the films was close to ideal. The anodic and cathodic peaks occurred at identical potentials, as predicted for highly adsorbed systems. The current was linearly dependent on scan rate for films under 1000 Angstroms in thickness.

The remarkable stability of the radical anions was observed by spectrophotometry. The radical anion of PAQ is green and the doubly charged anion is blue, and the color changes were observed and monitored for many cycles. Coulometry showed that 79% of the anthraquinone groups were reduced and oxidized in each cycle in film of 100 Angstrom thickness.

Charge transport in the films was investigated and a diffusion constant for charge transfer was determined as $D = 5.1 \times 10^{11}$ $cm^2/s$. Electrocatalytic studies were then conducted with these films. The PAQ films lowered the potential for the reduction of $O_2$ by 150 mV at current densities of 150 $mA/cm^2$. The polyvinylbenzophenone film produced a doubling in the reduction peak for tetrachlorobenzene and showed very good catalytic activity in chlorinated hydrocarbon systems.

REDOX POLYMERS ON SEMICONDUCTORS

Films of PAQ were coated on to Si crystal semiconductors and experiments were conducted with dimethyl sulfoxide (DMSO) as solvent. The polymeric films provided a great increase in the stability of the semiconductor in this solvent. A comparison of the bare semiconductor crystal, a semiconductor with anthraquinone in solution and a semiconductor coated with PAQ showed that the coated crystal produced the best performance. However,the electrocatalytic activity in $O_2$

reduction was marginal and the improvement was not sufficient to warrant concentrated study on this system. This was probably due to the fact that the energy level of $O_2$ is slightly below the conduction band, whereas for best catalytic purposes a substrate with a redox potential slightly below the conduction band is to be preferred.

## COATINGS OF ELECTRONICALLY CONDUCTING POLYMERS ON SEMICONDUCTORS

One of the disadvantages of the redox polymer coatings was the limited conductivity of the films in thicknesses over 1000 Angstroms. However, electronically conducting polymers, such as polypyrrole have very high electronic conductivity and can be utilized in films of considerable thickness. Films of polypyrrole were prepared on metallic substrates. Once the film was formed a suitable electrocatalytic group was incorporated by first reducing the film to expel the perchlorate anions, and then reoxidizing the film in the presence of a metal anion such as $PtCl_6^{-2}$. However, the Pt could readily be reduced to metallic Pt in a finely divided form which was deposited within the semiconductor. This provided a remarkable matrix in which a proven electrocatalytic element could be deposited in a relatively high concentration. The concentration and surface area of Pt in the immediate vicinity of the electrode was much higher than that attainable by other methods.

The uniformity of the films was investigated with a depth profile analysis by Auger spectroscopy. In the original method of forming these films most of the Pt was found in the outermost surface area. However, a technique was developed for obtaining a uniform distribution of Pt within the film.

These films produced very impressive results in an electrocatalytic study. The potential for oxygen reduction was reduced by 500 mV. At a given potential, a tenfold increase in current was obtained. The films with Pt dispersed uniformly throughout the film showed a four fold increase in current in comparison with those in which the Pt was deposited near the surface.

ELECTRONICALLY CONDUCTING POLYMERS ON SEMICONDUCTOR ELECTRODES

Polypyrrole films were coated onto semiconductors of Si with p and n-type doping. On n-type Si the polypyrrole is oxidized by the minority carrier when the semiconductor is illuminated. Unfortunately, polypyrrole is not ideal for this application because of its relatively high optical absorption. On p-type Si minority carriers reduced the polypyrrole when the film is illuminated.

A very unusual property has been found with these coatings. The equilibrium potential of a polypyrrole film adapts to the redox level of the substrate in solution, i.e. the degree of doping in the films is automatically adjusted so that the redox potential of the film and substrate reach equilibrium. Recent work now indicates that the redox potential of the film can be adjusted and pinned to any desired level relative to the semiconductor and the substrate. This involves immobilizing the anions in the film so that only electronic conduction can occur through the semiconductor and the redox process to undope the film is prevented. This new development provides a method of tuning the energy transfer characteristics of the semiconductor to the substrate and of optimizing these parameters.

## D. THE EFFECT OF CRYSTAL DAMAGE ON SELECTIVITY IN ANODIC AND CATHODIC ELECTRODE REACTIONS

As a second supporting area studies of the influence of damage on the crystals were undertaken because it was felt that it probably was necessary to have rather perfect crystal structure in order to get highly selective reactions. This suggestion was, therefore, investigated and found entirely valid. The conclusion of the studies was that, indeed, rather perfect crystals (not necessarily large crystals, but damage-free powder crystallites) would be necessary as the semiconductor electrode. A material with many dislocations or grain boundaries would lead to poor selectivity in the final product.

The actual study was done in two ways: A study of the effect of dislocations on the reduction of oxidizing agents,[6] and studies of their effect on both oxidation and reduction by examining electron transfer to and from dyes in solution.[7] The use of dyes is very convenient for such studies because one can study electrons going into the solid and electrons coming out of the solid in separate studies and control the rate of these electrode processes simply by eliminating the dye.

The results of these studies have been published in three papers, and are attached as Appendices B, C and D at the end of this report. The essence of the conclusion is that electrons can move not only from the conduction band into solution but can move through dislocation levels down to the Fermi energy of the material and thence into solution. This dislocation effect makes the semiconductor electrode behave more like a metal electrode and one loses the valuable selectivity properties of the semiconductor electrode. The same sort of behaviour occurs

with electron injection into the conduction band of the semiconductor--the electrons can come in at a much lower level than would be required were the electrons to enter directly into the conduction band--the electrode begins to act metallic.

As mentioned above, this leads to the requirement that for high selectivity in either oxidation or reduction reactions and specifically for the generation of stable cation radicals, one needs a relatively perfect semiconductor material as the electrode.

A substantially greater effort was made of oxidation studies on $TiO_2$ and of the radicals generated by holes. In the back-up studies of radicals, they were formed simpler systems than those required for alkane oxidation. This approach allows more detailed study of the radical generation processes, radical reactions, and how difficult it is to form radicals. These studies have just been prepared for publication and will be submitted at about the same time that this report is filed. The typewritten copy of the report is included as Appendix E.

The essence of the report is that the generation of radicals (as studied by "current doubling") will react with oxidizing agents in solution in a rather simple manner, and react with other organic molecules in solution in a somewhat more complicated fashion. In some interactions a less stable radical is formed (as observed by an increase in the current doubling). With some co-reactants no effect is observed indicating that neither the co-reactant capture the holes nor do they react with the radical once the hole is captured and a third interaction is a direct competition for the holes leading to a decrease

in the electron injection of the current doubling measurement. The various organic species (alcohols, acids, etc.) were studied and their interaction as above was determined, and their relative hole reactivity (hole capture cross-section) was determined. More work must be done to understand the basic chemistry behind the different kinds of behaviour.

E. STUDIES OF CATION RADICAL FORMATION BY HOLE OXIDATION OF ALKANES:

In our studies of alkanes, it was clear, initially, that a highly acid solvent would be necessary to stabilize the radicals generated. Two solvents have been studied: Triflic acid (trifluoromethane sulfonic acid monohydrate) and fluorosulfonic acid, $HSO_3F$. The fluorosulfonic acid is supposed to be a stronger acid (a high donor number) than the triflic acid, although both have been used in studies of metal electrodes of the oxidation of alkanes.

The objective using semiconductor electrodes is, of course, the highest stability of the cation radicals so formed and thereby the ability of these radicals to interact with other hydrocarbons in solution without being oxidized all the way to carbon dioxide and water (as is observed with metal electrodes).

In our studies of triflic acid it was found that propane, butane and to a small extent ethane showed current doubling (thus showing the formation of stable cation radicals) when there are no active species in solution. No current doubling was observed with methane added to the solution. To date no carbon dioxide has been observed to form during the oxidation of propane in triflic acid.

The temperature of the triflic acid (normally a solid at room temerature) was held at 160°C in order to optimize the current doubling. The cell used has only glass, teflon, and platinum in solution plus, of course, the $TiO_2$ electrode itself. Alternatively, measurements were made on Pt working electrodes. It was found with the Pt electrode that the current in the voltammogram was increased the order of 100 $\mu A/cm^2$ in the presence of propane and at a voltage between .8 and 1.5 volts (vs Pt).

In the solvent fluorosulfonic acid, on the other hand, no current doubling was observed. This does not necessarily mean that cation radicals were not formed, it simply means that they did not decompose by injecting electrons into the semiconductor--they were much less stable in the sulfonic acid solvent. In principal, as discussed above they should be much more stable and this problem has not yet been resolved. In variations to determine why current doubling is not observed with fluorosulfonic acid, we have tested at very low temperatures (-60°C), we have tested with oxygen rather than nitrogen as the carrier gas, and we have tested with varying amounts of current. It is found with high current that a film forms on the surface of the $TiO_2$ electrode and this may be part of the problem. If the titanium is slightly soluble in fluorosulfonic acid (it is soluble in sulfuric acid), the oxidation of the titania itself may compete with the propane for holes and this may be the reason why one does not get cation radicals from propane in the presence of fluorosulfonic acid.

F. RECOMMENDATIONS:

All of the evidence to date suggests substantial success in this approach to oligomerize low hydrocarbons into high hydrocarbons. The ability of the semiconductor electrode to form stable cation radicals has been shown in many systems and specifically has been demonstrated in alkane oxidation reactions in triflic acid. The very small amount of current doubling with methane added to the solvent suggests that even here a relatively unstable cation radical might be formed, but in any case, the studies of the reactions of these cation radicals with other alkanes in solution should be studied to determine whether the expected oligomerization does occur.

Because the study of radical formation from alkanes was started late in the program, we have just been able to show that the approach to room temperature oligomerization of low weight hydrocarbons is indeed highly promising, and may represent a valuable process. Because we feel the process does have such promise, we are continuing the investigation at a lower level with Energy Research Institute funds, while attempting to find support for a viable effort.

PUBLICATIONS: BASED ON THIS RESEARCH

1. B.L. Funt and S.R. Tan "The Photoelectrochemical Initiation of Polymerization of Styrene", J. Polymer Sci, Polymer Chem. Ed., 22, 605 (1984).

2. B.L. Funt and P.M. Hoang, "The Voltammetric Response of Solutions of Electroactive Polymers", J. Electrochem. Soc., 131, 2295 (1984).

3. P.M. Hoang, Steven Holdcroft and B. Lionel Funt, "Preparation and Properties of Electrodes Modified by Polymeric Films with Pendant Anthraquinone Groups", J. Electrochem. Soc., 132, 2129 (1985).

4. Steven Holdcroft and B. Lionel Funt "Electrocatalytic Reduction of Oxygen at Electrodes Modified by Films of Redox Polymers with Anthraquinone Moieties", Abstract for ACS Fall Meeting, Anaheim, Ca. September, 1986.

5. W.M. Sears and S. Roy Morrison, "Carbon Dioxide Reduction on Gallium Arsenide Electrodes", J. Phys. Chem., 89, 3295 (1985).

6. B. Li and S. Roy Morrison, "Effect of Damage on Selectivity in Semiconductor Electrode Reactions", J. Phys. Chem. 89, 1804 (1985).

7. B. Li and S. Roy Morrison, "Excited Dye Reactions on Damaged ZnO", J. Phys. Chem., 89, 5442 (1985).

8. S. Roy Morrison, "Problems and Potential in the Semiconductor/Electrolyte Approach to Solar Conversion, J. Photochem., 29, 55 (1985).

*Journal of Photochemistry*, *29* (1985) 55 - 70



# PROBLEMS AND POTENTIAL IN THE SEMICONDUCTOR/ ELECTROLYTE APPROACH TO SOLAR CONVERSION*

S. ROY MORRISON

*Simon Fraser Energy Research Institute, Simon Fraser University, Burnaby, British Columbia V5A 1S6 (Canada)*

## Summary

A general comparison of photoelectrochemical and solid state solar cells is made. It is concluded that although photoelectrochemical cells have problems, including corrosion and film formation, they have potential advantages over solid state cells for photovoltaic operation in the possibility of a lower cost. In a photosynthesis mode of operation, when the solar energy is stored as chemical energy, the use of a photoelectrochemical approach for direct conversion has potentially significant advantages over a combined solid state cell and metal electrolysis cell. The most interesting potential advantages arise in selectivity, where more desirable products can be generated, and in the use of suspended powders, where particularly low cost conversion could be realized.

## 1. Introduction

Extensive studies of semiconductors in electrolyte solutions with the objective of converting solar energy either to electrical energy directly or to stored chemical energy have been in progress since the report of Fujishima and Honda [1]. They demonstrated with $TiO_2$ that a photoproduced hole–electron pair could be used to dissociate water, storing the energy as hydrogen. The key property of semiconductors in solar energy conversion is the ability to separate the photoproduced hole from the photoproduced electron, thereby stabilizing the photoproduced hole until its energy can be converted to a useful form. This ability has been used since in many forms of photoelectrochemical solar energy conversion which generally can be classified as photovoltaic photoelectrochemical cells and photosynthesis photoelectrochemical cells (where for simplicity in description we shall include all reac-

*Paper presented at the Fifth International Conference on Photochemical Conversion and Storage of Solar Energy, Osaka, Japan, August 26 - 31, 1984.

0047-2670/85/$3.30

© Elsevier Sequoia/Printed in The Netherlands

tions where the photon energy is used to stimulate net chemical changes in the latter category).

A great amount of effort has been expended in research to develop a practical solar conversion device based on photoelectrochemical cells. Although such cells have not yet reached the market-place, a substantial amount of valuable scientific information has been generated by this research. The purpose of this contribution, however, is to discuss the potential of photoelectrochemical devices in practical solar energy conversion, emphasizing the practicality of the development while not minimizing its contribution to basic knowledge. Thus, in the present discussion, we shall discuss some of the features of photoelectrochemical devices which bear on the practicality of their future use as photovoltaic devices, where they must compete with solid state photovoltaic devices, and features of photoelectrosynthesis devices, where they must compete with a combination of solid state photovoltaic solar cells and electrosynthesis using metal electrodes. As the solid state solar cell, we shall emphasize the metal/insulator/semiconductor (MIS) Schottky barrier cell; it is analogous to the photoelectrochemical Schottky barrier cell, and so the comparison can be readily made. The MIS cell has about 20 Å of insulating oxide between the metal and the semiconductor.

The hoped-for current–voltage characteristics and the band model for an MIS or a photoelectrochemical Schottky barrier cell are shown in Fig. 1. In the n-type semiconductor used for illustration the double layer at the surface (the Schottky barrier) forces the holes to the surface and, under ideal conditions, is adjusted to force most of the photoproduced electrons to the back contact. The model represents an MIS solid state cell if a metal layer is

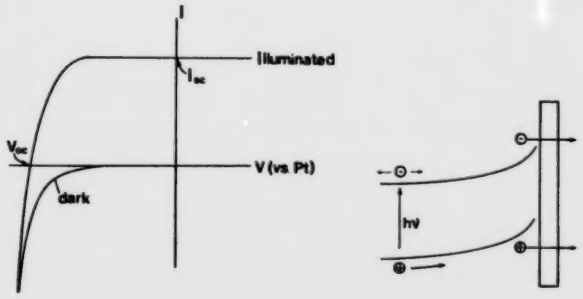


**Fig. 1. Ideal solar cell characteristics for an n-type semiconductor: (a) current–voltage characteristics, where with an illuminated sample a high photocurrent is maintained to a voltage cathodic enough that electrons flow to the surface in appreciable quantities (the optimum operating conditions are such that *IV* is maximum, with the voltage near the open-circuit voltage $V_{oc}$); (b) band model under optimum operating conditions, with some electrons reaching the surface (the semiconductor is shown with a wide band gap (insulating) film on the surface).**

deposited onto the insulator to collect the holes (and the low electron current) and represents a photoelectrochemical cell with a thin insulating film if an electrolyte is used to collect the holes and electrons arriving at the surface. In the discussion, we shall first describe the characteristics of photoelectrochemical cells that bear on their practical utilization. Specifically, we shall discuss corrosion and film formation because they may be the most serious problems associated with the practical utilization of photoelectrochemical devices. With this background, we can then discuss in more detail the advantages and disadvantages of the photoelectrochemical approach to solar energy conversion, compared with those of solid state cells.

## 2. Corrosion and film formation on semiconductor electrodes

### *2.1. Corrosion*

Photo-induced corrosion, a ubiquitous problem in photoelectrochemical cells [2], is almost always associated with holes [3]. In Fig. 2 we indicate a model for a hole, a missing valence electron in a reasonably covalent semiconductor lattice. Such a hole is produced as the first step in solar conversion, the absorption of the photon. The valence electron is excited to the next excited state (the conduction band), leaving the hole in the valence bond structure. The double bond is converted to a one-electron bond where the hole is localized. The hole is free to move through the crystal; other valence electrons jump into the empty bond that is the hole and the hole thus moves. Corrosion can occur if the hole reaches the surface.

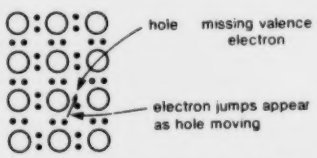


**Fig. 2. Schematic molecular model for a covalent semiconductor missing one valence electron, where the missing electron is a hole. The hole can move to the surface by successive neighbouring valence electrons moving into the unoccupied position, causing apparent movement of the hole.**

The "back bond" between the surface atom and the crystal is converted from a two-electron bond to a one-electron bond. If two holes occupy the same back bond of the surface atom, the bond is completely broken; there are no bonding electrons. Analysis suggests [4, 5] that the capture of one hole at a back bond of a surface atom is reversible, but that if two holes are captured on the same back bond the process is irreversible [4, 5] and corrosion results. Presumably the surface atom becomes hydrolysed (in an aqueous solution) and, once the surface atom coordinates to an $OH^-$ group or its equivalent, the corrosion process is irreversible.

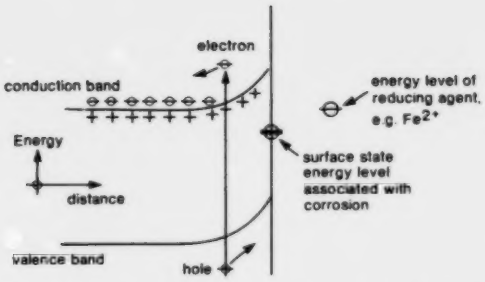


Fig. 3. Band model for corrosion: when a hole is captured on a back bond (energy level not shown), the remaining unpaired electron is at a higher energy level than a normal valence bonding electron. The higher energy level is shown as a surface state associated with corrosion. The energy level of a reducing agent ion in solution is also indicated.

The energy band model for the same process on an n-type semiconductor is shown in Fig. 3. Here a photon excites the valence electron from the energy levels in the valence band to the conduction band. Again, if one hole is captured on a back bond, the process is reversible, but the hole capture leaves the surface atom in the form of a radical (an atom with an unpaired electron). This unpaired electron has an energy level different from that of the normal valence electrons in the material and is expected to be at a substantially higher energy. Thus the surface state shown in Fig. 3, associated with corrosion, is in the midgap position. If a hole is captured on that surface state, as described above, the back bond is completely broken and corrosion results.

The most straightforward way to avoid photocorrosion is to use a strong reducing agent in solution, as indicated on the energy level diagram of Fig. 3. The electron from the reducing agent (say $Fe^{2+}$) transfers to the lower energy associated with the hole on the back bond of the surface atom, thus restoring the bonding electron to the surface atom and preventing corrosion. The competition for the photoproduced holes between the reducing agent in solution and corrosion can be monitored by observing the rate of generation of the oxidized form of the reducing agent in solution using a rotating ring disc electrode. Such a measurement permits corrosion by holes to be studied and the models to be analysed in some detail.

Figure 4 shows the results of such a measurement [6] where the "stabilization efficiency" (the ratio of hole capture by the reducing agent to the total hole current to the surface) is plotted as a function of the concentration of the reducing agent. Figure 4, curve a, shows the results for well-etched GaAs; curves b and c show the results for increasing mechanical damage (scratching with alumina powder). It is observed in Fig. 4 that the stabilization efficiency increases rapidly, but not linearly, as the concentration of the reducing agent increases. It is the analysis of such rate laws that leads to the model [4, 5] described briefly above, where the first hole capture at the back bond is reversible and the second hole capture is irreversible.

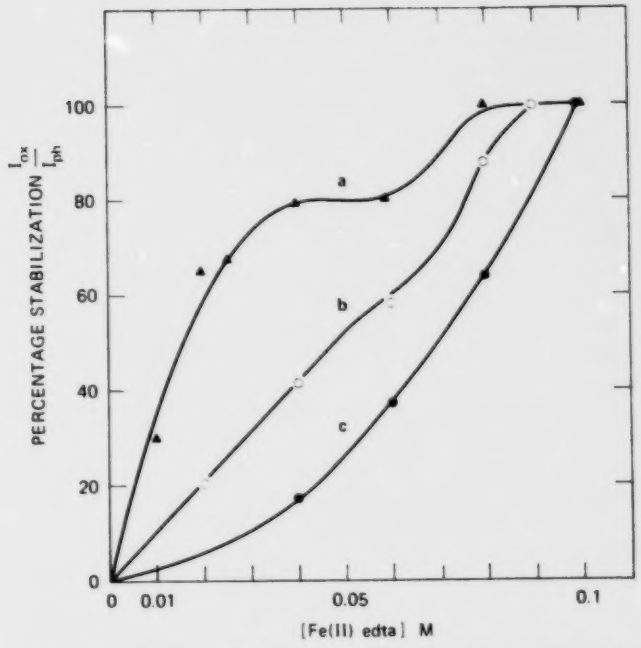


Fig. 4. Stabilization efficiency $S$ *vs.* concentration of the stabilizing agent ($S = I_{ox}/I_{ph}$ where $I_{ox}$ is the hole current oxidizing the reducing agent and $I_{ph}$ is the total photocurrent): curve a, surface well etched; curve b, mechanical damage to the surface; curve c, more mechanical damage to the surface.

Because mechanical damage has such a strong effect, the rate-limiting step in corrosion can be associated with defects. Through a study of the rate constants associated with the corrosion [4] it is suggested that the rate-limiting step in corrosion is hole capture at the back bond of an atom on a surface step.

We have discussed (Fig. 4) the use of stabilizing agents to prevent corrosion, but many other techniques have been used to induce stability and thus to make photoelectrochemical devices more practical. Such methods include the deposition of polymer films [7 - 12], the deposition of metal [13, 14] or tin oxide [15, 16] films onto the semiconductor (see Section 3.3), the use of insulators [17] or corrosion products [16], the use of layer compounds where the valence band electrons are in non-bonding orbitals [7, 12] and the use of intrinsically stable semiconductors such as titanates or iron oxide [18 - 20]. None of these has been completely satisfactory. For example, the layer compounds will corrode on edge planes although they are stable on the basal plane. Titanates are intrinsically quite stable but their band gap is large so that a small portion of the solar energy is adsorbed. Iron oxide is basically a low efficiency semiconductor in solar conversion, presumably because of defects in the material.

*2.2. Surface films*

The uncontrolled formation of surface films during operation is another serious problem in photoelectrochemical devices. The controlled use of surface films can be beneficial if they do not degrade the characteristics but passivate the surface. In some cases, such as for CdSe and InP, naturally conducting films which enhance the stability appear to form. In the case of InP, an $In_2O_3$ conducting film resulting from corrosion appears to passivate the surface [16]. However, if the conducting film does not prevent further corrosion it is not helpful.

Usually, however, films are undesirable. A "thick" insulating or semi-insulating film will substantially lower or even eliminate [21, 22] the solar energy conversion efficiency because it acts as a resistor in series with the device, and with any modest resistance very quickly the voltage output of the solar device is lost. If the film could be made thin enough (of the order of 20 Å) the film would be desirable. A thin insulating film has been shown to be beneficial both with solid state [23, 24] and with photoelectrochemical Schottky barrier cells [21], where in both cases improved conversion efficiency results and in the photoelectrochemical case improved corrosion resistance results. For example, it has been shown [21] that the stabilization efficiency is highest with an insulating film about 20 Å thick on the surface. This improved stabilization efficiency arises because a voltage appears across this insulating film due to the hole storage at the surface, and this voltage enhances the hole capture rate by the stabilizing agent. Improved conversion efficiency results because the thin film blocks the undesirable electron current to the surface, while permitting the desired hole current to the surface. Unfortunately, with photoelectrochemical cells it is difficult to maintain the film thickness at 20 Å; usually the film will either corrode or grow. Thus, with photoelectrochemical cells, surface films are in general undesirable, and the problem is to avoid surface film formation while still avoiding dissolution of the semiconductor electrodes.

Since films as little as 30 Å in thickness can be highly deleterious, such undesirable films can be invisible. Many reported cases of poor solar cell characteristics could be due to the presence of invisible and undetected films; tests with intentionally deposited insulating films present show characteristics [21] similar to those obtained in many cases of inefficient photoelectrochemical systems.

## 3. Potential advantages and remaining problems with photoelectrochemical photovoltaic cells

*3.1. The use of imperfect semiconductors*

One potential advantage of the photoelectrochemical photovoltaic cell is the relative insensitivity to poor material, *i.e.* to flaws in the crystal structure. A flaw in the semiconductor can effectively short out the solar cell with a metal/semiconductor cell. As indicated with Fig. 1, under ideal operating conditions a low flow of electrons to the metal should occur.

Because of the bulk levels associated with a scratch, dislocation or grain boundary, electrons can readily flow to the surface in the region of such flaws [25], while the flow is low (at the optimum level) elsewhere. A high electron flow of course counters the desired hole flow, and the conversion efficiency is reduced [26].

With a photoelectrochemical cell, such current through flaws would also occur but is limited by the electrolyte. First, whereas in the metal there is essentially an infinite density of states for the electrons to flow to, with the electrolyte the density of states is the ion density, and the flow is limited. Secondly, because the flaws are normally of limited area, diffusion limitations associated with the rate of diffusion of the ions to the flaw restrict the current to the flaw. Thus the photoelectrochemical cells can operate reasonably well [26] with flawed material.

With semiconductors where a suitable oxide can be formed to make an MIS cell as discussed in Section 1, the electrochemical cell no longer shows such an advantage. Specifically, with silicon and with GaAs [24], a thin oxide layer is intentionally formed on the surface of a Schottky barrier solar cell. This oxide effectively blocks the current of electrons to the surface while still permitting the holes to tunnel through to the metal. For this purpose the oxide should be of the order of 20 Å in thickness. As mentioned in Section 2.2, a similar oxide could also be very helpful in improving the efficiency of a photoelectrochemical solar cell, but in this case it is extremely difficult to maintain the oxide thickness at exactly the right value.

Thus, for some semiconductors, but not all, it can be anticipated that the photoelectrochemical photovoltaic cells will have an advantage in that in general poorer quality material can be used.

*3.2. Simplicity of design*

The major potential advantage of the photoelectrochemical photovoltaic solar cell over the solid state solar cell is its simplicity of design. In principle at least, a layer of semiconductor can be deposited in the bottom of a tray, the tray filled with a solvent, electrical contacts attached to the semiconductor and to a counterelectrode and electrical power collected when the semiconductor is exposed to the Sun.

Obviously the above is a gross simplification and in practice, for an efficient photoelectrochemical solar energy converter, the unit must be carefully designed [27] both with respect to the active components in the cells such as the semiconductor and the electrolyte [28] and with respect to hermetic sealing to avoid evaporation of solvent. To date, the "well-designed system" which has the conversion efficiency optimized to compete with solid state solar cells has not been lower in cost.

However, the cost of the photovoltaic systems is still the major problem in the general use of solar energy-to-electricity conversion for solid state cells. Thus, photoelectrochemical photovoltaic cells are still a serious candidate on the basis of their potentially low cost of production, if a suitable system is found.

*3.3. Electrolyte/metal/insulator/semiconductor cells*

By use of an electrolyte/metal/insulator/semiconductor (EMIS) configuration, the corrosion problem can be avoided somewhat while still retaining some of the design simplifications of the photoelectrochemical solar cells and thus perhaps a cell lower in cost than the straightforward MIS cell can be produced. An EMIS cell is a cell with an MIS Schottky barrier and where the electrolyte is only used to make electrical contact to the metal. Alternatively, a conducting oxide, such as $In_2O_3$ or $SnO_2$, can be used in place of the metal.

*3.4. Remaining problems of photoelectrochemical photovoltaic cells*

The corrosion problem is still a general problem. Cases of electrodes which have been stable over many years have been reported, specifically in work on CdSe at the Weizmann Institute, but the stability seems to be at the expense of conversion efficiency. Other cells, such as the EMIS cell, have not been tested over the many years necessary.

The efficiency of photoelectrochemical cells in general is lower than that observed with MIS cells. There are several causes for lower efficiency that must be overcome. Usually the optimum electrolyte for high efficiency is not the same as the optimum electrolyte for corrosion resistance, and so a compromise must be made. Thus research must continue on corrosion (and on optimized electrolytes for efficiency) to reduce the need for corrosion control and to permit the high efficiencies possible. There are other sources of efficiency loss that must be minimized system by system. The electrolyte is often highly coloured, and so absorption loss in the electrolyte can lead to low efficiency. Alternatively, the electrode processes can have a significant overvoltage, leading to energy loss.

Studies to optimize the selectivity of carrier reactions should be emphasized to try to eliminate side reactions. The use of catalysts, the better understanding of selectivity on semiconductor electrodes and the choice of electrolytes must be studied with a view to preventing undesirable film formation, minimizing corrosion and minimizing electrolyte changes with time.

## 4. Advantages and remaining problems of photoelectrochemical photosynthesis

*4.1. Introduction*

Here we wish to assess photoelectrochemical photosynthesis cells where the solar energy is either stored in the form of chemical energy or it is used in a photoelectrosynthesis or photoelectrocatalytic process to synthesize valuable chemicals. The potential of this approach should be compared with the potential for development of effective photoelectrochemical photovoltaic cells. It should also be compared with a series arrangement combining a solid state photovoltaic cell and a metal electrochemical cell.

*4.2. Selectivity*

The semiconductor electrode seems to show a potential selectivity for certain chemical reactions and products which differs from the selectivity on a metal electrode and which could give the semiconductor electrode an advantage [29, 30]. This is illustrated by the reduction of $CO_2$ selectively to methanol [31, 32], a process that can occur with 100% efficiency on GaAs [32] (while in a saturated $CO_2$ solution reduction on metal electrodes yields only formic acid, a product of less interest in energy conversion). Unfortunately, little is known regarding the reasons for this difference in selectivity. The problems of determining whether the difference between metals and semiconductors is real and, if real, how to optimize the selectivity, are probably of paramount importance in the successful development of photosynthesis cells. More details are discussed in Section 4.5.

*4.3. The use of suspended powder*

What may be the greatest potential advantage of the photoelectrochemical photosynthesis approach over either solid state cells or photoelectrochemical photovoltaic cells is the possibility of using the semiconductor as a suspended powder rather than as an electrode of an electrochemical cell in converting solar energy [33 - 38]. In comparison with the photoelectrochemical photovoltaic cell described in Section 3, the cost of solar energy conversion using suspended powders and a synthesis reaction could be very low because the system (in principle) is simpler: a powder is suspended in an appropriate electrolyte solution, it is exposed to the Sun and the product is collected. This is design simplicity in its extreme. It also avoids to a great extent the photocorrosion problem because if the powder does corrode it is easily replaced when its activity declines.

To date, high efficiency with this approach has not been attained. The system is difficult to optimize. The photon striking the surface of the powder particle produces the photoproduced hole and the photoproduced electron in the semiconductor particle. The holes and electrons must be physically separated to avoid recombination (the return of the excited electron to the valence band). The photoproduced electron must reduce a species A at the surface; the photoproduced hole must not reoxidize $A^-$ but must oxidize a different species B at the surface. The two products thus generated must be useful and must be collected. Workers in this area have attempted to separate the hole reaction and the electron reaction by depositing catalysts on two sides of the powder particle. The approach has been moderately successful. For example, Graetzel and coworkers [37, 38] have reported the dissociation of hydrogen sulphide into hydrogen and sulphur. This approach seems to be the most promising for the successful low cost conversion of solar energy using a semiconductor/electrolyte system.

*4.4. Electrolyte/metal/insulator/semiconductor cells*

Metal overlayers have been used to avoid the corrosion problem in photoelectrosynthesis as in photovoltaic systems. With this approach the

possible advantage of improved selectivity is not realized, and thus, for example, such systems are not used for $CO_2$ reduction to methanol. However, many other energy storage reactions that are appropriate to metal electrodes are feasible.

*4.5. Combination systems*

Work is in progress on the combination of a photoelectrochemical photovoltaic cell and chemical storage in the same cell.

The system is designed so that when the solar energy is converted to the energy of the hole–electron pair this energy can be directly extracted as electrical energy (photovoltaic mode), or when the electrical energy is not immediately needed the energy can be stored by a suitable electrode reaction (photoelectrosynthesis mode, *i.e.* a battery [39]). The potential advantage of this particular system of solar energy conversion as opposed to a solid state cell–battery combination is the fact that the chemical storage capacity, being a part of the solar cell, is distributed over a wide area. Separate storage facilities are not required, and the biggest problem in the conversion of solar energy to electricity, namely the storage of the electrical energy until nightfall when the electrical energy is needed, is very simply overcome. However, there is no evidence to date that this approach would be lower cost than the solid state cell–battery combination.

Another combination that is feasible with the conversion of solar energy to chemical energy by a photoelectrochemical cell is the possibility of adding a small applied voltage when necessary. An example of this would be the photoelectrocatalysis of water on a $TiO_2$ photoelectrochemical cell, where the conduction band edge of the $TiO_2$ is just not quite energetic enough to reduce protons. A small applied voltage makes the overall reaction feasible. This is a poor example, of course, because the use of $TiO_2$ for solar energy conversion cannot be efficient because of the low absorption of solar energy by $TiO_2$. However, the example illustrates the principle.

*4.6. Selectivity as the most important problem*

With the exception of the case where a suspended powder is used, the ubiquitous photo-induced corrosion is a problem with the photoelectrosynthesis as with the photovoltaic approach to photoelectrochemical solar conversion. Continuing research into ways to avoid corrosion is needed in all photoelectrochemical device development. Other problems of Section 3.4 are also present in this case to a greater or lesser degree.

However, we feel that the most important problem to be analysed before successful photosynthesis devices can be developed is selectivity. Selectivity is even more important here than in the photovoltaic case. For powdered suspensions, highly selective hole and electron reactions must be developed to increase the efficiency of the energy conversion. In all cases, better models of selectivity on semiconductors must be developed to optimize the surface and thus the desired reactions.

Two possible origins of special selectivity with semiconductor electrodes as opposed to metal electrodes can be suggested. One is the selectivity in accordance with ionic energy levels, as suggested by the Marcus–Gerischer model. Only ions with energy levels isoenergetic with the band edges will be electroactive, according to this model. Unfortunately the selectivity fails in many experimental cases [40, 41] (although it is apparently valid in others [42, 43]) and it would be of value to determine whether the model is wrong or whether the model is incomplete in real cases.

Another possible origin of selectivity is surface states, intentional or otherwise. Special surface additives can provide surface states on the surface [43], *i.e.* energy levels to mediate the carrier transfer. With metals, such surface states would be less active because of the high density of electrons near the Fermi energy.

In our laboratory at Simon Fraser we are studying selectivity with surface treatments to stimulate preferred adsorption and to deposit active sites as well as carrying out experiments to study specific carrier reactions. Some early results obtained in our laboratory by Baofang Li, a visiting scientist from China, on specificity associated with electron transfer processes may be of interest, suggesting a possible reason for the failure of the Marcus–Gerischer model.

Figure 5 shows the Marcus–Gerischer model [44] for reduction by isoenergetic electron transfer from the conduction band of a semiconductor to two species, A and B, in solution. The gaussian curves on the right-hand side of Figs. 5(a) and 5(b) represent the distribution of energy levels for the ion according to the Marcus–Gerischer model. Now for an isoenergetic electron transfer it is clear that the electrons from the conduction band cannot

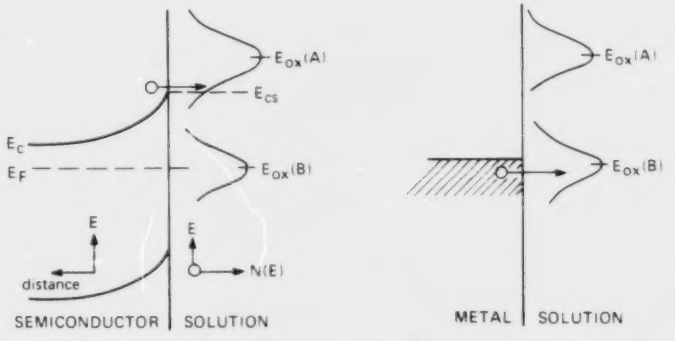


(a) (b)

**Fig. 5. A possible reason for semiconductor selectivity based on the Marcus–Gerischer model: (a) semiconductor band model with the "density of levels in solution" for two ions, A and B (with isoenergetic electron transfer the reduction of species A should be favoured); (b) equivalent model for a metal, with the Fermi energy in the metal determined by species B, but with a cathodic bias (with isoenergetic electron transfer the reduction of species B will always be favoured).**

transfer to species B because the energy level for species B has negligible probability of being at the conduction band energy. The energy level of species A is better located for electron transfer, with $E_{ox}$ approximately equal to the energy of the conduction band. This then should make the electrode highly selective for the reduction of species A. In contrast, with a metal electrode the reduction of species B should dominate, as in Fig. 5(b). However, experimentally, even with a semiconductor where the energy level of a species is well below the conduction band, such as ion B in Fig. 5, electron transfer is typically observed to occur at a high rate.

One possible reason suggested [44] for the preferred reduction of species B contrary to the Marcus–Gerischer model is described using Fig. 6. The reason is the presence of bulk energy levels associated with dislocations (imperfect crystal structure of the semiconductor). If enough energy levels are present in the band gap region, electrons from the conduction band could "trickle down" through these levels to the energy of $E_{ox}(B)$ and a high cathodic current will be observed. Other levels to mediate such electron transfer, such as surface states on the semiconductor [40 - 47], vibrational–rotational excited energy levels of the ion [48] or shifts in the ion energy level due to adsorption can be suggested. However, Baofang Li has emphasized the possible role of bulk states due to damage. Such damage has been shown to affect the electrode properties [49, 50], but the question here is whether it can remove the rate limitation imposed by the Marcus–Gerischer model.

In Li's experiments, various ions were studied at various pH values to vary a parameter $x$, the energy difference between the conduction band and the redox potential $E^\circ$ of a species in solution, where the energy determined

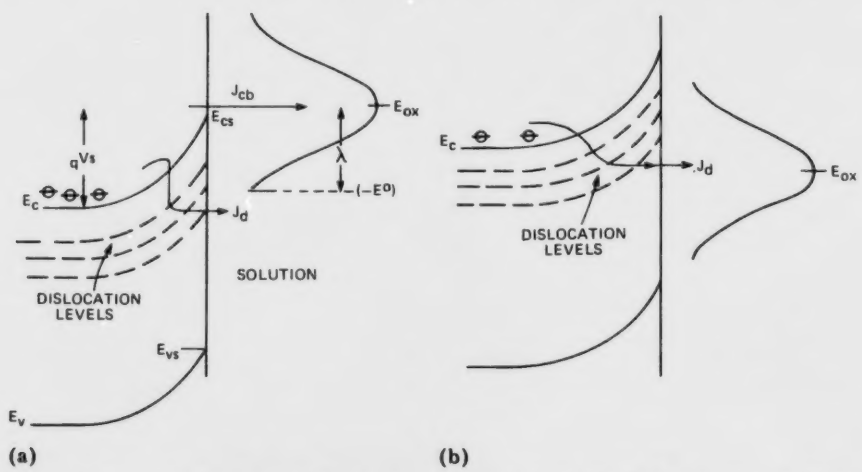


**Fig. 6. The possible influence of bulk flaws (energy levels) on semiconductor selectivity: (a) $E^\circ$ is almost as negative as the flat-band potential (little isoenergetic electron transfer through flaws); (b) $E^\circ$ is much more positive than the flat-band potential (all electron transfer through flaws).**

from the redox potential is an energy close to the bottom of the gaussian curve. Thus the value of $x$ for an oxidizing agent such as species A in Fig. 5(a) would be just above zero. The value for species B would be of the order of 1 V. If the Marcus–Gerischer model holds, the current should be low at $x \leqslant 0$ ($E^\circ$ is more negative than $V_{fb}$), increase rapidly as $x$ increases, pass through a maximum at $x \approx 1$ V ($E_{cs} \approx E_{ox}$), and decrease. If damage is destroying the selectivity, as suggested in Fig. 6(b), the current for the damaged surface should always be higher than that for the etched surface, with the difference increasing as $x$ increases.

The experimental results for a series of oxidizing agents with various values of $x$ on the abscissa as measured are shown in Fig. 7. On the ordinate we plot a parameter proportional to the logarithm of the current, namely the surface barrier potential $V_s$ at the semiconductor surface at constant current. Plotting this is equivalent, as indicated, to plotting the logarithm of the current at constant surface barrier potential. Results similar to that anticipated are observed, although the scatter is very large. The scatter is expected to be

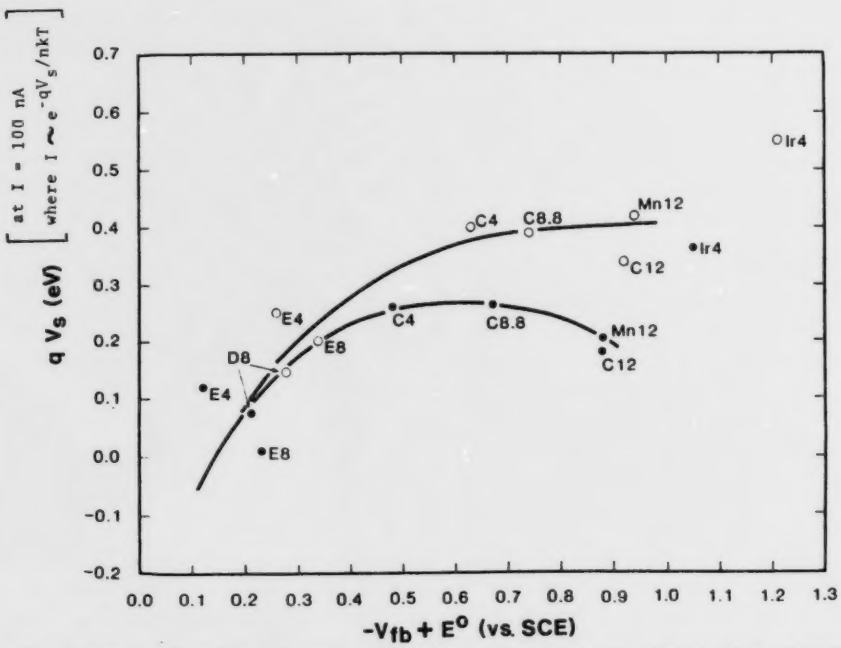


**Fig. 7. Effect of surface damage on cathodic current from the (0001) plane of ZnO to various ions in solution (concentration, $10^{-4}$ M in 1 M KCl): ○, measurements on the damaged surface; ●, measurements on the etched surface; points C, $[Fe^{III}(CN)_6]^{3-}$; points D, $[Fe^{III}(dtpa)_3]^{3-}$ (dtpa ≡ diethylenetriaminepentacetic acid); points E, $[Fe^{III}edta]^-$; points Ir, $[Ir^{III}Cl_6]^{3-}$; points Mn, $MnO_4^-$. The numerals indicate the pH in aqueous solution. (SCE, standard calomel electrode.)**

large because of the variation in the cross section for hole capture of the various species which cannot be taken into account. However, increasingly high values on the abscissa suggest that the current to the damaged surface becomes larger than the current to the well-etched surface by an increasing amount as $x$ increases. For example, for $MnO_4^-$ the current at constant surface barrier potential is higher by almost three orders of magnitude with the surface damaged. This suggests that dislocations are indeed active in transferring electrons to solution, contrary to the Marcus–Gerischer predictions.

Further experiments along this line are in progress. If the results continue to support the proposed model they suggest that, in cases of photoelectrochemical solar energy conversion where selectivity is important, semiconductors with few crystalline flaws must be used. Unfortunately there are few such cases; satisfactory materials could be silicon, germanium, epitaxial GaAs and, most practical, powder semiconductors that have not been subjected to mechanical damage.

## 5. Conclusions

Throughout the discussion the words "has potential" have been used very liberally to describe the advantages of photoelectrochemical cells. The research over the past years, since the original Fujishima–Honda publication [1], has exposed many problems in what initially appeared to be a rather simple concept for the conversion of solar energy. We have described some of these and urged appropriate research. There is no doubt that other workers in the field could list others. Many advances have been made in solving these problems, but most of them are still with us to a greater or lesser extent.

However, this same research has also shown us the great potential of the semiconductor/electrolyte approach to solar conversion and to electrochemistry. Let us consider photoelectrochemical photovoltaic cells; workers have obtained photoelectrochemical photovoltaic cells almost as efficient as the best solid state photovoltaic cells. The photovoltaic approach is far from dismissed and much active research is continuing in this area. However, the photoelectrochemical photosynthesis approach, converting solar energy or electrical energy to chemical energy, seems to be even more exciting. Although to date the efficiency of photosynthesis has been low, the approach could be extremely rewarding.

As a final remark we might compare the effort invested in three categories: solid state solar energy conversion, photoelectrochemical photovoltaic conversion and photoelectrochemical photoelectrosynthesis. The amount of time, study and money devoted to these three developments varies by orders of magnitude; the effort on solid state devices has been very large compared with the effort on photoelectrochemical photovoltaic devices, which in turn has been large compared with the effort on photoelectrochemical synthesis devices. It appears that the interest in synthesis devices is increasing rapidly at the present time and hopefully with a substantial

effort in that area we shall soon see some practical systems for direct solar energy conversion from optical to chemical energy.

## Acknowledgments

The experiments to study specific carrier reactions were supported by Energy, Mines and Resources, Canada Centre for Mineral and Energy Technology.

## References

1 A. Fujishima and K. Honda, *Nature (London), 238* (1972) 37.
2 K. Rajeshwar, P. Singh and J. Dubow, *Electrochim. Acta, 23* (1978) 1117.
3 H. Gerischer, *J. Vac. Sci. Technol., 15* (1978) 1422.
4 K. W. Frese, Jr., M. J. Madou and S. R. Morrison, *J. Electrochem. Soc., 128* (1981) 1939.
5 D. Vanmaekelbergh, W. P. Gomes and F. Cardon, *J. Electrochem. Soc., 129* (1982) 546; *J. Chem. Soc., Faraday Trans. 1, 79* (1983) 1391.
6 M. J. Madou, K. W. Frese, Jr., and S. R. Morrison, *J. Electrochem. Soc., 127* (1980) 987.
7 H. S. White, H. D. Abruna and A. J. Bard, *J. Electrochem. Soc., 129* (1982) 265.
8 K. Rajeshwar, M. Kaneko and A. Yamada, *J. Electrochem. Soc., 130* (1983) 38.
9 R. Noufi, A. J. Nozik, J. White and L. F. Warren, *J. Electrochem. Soc., 129* (1982) 2261.
10 B. Aurian-Blajeni, I. Taniguchi and J. O'M. Bockris, *J. Electroanal. Chem., 149* (1983) 291.
11 H. S. White, H. D. Abruna and A. J. Bard, *J. Electrochem. Soc., 129* (1982) 265.
12 L. Fornarini, F. Stripe and B. Scrosati, *J. Electrochem. Soc., 130* (1983) 2084.
13 Y. Nakato, S. Tonomura and H. Tsubomura, *Ber. Bunsenges, Phys. Chem., 80* (1976) 1002, 1289.
14 T. Kobayashi, H. Yoneyama and H. Tamura, *J. Electrochem. Soc., 130* (1983) 1706.
15 F. Decker, J. Melsheimer and H. Gerischer, *J. Electrochem. Soc., 130* (1983) 2173; *Isr. J. Chem., 22* (1982) 195.
16 H. J. Lewerenz, D. E. Aspnes, B. Miller, D. Malsu and A. Heller, *J. Am. Chem. Soc., 104* (1982) 3325.
17 D. S. Ginley, R. J. Baughman and M. A. Butler, *J. Electrochem. Soc., 130* (1983) 1999.
18 J. H. Kennedy and M. Anderson, *J. Electrochem. Soc., 130* (1983) 849.
19 K. Itoh and J. O'M. Bockris, *J. Electrochem. Soc., 131* (1984) 1266.
20 P. Iwanski, J. S. Curran, W. Gissler and R. Memming, *J. Electrochem. Soc., 128* (1981) 2128.
21 D. Canfield and S. R. Morrison, *Appl. Surf. Sci., 10* (1982) 493.
22 B. H. Loo, K. W. Frese, Jr., and S. R. Morrison, *Surf. Sci., 109* (1981) 75.
23 S. J. Fonash, *J. Appl. Phys., 47* (1976) 3597.
24 R. L. van Meirhaighe, F. Cardon and W. P. Gomes, *Phys. Status Solidi A, 59* (1980) 477.
25 S. R. Morrison, *J. Electron. Mater., 11* (1982) 21.
26 A. S. Cogan, *Appl. Phys. Lett., 44* (1984) 539.
27 A. J. Bard, *J. Phys. Chem., 86* (1982) 172.
28 T. Inoue, C. Weber, A. Fujishima and K. Honda, *Bull. Chem. Soc. Jpn., 53* (1980) 334.

29 M. A. Fox, *Acc. Chem. Res.*, *16* (1983) 314.
30 M. Fujihira, Y. Satoh and T. Osa, *Chem. Lett.*, (1981) 1053.
31 M. Halmann, *Nature (London)*, *275* (1978) 115.
32 D. Canfield and K. W. Frese, Jr., *J. Electrochem. Soc.*, *130* (1983) 1772.
33 H. Hada, Y. Yonezawa and M. Saikawa, *Bull. Chem. Soc. Jpn.*, *55* (1982) 2010.
34 M. D. Ward, J. R. White and A. J. Bard, *J. Am. Chem. Soc.*, *105* (1983) 27.
35 J. Manassen, *Isr. J. Chem.*, *22* (1982) 190.
36 S. Sato, *J. Phys. Chem.*, *87* (1983) 3531.
37 M. Graetzel, *Biochem. Biophys. Acta*, *683* (1982) 221.
38 K. Kalyinasundaram, E. Borgarello and M. Graetzel, *Helv. Chim. Acta*, *64* (1981) 362.
39 Y. Yonezawa, M. Okai, M. Ishino and H. Hada, *Bull. Chem. Soc. Jpn.*, *56* (1983) 2873.
40 K. W. Frese, Jr., *J. Electrochem. Soc.*, *130* (1983) 28.
41 P. A. Kohl and A. J. Bard, *J. Am. Chem. Soc.*, *97* (1975) 9427.
42 R. A. L. Vandenberghe, F. Cardon and W. P. Gomes, *Surf. Sci.*, *39* (1973) 368.
43 S. R. Morrison, *Surf. Sci.*, *10* (1968) 459.
44 S. R. Morrison, *Electrochemistry at Semiconductor and Oxidized Metal Electrodes*, Plenum, New York, 1981.
45 J.-N. Chazalviel, *J. Electrochem. Soc.*, *129* (1982) 963.
46 K. Rajeshwar, *J. Electrochem. Soc.*, *129* (1982) 1003.
47 J. J. Kelly and R. Memming, *J. Electrochem. Soc.*, *129* (1982) 730.
48 H. Gerischer, *International Society for Electrochemistry Berkeley Meet., August 1984.*
49 T. Kobayashi, H. Yoneyama and H. Tamura, *J. Electroanal. Chem.*, *138* (1982) 105.
50 S. R. Morrison and T. Freund, in A. Franklin (ed.), *Proc. National Bureau of Standards Workshop on Electrocatalysis on Non-metallic Surfaces, 1975*, U.S. Government Printing Office, Washington, DC, p. 139.

APPENDIX A

Reprinted from The Journal of Physical Chemistry, 1985, 89, 3295.
Copyright © 1985 by the American Chemical Society and reprinted by permission of the copyright owner.

# Carbon Dioxide Reduction on Gallium Arsenide Electrodes

**W. M. Sears* and S. Roy Morrison**

*Simon Fraser Energy Research Institute, Simon Fraser University, Burnaby, British Columbia, Canada V5A 1S6* *(Received: December 14, 1984)*

Studies of carbon dioxide reduction by conduction band electrons from gallium arsenide single-crystal electrodes were undertaken, to determine the degree of product selectivity. High Faradaic efficiencies for methanol production have been reported in the literature, and our main purpose here was to extend this work to highly doped p-type material to study the effect of cathodic current produced from avalanche breakdown. In doing so, we found that a reinterpretation of the reduction process is necessary. Our most striking result was the detection of open circuit (dark) reduction of carbon dioxide to methanol. This occurred at the rate of 0.1 $\mu$mol/(h cm$^2$) on the As face of the heavily doped p-type GaAs. A slightly higher rate (50%) was observed for a moderately doped n-type crystal. Some formaldehyde production was also seen but at a much smaller rate (1/5). We determined that this rate is indeed constant with surface area and time. A measurement on the opposite face (Ga) showed very little methanol production. The (100) face gave an intermediate result. It was also determined that damaging the surface greatly reduced methanol production while increasing the amount of formaldehyde. Closed circuit measurements under cathodic bias showed reduction of carbon dioxide as indicated by the disappearance of hydrogen bubbles when the carbon dioxide gas was introduced. The product was almost certainly formic acid as no additional methanol or formaldehyde (over the open circuit results) was detected at either high current (10 mA) or low current (0.2 mA). We explain this result in terms of dissolution (or corrosion) of the semiconductor in carbonic acid. GaAs plus dissolved carbon dioxide would form hydroxides of gallium and arsenic plus methanol (or possibly formaldehyde). This acid etch of the sample only needs to proceed at a rate of about 300 Å/h to explain our results on the As face.

## Introduction

There have been a number of studies on the electrocatalytic reduction of $CO_2$ at metal electrodes.[1,2] It has been found that $CO_2$ reduces to formic acid at high current efficiencies with some indication of further reduction to formaldehyde and methanol. Because of a large overvoltage, however, the electrical conversion efficiency is very low.

In an attempt to overcome these problems, there have been recent studies on the use of semiconductor electrodes in the reduction of $CO_2$.[3-16] As electrons come off the conduction band at a fixed energy, semiconductors promise a degree of selectivity not normally observed with metals. Much of the recent work has involved the use of semiconductor powders which have the advantage of a large surface area and relative ease of preparation.[10-12] The most interesting result has been the efficient reduction of carbon dioxide to methanol which supports the hope of semiconductor selectivity.[3,4,6,8,9-14]

Electrocatalytic reduction of $CO_2$ is expected to proceed in a stepwise fashion according to these equations.

$$CO_2 + 2e^- + 2H^+ \rightarrow HCOOH \quad (1)$$

$$HCOOH + 2e^- + 2H^+ \rightarrow CH_2O + H_2O \quad (2)$$

$$CH_2O + 2e^- + 2H^+ \rightarrow CH_3OH \quad (3)$$

$$CH_3OH + 2e^- + 2H^+ \rightarrow CH_4 + H_2O \quad (4)$$

Each of these steps involves at least four substeps with the formation of intermediate ions and radicals. The details can be found in ref 4. Without going into details, we can state that the redox potentials of these reactions lie at about −1 V (SCE).[11] The conduction bands of many semiconductors lie at potentials in this region.

In this paper we will look at $CO_2$ reduction on GaAs single-crystal electrodes. Enhanced methanol production has been reported by a number of papers,[3,4,6,8] and we decided to see how this would work out with heavily doped p-type material. Under reverse breakdown conditions electrons would emerge at various energies just above the conduction band.

Because of its importance later in the paper, we should note here some of the features of GaAs corrosion in aqueous solution. GaAs corrosion in acidic medium proceeds as a complete dissolution of $Ga^{3+}$ and $As^{3+}$ ions. This also happens in strong basic solution, and the oxides are in fact most stable at neutral pH.[17-22] Normally this is a problem under anodic bias although for acid etches not a necessary condition.

## Experimental Section

*Sample Preparation.* The GaAs crystals used in this work were bought from Crystal Specialties Inc., Monrovia, CA. The n-type

(1) R. G. Russell, N. Kovac, S. Srinivasan, and M. Steinberg, *J. Electrochem. Soc.*, **124**, 1329 (1977).
(2) S. Kapusta and N. Hackerman, *J. Electrochem. Soc.*, **130**, 607 (1983).
(3) D. Canfield and K. W. Frese, Jr., *J. Electrochem. Soc.*, **130**, 1772 (1983).
(4) K. W. Frese, Jr., and D. Canfield, *J. Electrochem. Soc.*, in press.
(5) I. S. Sarfati, Ph.D. Thesis, Polytechnic Institute of Brooklyn, 1968.
(6) B. Aurian-Blajeni, M. Halmann, and J. Manassen, *Sol. Energy Mater.*, **8**, 425 (1983).
(7) G. Ertl and J. Tornau, *Z. Phys. Chem.* (*Munich*), **82**, 21 (1972).
(8) M. Zafrir, M. Ulman, Y. Zuckerman, and M. Halmann, *J. Electroanal. Chem. Interfacial Electrochem.*, **159**, 373 (1983).
(9) M. Halmann, *Nature* (*London*), **275**, 115 (1978).
(10) M. Ulman, A. H. A. Tinnemans, A. Mackor, B. Aurian-Blajeni, and M. Halmann, *Int. J. Sol. Energy*, **1**, 213 (1982).
(11) B. Aurian-Blajeni, M. Halmann, and J. Manassen, *Sol. Energy*, **25**, 165 (1980).
(12) B. Akermark, U. Eklund-Westlin, P. Baeckstrom, and R. Lof, *Acta Chem. Scand., Ser. B*, **B34**, 27 (1980).
(13) J. C. Hemminger, R. Carr, and G. A. Somorjai, *Chem. Phys. Lett.*, **57**, 100 (1978).
(14) A. Monnier, J. Augustynski, and C. Stalder, *J. Electroanal. Chem. Interfacial Electrochem.*, **112**, 383 (1980).
(15) A. H. A. Tinnemans, T. P. M. Koster, D. H. M. W. Thewissen, C. W. de Kreuk, and A. Mackor, *J. Electroanal. Chem. Interfacial Electrochem.*, **145**, 449 (1983).
(16) J. Augustynski, *J. Electroanal. Chem. Interfacial Electrochem.*, **145**, 457 (1983).
(17) K. W. Frese, Jr., and S. R. Morrison, *J. Electrochem. Soc.* **126**, 1235 (1979).
(18) K. W. Frese, Jr., M. J. Madou, and S. R. Morrison, *J. Electrochem. Soc.*, **128**, 1527 (1981).
(19) K. W. Frese, Jr., M. J. Madou, and S. R. Morrison, *J. Electrochem. Soc.*, **128**, 1939 (1981).
(20) M. M. Faktor, D. G. Fiddyment, and M. R. Taylor, *J. Electrochem. Soc.*, **122**, 1566 (1975).
(21) A. Yamamoto and S. Yano, *J. Electrochem. Soc.*, **122**, 260 (1975).
(22) K. W. Frese, Jr., M. J. Madou, and S. R. Morrison, *J. Phys. Chem.*, **84**, 3172 (1980).

0022-3654/85/2089-3295$01.50/0 © 1985 American Chemical Society

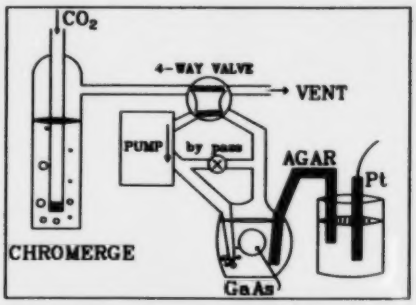


**Figure 1.** Circulation system used to study $CO_2$ reduction on GaAs.

crystals were doped with Si to a carrier concentration of $10^{16}$ $cm^{-3}$ and were obtained as (111) wafers. The p-type crystals were doped with Zn to a carrier concentration of $3 \times 10^{19}$ $cm^{-3}$ and were obtained both as (111) and (100) wafers.

The As and (100) faces were polished chemomechanically with a solution of 5% $Br_2$ in methanol. The solution was soaked into a large sheet of filter paper placed on a flat glass plate. The sample could then be physically polished on this surface. This technique works very well and gives a highly polished surface.

The Ga face cannot be polished this way and is in fact much more inert than the As face. However, we were able to use a similar chemomechanical method with a solution of 49% $H_3PO_4$ + 11% $HNO_3$ at 60 °C.[23]

After polishing the surfaces were rinsed with methanol and 10% HCl.

Ohmic contact was made to the GaAs electrodes with Ga–In eutectic. For the lower doped n-type material this was annealed in hydrogen at 500 °C for about 1 h (before polishing). Contacts were sealed and the sample was mounted with 5-min epoxy. Black wax or RTV silicone rubber cement was used to mask the electrode.

The GaAs electrodes were then dried thoroughly (sometimes under vacuum) to eliminate any remaining methanol or organic contaminant.

*Apparatus.* Figure 1 shows schematically the apparatus that was used to study $CO_2$ reduction on GaAs electrodes. Anaerobic high-purity carbon dioxide from Linde Gas was first bubbled through a solution of Chromerge in concentrated sulfuric acid to remove unwanted organics. The gas was then admitted to a Teflon pump driven circulation system through a four-way switching valve. The system and the electrolyte were usually purged with $CO_2$ for about 10 min in the flow through position of the value before switching to circulation.

The sample chamber was built to hold a small volume of electrolyte, about 10 mL. The inlet tube contained fritted glass to disperse the $CO_2$ gas. The GaAs electrode was mounted through a ground glass joint from the back. The electrolyte usually used was 0.2 M KCl. For $I/V$ measurements a Ag/AgCl wire was inserted into the sample chamber as a reference electrode. This was not used in catalysis as it caused a transfer of metallic silver to the GaAs electrode.

The counterelectrode, Pt, was kept in a separate electrolytic solution (KOH) to separate products and joined to the working cell by an Agar bridge.

*Gas Chromatography.* The electrolytic solution from the GaAs catalytic cell was analyzed with a Varian Vista 6000 gas chromatograph which was controlled by the Varian CDS 401 computer dedicated to that system. The data from this analysis were then transferred via a communication line to an IBM PC microcomputer where more efficient data and file manipulation were possible.

Direct syringe injection of the liquid into a Porapak T column allowed the separation of formaldehyde and methanol from the water. A flame ionization detector (FID) provided the signal. The integrated peak areas of these two compounds were calibrated with standard solutions. Figure 2 shows a typical plot where the concentrations are of the same magnitude as the experimental results.

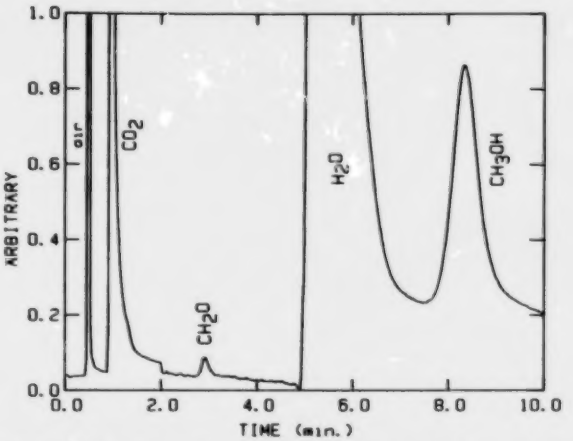


**Figure 2.** Gas chromatic separation of 17 ppm methanol and 20 ppm formaldehyde in aqueous solution using a column of Porapak T.

**TABLE I: Open Circuit Reduction on GaAs**

| sample | time, h | product | concn, ppm | no. of mol ($\times 10^{-6}$) | no. of mol/(h $cm^2$) ($\times 10^{-6}$) |
|---|---|---|---|---|---|
| p-type As | 19 | $CH_3OH$ | 11 | 2.2 | 0.10 |
| face | | $CH_2O$ | 2 | 0.5 | 0.02 |
| p-type As face ($^1/_4$ the area) | 17 | $CH_3OH$ | 3 | 0.6 | 0.12 |
| p-type Ga face | 20 | $CH_3OH$ | 0.8 | 0.16 | 0.014 |
| p-type Ga face | 71 | $CH_3OH$ | 2 | 0.4 | 0.009 |
| p-type (100) | 17 | $CH_3OH$ | 5 | 1.3 | 0.08 |
| n-type As | 18 | $CH_3OH$ | 8 | 2.7 | 0.15 |
| face | | $CH_2O$ | 2 | 0.5 | 0.02 |
| n-type As | 66 | $CH_3OH$ | 50 | 12 | 0.18 |
| face | | $CH_2O$ | 7 | 1.8 | 0.03 |
| n-type As | 18 | $CH_3OH$ | 2 | 0.5 | 0.03 |
| face (damaged surface) | | $CH_2O$ | 4 | 1.0 | 0.06 |

## Results

*Measurement of Background Impurities in $CO_2$.* A number of background measurements were done to determine the amount of methanol (and formaldehyde) contained in the distilled water solvent used in these experiments plus the amount trapped out of the carbon dioxide gas. Using the gas chromatograph, we detected a methanol impurity in distilled water of 1 ppm. As described in the last section, carbon dioxide was bubbled through the sample chamber which contained an electrolyte of 0.2 M KCl in distilled water for about 10 min before switching to a closed circulation system. This measurements was performed with a blank (no semiconductor) plug in place of the electrode. When the carbon dioxide was not bubbled through a Chromerge solution, a methanol background of 20 ppm was observed. When the Chromerge solution was used, the concentration detected was only that of the original distilled water (1 ppm).

No formaldehyde was detected in these background measurements.

*Open Circuit Results.* In this section we will present the carbon dioxide reduction observed on GaAs in the dark under open circuit conditions. The electrolyte we used when saturated with carbon dioxide gas produced a weak acid (carbonic acid buffer) at a pH of 4. No reducing agent was added.

Table I lists the results of various open circuit experiments. The p-type material used was heavily doped ($3 \times 10^{19}$ $cm^{-3}$) while the n-type material was moderately doped ($1 \times 10^{16}$ $cm^{-3}$). Despite the fact that there was no net current flow $CO_2$ reduction still occurred. Methanol production at the rate of about 0.1 μmol/(h $cm^2$) occurred on the As surface, the ($\bar{1}\bar{1}\bar{1}$) face, of well-polished

(23) W. Kern, *RCA Rev.*, 39, 278 (1978).

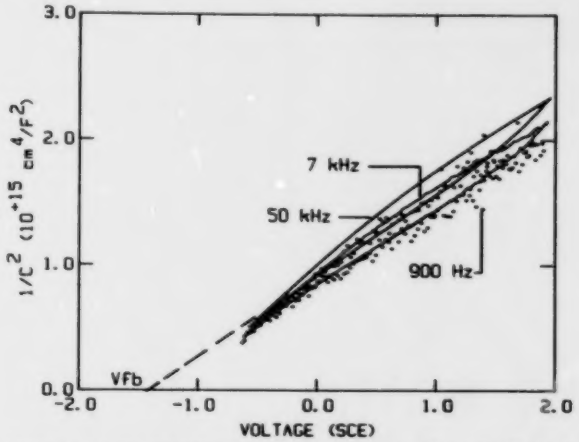


**Figure 3.** Mott–Schottky frequency dependence of n-type GaAs in neutral electrolyte at pH 4.3 with respect to a standard calomel electrode.

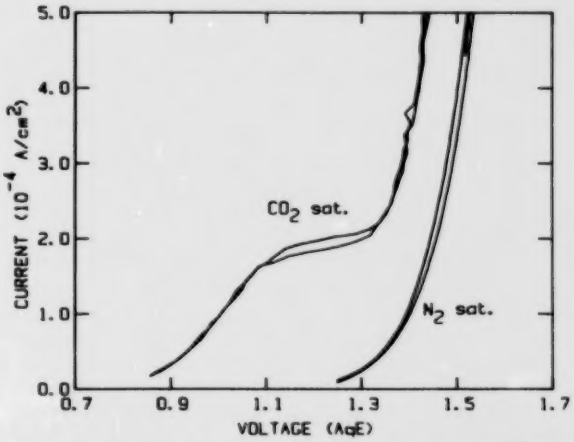


**Figure 4.** Cathodic $I/V$ of p-type GaAs showing reverse breakdown currents in $N_2$- and $CO_2$-saturated solutions with respect to a Ag/AgCl reference electrode.

single crystals. This occurred for both the n- and p-type samples with an approximately 50% greater yield for the n-type. Some formaldehyde was also seen with a production rate of 0.02 μmol/(h cm$^2$).

That this yield of methanol varies with the surface area of the crystal is shown by the reduced area measurement in Table I. That the yield varies with the time of illumination is shown by the 66-h run on the n-type sample.

Measurements on the gallium surface, the (111) face, produced very little methanol. This is an important result considering the relative stability of this face over the arsenic in aqueous solutions. The mixed face, (100), measurement gave a somewhat intermediate result.

Damaging the surface of the sample, by mechanical grinding, greatly reduced the methanol production while increasing the production of formaldehyde.

*Current Driven Results.* Figure 3 shows the results, on the medium doped n-type sample of GaAs, of a Mott–Schottky scan. This measurement was done in a weak solution of HCl. Scans at 900 Hz, 7 kHz, and 50 kHz are shown which indicate good frequency independence and give a flat-band potential of −1.39 V (SCE). From the slope a doping density of about $2 \times 10^{16}$ cm$^{-3}$ can be inferred by assuming a dielectric constant of 11.1[24] and a surface area of 0.5 cm$^2$. A measurement in strong HCl (pH 0) gives a flat band at −1.11 V (SCE) whereas in KOH at pH 12 a value of −1.80 V (SCE) was seen. These three numbers give shifts which are very close to the expected value of 59 mV/pH.

In our experiments on the reduction of $CO_2$ by electrons, we thus expect these electrons to come off the conduction band into solution at about 1.4 eV (SCE). This compares well to an earlier value.[17]

Figure 4 and 5 respectively are the cathodic $I/V$ characteristics, in the dark, of the heavily doped p-type and the moderately doped n-type material showing the change in reduction current when $CO_2$ is bubbled into solution. The solution used is 0.2 M KCl purged with $N_2$. The reference electrode is a Ag/AgCl wire which in 0.2 M KCl is +0.011 V (SCE).

Figure 4 shows reverse breakdown at about 1.5 V where, in the $N_2$-purged solution, water is being reduced to form hydrogen gas. At high currents the gas bubbles can be clearly seen evolving from the surface of the electrode. When carbon dioxide is introduced, this bubbling mostly disappears showing that $CO_2$ reduction is now dominant. The reduction starts at voltages more negative than −0.8 V and shows a slight saturation before breakdown.

Figure 5 shows very much the same results on the forward current of n-type GaAs. Here reduction of $CO_2$ begins at −1.1 V.

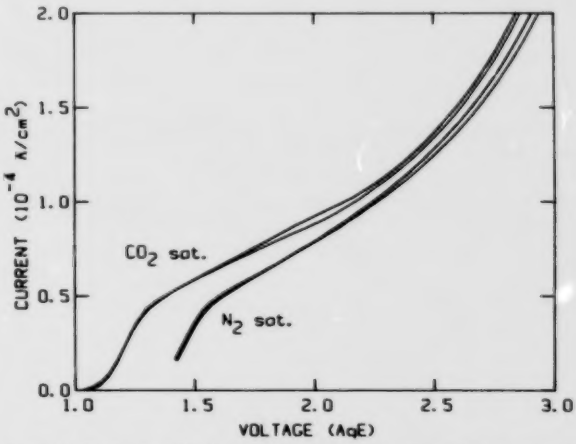


**Figure 5.** Cathodic $I/V$ of n-type GaAs showing forward bias currents in $N_2$- and $CO_2$-saturated solutions with respect to a Ag/AgCl reference electrode.

$CO_2$ reduction experiments were performed at a cathodic current of 10 mA on p-type GaAs. The resultant production of methanol (or formaldehyde) observed was at the same level as stated in Table I, the open circuit results. Lower current (0.2 mA) measurements and the use of the n-type sample gave the same result. No additional methanol production was observed. The addition of the current seemed to result in only formic acid.

*Miscellaneous Results.* We looked for catalytic effects on open circuit GaAs surfaces in a solution of formic acid, but no $CO_2$ reduction was observed.

We also tried "catalytic" measurements on GaAs powder in $CO_2$-saturated solution, where the powder was prepared by grinding a single crystal. Again there was little evidence of methanol production. It would seem that a well-polished crystalline surface is necessary.

## Discussion

The surprising conclusion of this paper is that the production of higher reduction products, formaldehyde or methanol, from $CO_2$ on GaAs electrodes is an open circuit phenomenon. Cathodic current seems to result in only the production of formic acid. We will try to explain this effect in terms of dissolution (or corrosion) of the semiconductor in carbonic acid. If true, this will have an important effect on the interpretation of measurements on other semiconductors, particularly III–V's. The net effect of this dis-

(24) M. Hass, "Semiconductors and Semimetals", Vol. 3, R. K. Willardson and A. C. Beer, Eds., Academic Press, New York, 1967.

solution would be the following

$$GaAs + H_2CO_3 + 4H_2O \rightarrow Ga(OH)_3 + As(OH)_3 + CH_3OH \quad (5)$$

where gallium and arsenic hydroxide are soluble in slightly acidic solution. This final equation would be the result of many intermediate steps involving ionic and radical forms much as in eq 1–4. Rewriting this equation in an acid form, we get

$$GaAs + (H^+ + HCO_3^-) + 4H_2O \rightarrow (H^+ + H_2GaO_3^-) + (H^+ + H_2AsO_3^-) + CH_3OH \quad (6)$$

Using information from Latimer,[25] we calculate a free energy change of approximately zero for this reaction. This implies a marginal reaction which may continue to the right as long as the methanol concentration is low. We could also add six electrons and six holes to the above equation to represent the reduction of $CO_2$ and oxidation of GaAs as joined through the semiconductor bands.

We will now review the experimental results in light of this model.

The methanol production rate of 0.1 μmol/(h cm$^2$) from Table I corresponds to a 270 Å/h disappearance of GaAs which certainly is not an impossible rate, even for a weak acid.

As intimated in the last section, the data on the gallium face and the mixed (100) face support this conclusion as the gallium face is very hard to etch (or dissolve) in acid solution at room temperature.[23]

The result on a damaged crystal is interesting in that as well as a loss in methanol there is a marked increase in formaldehyde production. Adding this to the lack of a noticeable effect on GaAs powder, we are led to the conclusion that a chemically polished surface is necessary. We might conclude that surface states destroy the coupling indicated by eq 5 and that holes from the valence band and electrons from the conduction band are needed to oxidize the semiconductor and to reduce the $CO_2$.

We are also led, by the absence of an effect involving formic acid, to the conclusion that a formic acid intermediate is not involved in eq 5. The result on the damaged surface suggests that formaldehyde is, however, an intermediate.

As mentioned, the addition of cathodic current to the GaAs electrode added only formic acid to the products and, as formic acid had no effect on the corrosion of the electrode, the result was the same amount of methanol (or formaldehdye) as observed in open circuit.

Relating this to previous measurements of electrocatalysis on GaAs electrodes,[3,6,8] we note that the bulk of past experiments relate to the indisputable fact of $CO_2$ reduction. We see, by our experiments, that this can be understood almost entirely by the production of formic acid. The amounts of methanol (or formaldehyde) observed in these papers are small in absolute terms and therefore, as far as we can tell, can be explained by the open circuit effect presented here. The drop-off of methanol production (efficiency) with increasing current density observed in the literature also fits in very well if this production is in reality independent of current.

The generation of methanol by straight chemical reaction with GaAs coupled with the lack of methanol generation by reduction of $CO_2$ with conduction band electrons is very surprising. The tentative conclusion is that a very special reaction route must be followed during the chemical reaction on a well-etched ($\bar{1}\bar{1}\bar{1}$) surface, a reaction route that involves absorbed intermediate reducible complexes and bypasses the brute force reduction of the formate ion.

*Acknowledgment.* Financial support for this research was supplied by Energy, Mines and Resources, Ottawa. We also thank the other members of the Energy Institute for their unrestrained criticisms at weekly meetings.

**Registry No.** $CO_2$, 124-38-9; GaAs, 1303-00-0; $CH_3OH$, 67-56-1; $CH_2O$, 50-00-0; KCl, 7447-40-7.

(25) W. M. Latimer, "Oxidation Potentials", 2nd ed., Prentice-Hall, Inc., New York, 1952.

APPENDIX B

Reprinted from The Journal of Physical Chemistry, 1985, 89, 1804.
Copyright © 1985 by the American Chemical Society and reprinted by permission of the copyright owner.

# Effect of Damage on Selectivity in Semiconductor Electrode Reactions

**Baofang Li[†] and S. Roy Morrison***

*Energy Research Institute, Simon Fraser University, Burnaby, British Columbia, Canada V5A 1S6*
*(Received: August 27, 1984; In Final Form: December 18, 1984)*

According to the Marcus–Cerischer model for electron transfer from bands of a semiconductor to ions in solution, strongly exothermic reactions should be hindered. One possible mechanism for such reactions occurring rapidly is tested. This is a mechanism where the carriers are assumed to "trickle down" through dislocation levels in the solid. A comparison of well-etched (low dislocation density) and mechanically polished (high dislocation density) electrodes shows a significantly higher current on the polished samples, qualitatively supporting the simple theory. The study was done on the Zn face (0001) of ZnO, and it is shown that, contrary to earlier reports on ZnO, the flat-band potential for this face is insensitive to pH for near-neutral aqueous solutions. This is attributed to low electric fields at this surface. A series of oxidizing agents were tested, including many iron complexes, permanganate, and quinone. The problems of applying the Marcus–Geriseher model to species that become hydrolyzed upon reduction, such as quinone, are discussed. A method of estimating the energy level of such ions is proposed.

## Introduction

Semiconductor electrodes for the electrochemical conversion of species in solution have been a subject of substantial interest in recent years.[1-3] An important reason for interest is the significant difference in selectivity in electrosynthesis reactions between semiconductors and metals. For example, photoproduced electrons in p-type gallium arsenide under certain conditions have been found[1] to convert $CO_2$ into methanol with 100% efficiency, whereas the reduction of $CO_2$ on metals leads to formic acid as the dominant product. Other reactions on semiconductor electrodes that have stimulated particular interest are the photo-Kolby[4] and the photo-Fenton[5] reactions. The objective of the present study was primarily to examine models for selectivity in such electrode reactions and, more directly, to test a possible reason for lack of selectivity under certain circumstances. During the course of the study, other interesting features of semiconductor electrochemistry were encountered and are discussed: experimentally, the unique pH dependence of the flat-band potential on the Zn face of ZnO; theoretically, a possible way to describe by the Marcus–Gerischer energy level model energy levels involving hydrolysis of the product.

The Marcus–Gerischer model of semiconductor electrode reactions[6] suggests why semiconductors should be different from metals in their selectivity. Electron exchange between the semiconductor conduction band (for example) and various species in solution, according to this model, should occur dominantly with ions for which there is a high probability that their energy level is isoenergetic with the conduction band edge, $E_{cs}$. According to the model the energy level of each given oxidizing agent has a certain energy level of highest probability, $E_{ox}$, as indicated in Figure 1, for arbitrary oxidizing agents A and B and the probability that the energy is at another energy, $E_c$, decreases in a Gaussian fashion with $E_c - E_{ox}$. If $E_c$ is the band edge of the active band of the semiconductor, and $E_{cs} - E_{ox}$ is large, the electron exchange with the band should be very poor. To a first approximation, according to the model, $E_{cs} - E_{ox}$ is independent of voltage in many cases of interest for a given species and semiconductor. This leads to a highly selective electrode. Either the band edge $E_{cs}$ is near $E_{ox}$, so the species is active, or far from $E_{ox}$, so the species is inactive. With metals, on the other hand, the equivalent parameter is the difference $E_{ox} - E_F$ between $E_{ox}$ and the Fermi energy is the metal. Because of the dependence of the Helmholtz double layer on the electroactive species, this difference is somewhat similar for all metals and all dominant redox couples, where we define the "dominant" redox couple as the electroactive species in the solution that controls the open-circuit electrode potential.

Experimentally it has been found in many cases[7] that the activity of various species at the semiconductor surface do not follow the predictions of the Marcus–Gerischer model. Specifically it is found that when the energy level $E_{ox}$ becomes much lower than the conduction band edge ($E_{cs} - E_{ox}$ large and positive) the electron

[†]On leave from Institute of Photographic Chemistry, Academia Sinica, Beijing, China.

(1) D. Canfield and K. W. Frese, Jr., *J. Electrochem. Soc.*, **130**, 1772 (1983).
(2) A. C. C. Tseung, B. S. Hobbs, and A. D. S. Tantram, *Electrochem. Acta*, **15**, 473 (1970).
(3) M. A. Fox, *Acc. Chem. Res.*, **16**, 314 (1983).
(4) R. E. Schwerzel, N. J. Byker, D. G. Vutetakis, and V. E. Wood in "Photoelectrochemistry: Fundamental Processes and Measurement Techniques" W. W. Wallace, A. J. Nozek, and S. K. Deb, Ed., Electrochemical Society, Princeton, NJ, 1982.
(5) M. Fujchua, Y. Satoh, and T. Osa, *Chem. Lett.*, 1053 (1981).
(6) S. R. Morrison, "Electrochemistry at Semiconducting and Oxidized Metal Electrodes", Plenum, New York, 1981.
(7) See, for example P. A. Kohl and A. J. Bard, *J. Am. Chem. Soc.*, **99**, 7531.

0022-3654/85/2089-1804$01.50/0 © 1985 American Chemical Society

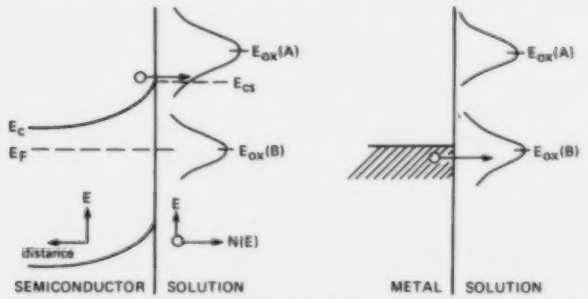


**Figure 1.** Energy level model for two oxidizing agents, A and B, at a semiconductor and a metal electrode. Reduction of A will be preferred on the semiconductor, reduction of B will be preferred on the metal, in isoenergetic electron transfer processes.

transfer to the energy level maintains a high value rather than decreasing as would be predicted by the Marcus–Gerischer model. Examples of this are reviewed in ref 6. The suggestion in ref 6 to explain this variation was that either surface states or flaw states in the semiconductor permitted the electrons to trickle down to the energy level of the oxidizing agent rather than emerge at the energy of the conduction band edge. This means that a damaged or a badly dislocated crystal will not have the selectivity of a perfect single crystal surface. The work of Kobayashi et al.[8] and that of Morrison and Freund[9] show that indeed there is a significant difference in electrode behavior depending on the presence of surface damage.

The approach in this work was to attempt directed experiments to test the theory proposed in ref 6 and determine whether damage does destroy the selectivity. We use zinc oxide as a test semiconductor because[9] zinc oxide can be etched to give a "perfect surface" as far as can be determined by the electrical properties of the semiconductor electrolyte interface. Then this "perfect surface", henceforth called the "etched surface", can be mechanically damaged (dislocations introduced) to distinguish clearly the difference between the etched and the damaged surface. Mechanical surface damage to the material results in dislocation loops penetrating deeply into the zinc oxide.[9] The dislocations can be considered bulk defects produced near the surface. We measure the effect of this reasonably high dislocation density on the electron transfer characteristics by comparing the capture cross section or current flow to various species in solution where the value of $E_{ox} - E_{cs}$ is varied, with $E_{ox}$ values from above the conduction band edge to somewhat below the conduction band edge.

## Analysis

As we are interested in electron capture from the zinc oxide conduction band by oxidizing agents, we use the band model as indicated in Figure 2, where we show the band model for ZnO (3-eV bandgap) and well-behaved ions in solution for which the standard electrode potential $E°$(SCE) is related to $E_{ox}$ by the reorganization energy $\lambda$ as shown. We have ignored the possibility in Figure 2 that the zinc oxide may have surface states close to the conduction band. Such states would not have a significant effect on the overall model, at least to a first approximation. In Figure 2a we illustrate the case where the energy $E_{ox}$ of the ion is above the conduction band edge at the surface $E_{cs}$ or, in the approximation we will be using, $E_{ox}$ is above $V_{fb}$, the flat-band potential of the $n$-type zinc oxide. In this case, in accordance with the Marcus–Gerischer model, we should observe a current $J_{cb}$ due to direct electron transfer from the conduction band at the surface to the energy levels of the oxidizing agent in solution. If the surface is damaged we should also perhaps measure a current $J_d$, which is the current that trickles through the damaged region as indicated. In Figure 2b, the current $J_{cb}$, in accordance with the Marcus–Gerischer model, should be close to zero, whereas the current $J_d$ should be the same or more in this case than in the case of Figure 2a.

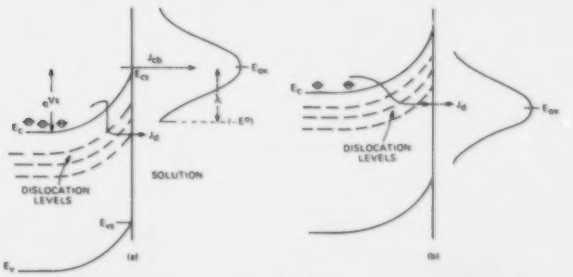


**Figure 2.** Model for decreased selectivity of a ZnO cathode due to dislocations, using the representation of energy levels in solution introduced by Gerischer and discussed in ref 6. Two routes for electrons transfer are indicated, direct from the conduction band ($J_{cb}$) and indirect through dislocation levels ($J_d$). For example, if for zinc oxide the conduction band edge is at −0.4 V SCE, the oxidizing agent in a could be ferricyanide, the oxidizing agent in b, hexachloroiridate.

Specifically eq 1 should describe the total cathodic current $J$

$$J = J_{cb} + J_d = n_b \bar{c} \sigma \lambda c_{ox} d \exp -(E_{ox} - E_{cs})^2/4\lambda kT \exp(-qV_s/kT) + bf(E_{ox} - E_{cs}) \exp(-qV_s/nkT) \quad (1)$$

to the oxidizing agent. The first term in eq 1 is one of the possible expression, in accordance with the Marcus–Gerischer model, for electron transfer to the oxidizing agent from the conduction band.[6] The second term is intended to represent electrons trickling through the levels associating with dislocations at the surface. The parameter $\sigma$ is the capture cross section for electrons, $\bar{c}$ is the average thermal velocity of electrons, $c_{ox}$ is the concentration of the oxidizing agent, $d$ is a distance parameter of the order of 15 Å, and $\lambda$ is the reorganization energy of the ion in solution. $V_s$ is the surface barrier as indicated in Figure 1a. The rest of the factors in the first term are indicated in the band models of Figure 1 or are standard symbols. The current depends on $V_s$ because the density of electrons at the surface is $n_b \exp(-qV_s/kT)$ and depends on $(E_{ox} - E_{cs})$ according to the Marcus–Gerischer model. In the second term $B$ is a constant, $f(E_{ox} - E_{cs})$ is some function of the difference $(E_{ox} - E_{cs})$. This function may have the same form as the exponential in the first term but, if trickling through the dislocation levels is the rate-limiting step for this electron transfer, $f$ may equal unity. The second term indicates that the current through the damaged region should depend on the surface barrier $V_s$. Here $n$ is a factor known in semiconductor device technology as the "quality factor" for Schottky barrier diodes and varies from 1 to 3 and possibly higher. Studies[10] of the possible leakage current through dislocation pipes or grain boundaries, at the surface of Schottky barrier diodes such as we have here, suggest that $n$ may be 2 or slightly higher for dislocations. The studies in ref 10 assume the increased current through such defects is dependent upon electrons from the conduction band being activated over the barrier surrounding the defect. When the carriers are on the defect, it is assumed they are able to move to the surface. An alternate possibility involving tunneling to or from such defect levels could occur but seems unlikely considering the low doping level of the zinc oxide used (about 5 ohm cm).

We assume that for ZnO

$$V_s = V_a + V_{fb} \quad (2)$$

where $V_a$ is the applied voltage and $V_{fb}$ the flat-band potential, both measured relative to a common reference electrode. This assumption implies the Helmholtz voltage does not depend on $V_a$ in the $V_a$ span used.

It is observed in eq 1 that when the surface is damaged the slope of the plot of log $J$ vs. $V_s$ will not be 60 mV/decade as predicted

(8) T. Kobayaski, H. Yoneyama, and H. Tamura, *J. Electroanl. Chem.*, 138, 105 (1982).

(9) S. R. Morrison and T. Freund in "Electrocatalysis on Non-Metallic Surfaces", A. D. Franklin, Ed., National Bureau of Standards, Washington, DC, 1976, Spec. Pub. No. 455.

(10) S. R. Morrison, *J. Electron Mater.*, 11, 21 (1982).

by the first term of eq 1. Thus a plot of $\sigma[x]$ as was done earlier,[11] where the theoretical slope of 60 mV/decade was observed, is not feasible in these experiments. As will be described later we will represent the results with $x$ on the abscissa, where $x = -V_{fb} + E^\circ$ and values of $V_s$ on the ordinate that lead to a constant current. Here $E^\circ$ is the standard electrode potential of the redox couple referred to calomel. The parameter $x$ is close to the difference between $E_{cs}$ and $-E^\circ$ in Figure 2, $x$ being positive if $E_{cs}$ is about $E^\circ$ in the band model.

In such plots we will be expecting a variation as follows. As suggested in Figure 1, when $x$ is zero or negative we expect both the currents $J_{cb}$ and $J_d$ to be low. As $x$ approaches $\lambda$, we expect $J_{cb}$ to be at a maximum, for here $E_{cb} = E_{cs}$. In this region, as indicated Figure 2a, $J_d$ may still be low. As $x$ increases above $\lambda$, approaching the configuration of Figure 2b, we expect $J_{cb}$ to decrease and $J_d$ to dominate.

In eq 1 it is observed that the first term is expected to vary linearly with the concentration of oxidizing agent. On the other hand, the second term, $J_d$, may be insensitive to the concentration of oxidizing agent. This will be so if, in the second term, the rate-limiting step is the movement of current through the damaged region rather than electron exchange at the surface. Thus the relative magnitude of the two terms is expected to change with concentration. Experimentally we have used a reasonably low concentration of the oxidizing agent to try to emphasize the second term over the first term in the expression.

It is clear that, in general, we do not expect a smooth curve in a plot according to eq 1 because we are varying the oxidizing agent in solution to vary $x$. Therefore presumably we are varying $\sigma$, the capture cross section, and $\lambda$, the reorganization energy in eq 1. Thus we expect a considerable scatter in the results, and, as will be seen, we realize this expection, although, fortunately, the effect of the dislocations dominates over the effect of the varying $\lambda$, so the results are meaningful.

## Experimental Section

The ZnO single crystals were obtained many years ago from 3M Co., grown from the vapor phase. The $c$ faces are exposed; the crystals are about 6 mm in diameter. In the work to be discussed the zinc plane, the (0001) plane, of zinc oxide was used. This was done because of the resistance to etching of the zinc plane that has been observed in dilute etches. Unfortunately as will be seen, we were unable to take advantage of this characteristic because, as will be discussed below, the damaged regions, where other planes are exposed, apparently did etch rapidly at pH below about 4.

The oxidizing agents used were all reagent grade as obtained from the manufacturer. The supporting electrolyte in aqueous solvent was 1 M KCl, with the pH adjusted with KOH or KCl. In cases where the pH was adjusted to about 8.5, a borate buffer was used.

The electroactive species were primarily based on the ferric complexes ferricyanide, ferric EDTA (ethylene diamine tretraacetic acid), and ferric DTPA (diethylenetriaminepentacetic acid). For further shifts of $x = (-V_{fb} + E^\circ)$ the pH was changed while keeping the same oxidizing agent. Such pH changes were used to shift $V_{fb}$ of the zinc oxide at constant $E^\circ$ and provided shifts of $s$ with constant capture cross section and $\lambda$. Other species tested (besides iron) were quinone and potassium permanganate. Quinone has been extensively studied by Memming and Moellers[12] who suggested a redox potential for the quinone/semiquinone couple and this is the $E^\circ$ assumed in these studies. However, the energy level assignment in this case cannot be simple $-E^\circ$ because at moderate pH quinone is not expected to be hydrolyzed whereas semiquinone is. The assigned value of $x$ will be discussed later.

The sample preparation and measurement technique used was designed to measure a clean, "dislocation free" surface (when specifying an etched sample). As was discussed in ref 9 the zinc face of zinc oxide does not etch appreciably in dilute acids; however, it does etch, although slowly, in 85% $H_3PO_4$. The surfaces were thus prepared by first etching for the order of 1 h in 85% $H_3PO_4$, then for the order of less than 1 min in nitric acid. Because it was found in some cases that a surface film seemed to develop on an electrode during the cathodic current flow, the runs were made as follows. After an etch as above a single sweep, from a voltage slightly anodic to sufficiently cathodic to register about two decades of measurable current flow, was made while the capacity and the current were simultaneously measured. The sweep rate was 10 mV/s. Before another measurement was made the sample was removed, etched for 15 min in phosphoric acid, for 10 s in nitric acid, and only then was the next run made. This treatment was followed for all the measurements on etched surfaces.

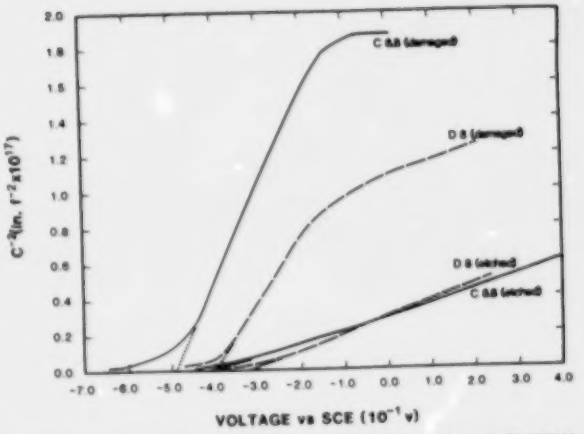


**Figure 3.** Mott–Schottky plots for damaged and for etched ZnO (0001) surfaces. Ferricyanide at pH 8.8 (C 8.8) and $Fe^{3+}$(DTPA) at pH 8 (D 8) are compared. The high slope of the dampaged curves is interpreted as electron trapping in the space charge region.

"Damaged surfaces" for comparison were prepared by damaging the surface following the above etch treatment (again done for each sweep), by rubbing the surface with alumina powder on a "Q-tip". The sample was then held in the dark above the solution for 15–20 min before immersing it in the solution for the cathodic sweep. The reason for maintaining the sample in the dark throughout was to avoid variations that were otherwise observed in the current, apparently associated with room light impinging on the sample. It was found that reproducible results were found if the above procedure was followed. Presumably the effect of the light was associated with trapping of photoproduced holes on dislocations[9] during exposure to room light and it is necessary to allow time for recombination with the sample held in the dark.

The value of $V_{fb}$ was obtained by Mott–Schottky plots. The capacity was measured as a function of frequency for both the etched and damaged surfaces. There was no significant frequency dependence between 1 and 20 kHz on the etched surface, but with the damaged surface the slope of the Mott–Schottky plot varied with frequency. Extra capacity at low frequency associated with storage of charge in the dislocation levels was presumably the caused for this frequency dependence. However, the flat-band potential as measured was independent of frequency, and as this was the only parameter of interest to us, we accepted the flat-band potential as observed.

## Results

*Variation of Flat-Band Potential with pH for the Zn (0001) Face of ZnO.* As discussed above, pH variations were used to vary $V_{fb}$. Typical results for Mott–Schottky plots for etched and damaged ZnO surface are shown in Figure 3. Under identical conditions otherwise $V_{fb}$ is found to be shifted negative for the damaged surface. The reason was not studied; it was assumed that electron trapping at dislocation levels was the cause. With this trapping model, the extra electric field in the Helmholtz region due to electrons trapped very near the surface would lead to the

(11) S. R. Morrison, *Surf. Sci.*, 15 363 (1969).
(12) R. Memming and F. Moellers, *Ber. Bunsenger. Phys Chem.*, 73, 475 (1972).

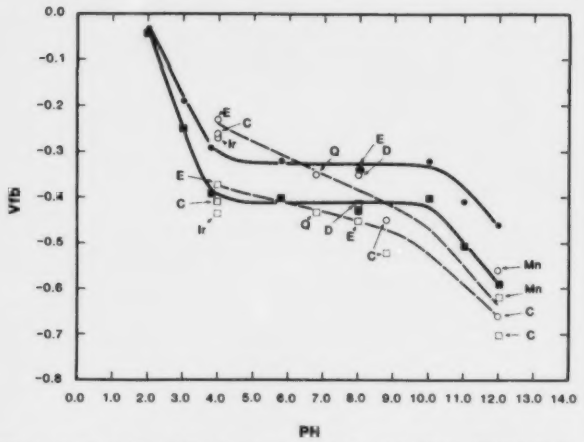


**Figure 4.** Variation of flat-band potential $V_{fb}$ with pH for (0001) ZnO. The solid lines show results with no electroactive species present; the dashed lines show results with electroactive species present as indicated: C, ferricyanide; D, $Fe^{3+}$(DTPA); E, $Fe^{3+}$(EDTA); I, $Ir^{3+}$(Cl); Mn, $MnO_4^-$; Q, quinone. The round symbols represent readings on an etched surface, the square symbols on a damaged surface. The insensitivity of $V_{fb}$ to pH between pH 4 and pH 10 is unexpected.

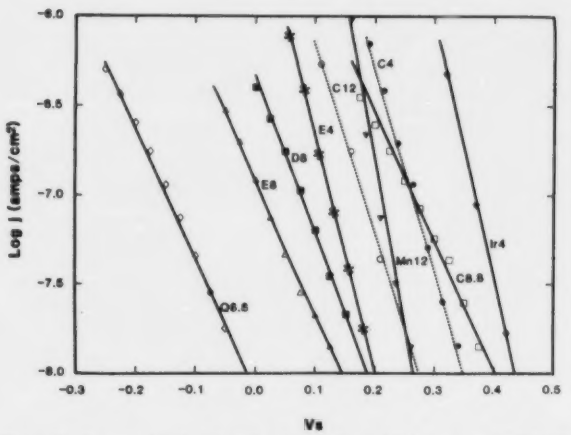


**Figure 5.** Current/surface barrier curves for oxidizing agents ($10^{-4}$ M) on etched ZnO. For symbols code, see caption of Figure 4, the numbers refer to pH.

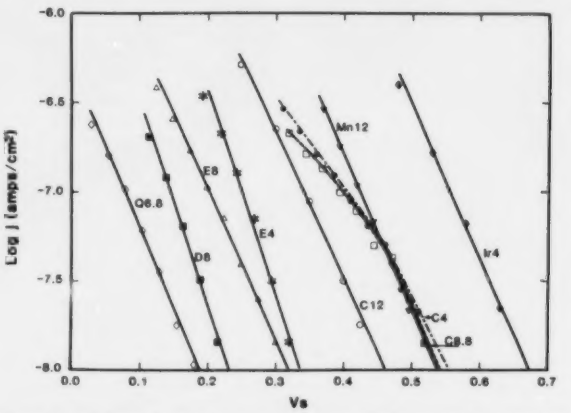


**Figure 6.** Current/surface barrer curves for oxidizing agents ($10^{-4}$ M) on damaged ZnO. For symbols code, see caption of Figure 5.

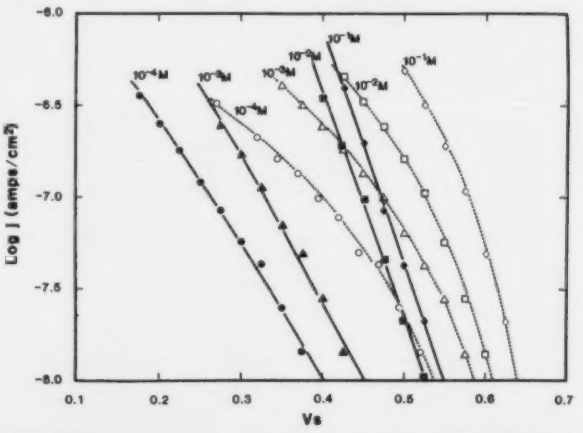


**Figure 7.** Plots of current vs. surface barrier $V_s$ for damaged (solid lines) and etched (dashed lines) ZnO. Results for various concentrations of $K_3Fe(CN)_6$ at pH 8.8 are shown. Note the excess current due to the damage, greatest (in terms of $\Delta V_s$) at low concentration and low current.

more negative flat-band potential. It is observed that for the damaged surface there are two slopes. The slope near $V_{fb}$ is much higher than the slope when $V_s$ is very anodic. This has been observed before[11] and is attributable to electron trapping (lowering the positive charge density) at dislocation levels. When $V_s$ is high enough to permit ionization, the slope should decrease, and this appears to occur at about $V_s \sim 0.3 \pm 0.1$ V (with $V_s$ obtained from eq 2), suggestive that at this energy the concentration of dislocation levels becomes high. A rather unusual dependence of flat-band potential vs. pH was found for zinc oxide. In earlier studies Lohmann[13] observed that on ZnO the flat-band potential varied with pH at the rate of 60 mV/pH unit. Our results are shown in Figure 4. It is observed that $V_{fb}$ is relatively insensitive to pH between pH 4 and pH 10 for the etched surface with no electroactive species (in this case solely KCl is the electrolyte with the pH adjusted by using KOH and KCl). The same insensitivity is observed for the case where the surface is damaged, but the flat-band potential is more negative by the order of −0.1 V. With the electroactive species present in the solution, at a concentration the order of $10^{-4}$ M, there may be an effect on the flat-band potential making it vary with pH in this region, but the effect may lie within probable error. In any case the variation is still much less than 60 mV/pH unit.

It is observed that at pH 2 the flat-band potentials of the etched and the damaged surfaces are identical. we also found, although not shown, that the current/voltage characteristics with oxidizing agents in solution were also identical for the damaged and etched surfaces when the pH was between 1.3 and 2. Another complication found in this pH range was a high anodic current when the sample was first immersed in the solution. This current died away after 5–10 min, but during this period our measurements could not be made because as the voltage was swept cathodic one could not distinguish the decrease of the anomalous current from the cathodic current of interest. We suspect this high anodic current represented electrochemical etching at the dislocations, so that when this current died away, we were no longer studying the "damaged" surface. Because of these factors our results for such ions as the ceric ion and the ferric (aquo) ion, where a very low pH is required, are not reported.

In Figures 5 and 6 we show our results for the current as a function of surface barrier, $V_s$ ($= V_a - V_{fb}$, where $V_a$ is the applied voltage). It is observed that, in general, the slope of the current/voltage characteristic is in general greater than 60 mV/decade, as was observed earlier for the (0001) face. However, it is nonetheless clear that, as expected from eq 1, the slopes observed with the etched surface are closer to 60 mV/decade than the slopes observed with the damaged surface. In principle, we can distinguish between $J_{cb}$ and $J_d$ by using eq 1 with $J_{cb}$ set equal to the current on an etched surface. However, the values of $J_d$ thus obtained are hard to interpret, possibly because of the unknown factor that leads to the nonideal slope with the etched surface.

(13) F. Lohmann, *Ber. Bunsenger. Phys. Chem.*, **70**, 428 (1966).

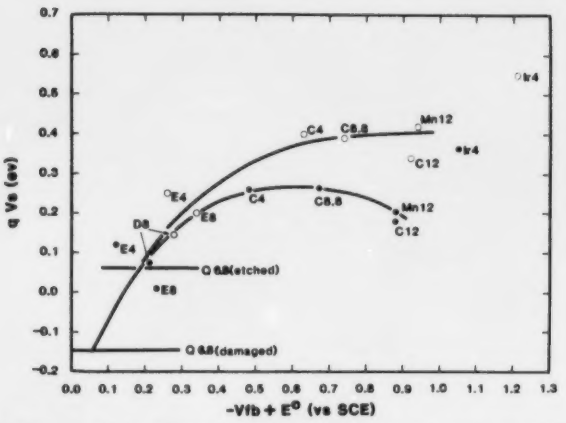


**Figure 8.** Cathodic current vs. the depth of the "energy level" $-E^\circ$ below the conduction band edge, showing much higher currents for damaged surfaces. The excess cathodic current is represented by the surface barrier needed to reduce the current to 100 nA/cm²—a high $V_s$ implies a very high current would flow if the measurements could be taken at constant $V_s$. The difference in energy levels is approximated by using $V_s$ instead of the more accurate $E_{cs}$ in calculating the abscissa.

Figure 7 shows a typical curve for the current/voltage characteristics with varying $c_{ox}$, showing how the curves are similar at high $c_{ox}$ where the first term in eq 1 dominates.

Figure 8 shows a summary of the results at $c_{ox} = 10^{-4}$ M for each of the oxidizing agents tested. On the ordinate we plot the surface barrier $V_s$ required for a current of 100 nA/cm². On the abscissa we indicate the presumed energy level of the ion relative to the conduction band; specifically we plot $x = -V_{fb} + E^\circ$ (all vs. SCE) where for all species except quinone $E^\circ$ is the standard electrode potential, and $V_{fb}$ is the measured flat-band potential.

The value of $x = -V_{fb} + E^\circ$ for quinone/semiquinone is shown as a broad line with, at one end, the "$E^\circ$" value taken as the potential of the first reduction wave of quinone on a Pt electrode at pH 6.8, the pH used in the ZnO experiment. At the other end the "$E^\circ$" value is taken as the standard electrode potential for the quinone/semiquinone couple. As will be suggested in the Discussion section, neither value is appropriate; rather an intermediate value is most probable.

When examining Figure 8 it should be kept in mind by comparing Figure 7 that the ordinate used, $V_s$, is an extremely insensitive function: for example, in the case of Mn, damaging the ZnO surface leads to an increase in $V_s$ of only 0.21 V at constant current as shown, but leads to a factor of 300 difference in current at constant $V_s$ (extrapolating the damaged surface curve).

It is observed that the results for $IrCl_6^{-3}$ are inconsistent with the pattern, insofar as the ordinate, the value of $V_s$, is concerned (although consistent insofar as the large difference between the etched and damaged values is concerned). The reason for the large current is not clear. It could be because at pH 4 the $IrCl_6^{3-}$ adsorbs on the surface, or it could be because the $IrCl_6^{3-}$ is reduced to Ir metal and we are observing the current/voltage characteristics of a ZnO/metal Schottky barrier instead of a ZnO/electrolyte Schottky barrier. Either of these effects could lead to the observed trend, where the current associated with the damaged surface is much greater than that associated with the etched surface, as expected, but both are higher than expected (at constant $V_s$).

In general, the relationship between $qV_s$ and $x$ follows the model of Figure 2. It is observed, subject to the scatter of the results, that the value of $V_s$ necessary to pass 100 nA/cm² approaches zero and becomes negative as the value of $x$ approaches zero. This suggests that as the conduction band edge approaches the same energy as the $(-E^\circ)$ level of the oxidizing agent, the current rapidly approaches zero. This could be expected from the simplest model. As indicated in Figure 2a if $(-E^\circ)$ is at or above the conduction band edge one expects very little current flow. As the value of $x$ becomes more positive the configuration moves from Figure 2a to Figure 2b and the current is observed to increase for both the etched and damaged surface and then possibly to decrease for the etched surface.

## Discussion

*The Flat-Band Potential for the (0001) Face of ZnO.* The behavior of the flat-band potential, as observed in Figure 2, is quite unusual for oxide semiconductors. It is normally anticipated that the surface of the oxide semiconductor will become hydroxylated so that the adsorbed charge that induces the Helmholtz potential will depend directly on the pH, giving 60 mV/pH unit shift in the flat-band potential. The insensitivity of the flat-band potential to pH for the zinc surface of the zinc oxide suggests that the surface is not so hydroxylated. It suggests that, in the region of intermediate pH values, the ligands at the surface are more accurately represented as water molecules rather than adsorbed protons and hydroxyl ions. In turn this would suggest a low field strength beyond the (0001) surface of ZnO, too low to dissociate the adsorbing water molecules.

The reason that $V_{fb}$ is more negative for the damaged surface than for the etched surface may be related to electron trapping on dislocations. Substantial trapping near the surface may affect the Helmholtz double layer potential.

*The Energy Levels of Quinone.* The reduction of quinone is complicated by the expectation that at low pH where $E^\circ$ is measured, the product, semiquinone, is hydrolyzed. Thus the standard electrode potential includes the energy of hydrolysis, whereas the electron transfer to an energy level may occur before or after the hydrolysis. To our knowledge this complication has not been considered in the literature. However, it is important in the present interpretation of Figure 7, for the effective value of $x$, the difference between the conduction band edge and the energy level in solution, depends critically on the assignment of the energy level in solution. The discussion below can be applied to other cases where inner-sphere chemical reorganization occurs before or after electron transfer, with minor changes.

We will assume there are three chemical routes possible for the reduction of quinone Q to semiquinone QH:

$$e^- + Q = Q^- \qquad (3a)$$

$$Q^- + H^+ = QH \qquad (3a')$$

$$Q + H^+ = QH^+$$

$$e^- + QH^+ = QH \qquad (3b)$$

$$e^- + H^+ = H\cdot$$

$$H\cdot + Q = QH \qquad (3c)$$

With this we are assuming there are three dominant species that could capture the electron leading to semiquinone. We immediately reject reaction 3c as probably involving too high an activation energy under the present conditions. Reaction 3b, where the electron transfer is to the species $QH^+$, would probably dominate at high proton concentration, but in our case, where the pH is 6.8, we suggest that eq 3a and 3a′ dominate the kinetic route of the reaction. The electrode potential of the Q/QH couple is related to the standard electrode potential $E^\circ_{Q/QH}$ by the Nernst equation:

$$E = E^\circ_{Q/QH} - kT \ln \frac{[QH]}{[Q][H^+]} \qquad (4)$$

If we believe reaction 3a, followed by reaction 3a′, is the dominant route for the reaction, we are interested in the "standard electrode potential", $E^\circ_{Q/Q^-}$, of the $Q/Q^-$ couple, which by the Nernst equation is related to the observed electrode potential by

$$E = E^\circ_{Q/Q^-} - kT \ln [Q^-]/[Q] \qquad (5)$$

Now if the free energy of the chemical reaction 3a′ is $\Delta G$, we have

$$[QH]/[Q^-][H^+] = \exp(-\Delta G/kT) \qquad (6)$$

hence

$$kT \ln [Q^-] = \Delta G + kT \ln [QH]/[H^+] \quad (7)$$

Substituting eq 7 in to eq 5 yields

$$E = E^\circ_{Q/Q^-} - \Delta G - kT \ln [QH]/[Q][H^+] \quad (8)$$

Naturally, independent of the reaction route, the electrode potential $E$ must be the same at equilibrium, so comparing (4) and (8) we obtain

$$E^\circ_{Q/Q^-} = E^\circ_{Q/QH} + \Delta G \quad (9)$$

If, as can be expected, (3a′) is exothermic, $\Delta G$ is negative, and the energy level ($E^\circ_{Q/Q^-}$) in Figure 1 is nearer the conduction band than ($-E^\circ_{Q/QH}$) by [$\Delta G$] electronvolts. In Figure 8 the appropriate value of $x$ for quinone is in the region indicated, to the left of the positive limit by the amount of [$\Delta G$].

*Current Flow through Dislocation Levels.* In Figure 8 it is observed that, in general, the results do follow the anticipated behavior as described in the theoretical section. If $-E^\circ$ is above the conduction band in Figure 2a ($x \lesssim 0$) very little current passes from the zinc oxide to the species in solution. As $x$ increases, the curves for the etched and damaged electrodes seem to diverge. For the etched electrode, there is some evidence of a peak in the current and a subsequent decrease in accordance with expectations of the Marcus–Gerischer model. With the damaged surface, on the other hand, as could be expected following the arguments related to Figure 2b, the current is maintained at a high level, presumably primarily due to $J_d$. By the simplest model the current $J_d$ through dislocation levels should become significant when the energy level $-E^\circ$ (see Figure 2) drops below the energy levels associated with the dislocations. From the location of the knee in the Mott–Schottky plots for damaged surfaces (Figure 2) a value of ($V_{fb}$ − 0.3) eV is suggested as the upper edge of the dislocation band. The results of Figure 8, are not inconsistent with such a simple model; the divergence of the two curves could indeed begin at about $x \sim 0.3$ eV.

In the case of the EDTA and the cyano complexes of iron, the pH was changed through a region where the redox potential was observed to show little shift with pH (as measured by a platinum working electrode). Unfortunately, as indicated in Figure 3, the flat-band potential did not shift nearly to the extent that was anticipated, so the shift in the value of $x$ was less than hoped. In the case of the EDTA the shift was very small, close to the probable error of $V_{fb}$. However, a significant increase in the current was observed at pH 4 over that at pH 8. The higher current is perhaps associated with another complex of EDTA that begins to appear at pH 4 or with strong adsorption at pH 4 of the EDTA itself onto the zinc oxide surface. The ferricyanide, which is not expected to adsorb, shows the expected behavior. Presumably at pH 12 one might expect a small fraction of the ferricyanide to be present with a cyano ligand exchanged for a hydroxyl ligand. However, either the hydroxylated compound has a low capture cross section or there is a negligible fraction thereof, as a total current is low at pH 12. Thus the presence of a fraction of partially hydroxylated iron does not alter the conclusion that the capture cross section of the hexacyanoferrate ions decreases at high pH, or at high $x$. Electron capture by the permanganate ion is higher than that of the ferricyanide ion at pH 12, but one can accept such differences with different ions.

## Conclusions

The most important conclusion that one can draw from the above study is the apparent qualitative agreement with the model described under Analysis, where the presence of a damaged surface (dislocations) is proposed as one reason for the high activity in exothermic electrode reactions. The model suggests that the Marcus–Gerischer theory in its simplest form may not apply to semiconductor electrodes unless they are prepared with a minimal concentration of flaws at the surface. With most electrodes, especially those for which techniques of material preparation are not sophisticated, one expects a very high density of dislocations built into single crystals and an extremely high density of dislocations built into most compressed powder, polycrystalline or film electrodes. Zinc oxide was chosen for the present study because, as was shown in earlier studies, by suitable etching deep channels are apparently etched at any dislocations emerging at the surface so that the dislocations are no longer active. This feature permitted the present study to be made. Similar studies could be made on dislocation-free silicon, dislocation-free germanium, and probably epitaxially grown CaAs. Powders prepared by precipitation and not subjected to mechanical treatment (such as compression) could be relatively dislocation-free. Few other materials could be relied upon to have the required low dislocation density.

Another feature of interest identified by the present paper, although perhaps not of such great import, is the insensitivity of the flat-band potential to pH in an extended pH range for the zinc face of the ZnO. This is quite unusual for an oxide semiconductor, although similar behavior has been observed[14] on an oxide-covered silicon electrode. As described in the discussion we suggest the (0001) surface is characterized by low electric fields such that the ligands are water molecules rather than protons and hydroxyl ions. Yates et al.[15] provide a more mathematical description in terms of the strength of the surface acid and basic sites.

Finally, the assignment of energy levels for cases where oxidation or reduction involves changes in inner-sphere composition was discussed. It was indicated that the energy level in solution can no longer be represented by the redox potential of the electroactive couple, and so the Marcus–Gerischer model in its simplest form must be appied with caution. For the case of interest here, quinone, an energy level was estimated, using an approach applicable to other systems. It is this problem of energy level assignment which makes the application of the model to the kinetics of such reactions as proton reduction to hydrogen very complicated. The direct application of the simple model, as has been done[16] to prove the Marcus–Gerischer model wrong, cannot be used as a valid test of the model.

*Acknowledgment.* This work was supported by Energy, Mines and Resources, Canada.

**Registry No.** $Fe^{III}$(DTPA), 20438-93-1; $Fe^{III}$(EDTA), 17099-81-9; $Ir^{III}(Cl)_6$, 14648-50-1; $MnO_4^-$, 14333-13-2; ZnO, 1314-13-2; ferricyanide, 13408-62-3; quinone, 106-51-4.

(14) M. J. Madou, B. H. Loo, K. W. Frese, and S. R. Morrison, *Surf. Sci.*, **108**, 135 (1981).
(15) D. E. Yates, S. Levine, and T. W. Healy, *J. Chem. Soc., Faraday Trans. 1*, **70**, 1807 (1974).
(16) J. O'M. Bockris and S. O. M. Khan in "Quantum Electrochemistry", Plenum, New York, 1979.

APPENDIX C

Reprinted from The Journal of Physical Chemistry, 1985, *89*, 5442.
Copyright © 1985 by the American Chemical Society and reprinted by permission of the copyright owner.

# Excited Dye Reactions with Damaged Zinc Oxide†

**Baofang Li‡ and S. Roy Morrison***

*Simon Fraser Energy Research Institute, Simon Fraser University, Burnaby, B.C., Canada V5A 1S6*
*(Received: July 1, 1985)*

Electrochemical studies of electron exchange between dyes and the conduction band of ZnO are reported, emphasizing the effect of dislocation levels (surface damage) on the exchange. It is found with rhodamine B that anodic electron injection from the excited dye is enhanced substantially by the presence of dislocations. Cathodic electron flow to the ground state of the rhodamine B (while the dye is excited) is also substantial in the presence of dislocations. In the case of rose bengal, the anodic electron injection from the excited dye and the cathodic electron flow to the ground state of the excited dye are each increased, but only moderately, by dislocation levels. The results are interpreted as suggesting that the energy levels of the dislocations act as transfer levels for electron flow in either direction between the conduction band and those surface levels of the dyes located in the bandgap region.

## Introduction

In an earlier contribution[1] the effect of damage (surface dislocation loops) on electron transfer from the n-type zinc oxide (0001) face to various ions in solution was studied. It was observed that for energy levels well below the conduction band a substantial increase in current was observed associated with the damage. It was suggested that electrons could move through dislocation levels to the surface, where they could, in an isoenergetic electron-transfer process, transfer to the energy levels in the solution. This provided some clarification on the role of dislocation levels in electrode reactions.

For many years studies have been made of the reaction of excited dyes on zinc oxide.[2,3] The interest was undoubtedly

† Supported by Energy, Mines and Resources, Canada.
‡ Visiting Scientist from the Institute of Photographic Chemistry, Academia Sinica, Beijing, China.

(1) Li, B.; Morrison, S. R. *J. Phys. Chem.* **1985**, *89*, 1804.
(2) Hauffe, K.; Pusch, H.; Range, J.; Rein, D. In "Current Problems in Electrophotography"; Hauffe, K., Berg, W., Eds.; deGruyter: Berlin, 1972.
(3) For more recent reviews of dye sensitization of ZnO, see: Hirschwald, W. "Current Topics in Material Science"; North-Holland: Amsterdam, 1980; Vol. 6. Morrison, S. R. "Electrochemistry at Semiconductor and Oxidized Metal Electrodes"; Plenum Press: New York, 1981.

0022-3654/85/2089-5442$01.50/0 © 1985 American Chemical Society

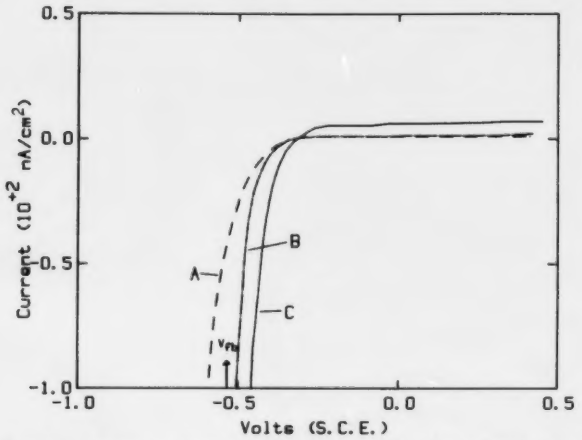


**Figure 1.** Current/voltage characteristics of etched ZnO with the dye rose bengal. Curve A: Blank (no dye or illumination); curve B: dark with dye present; curve C: illuminated at dye wavelength with dye present. The flatband potential indicated is measured by Mott–Schottky measurements in the dark with the dye present.

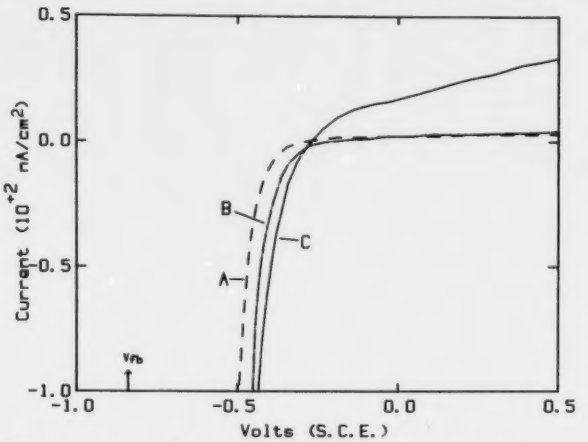


**Figure 2.** Current/voltage characteristics of damaged ZnO, ZnO with surface dislocation loops present. The dye is rose bengal. For code, see Figure 1 caption.

stimulated initially by the interest in zinc oxide as an electrophotographic material where, to make the zinc oxide sensitive to visible light, dyes were introduced on the surface. As the dyes were excited, electrons could be injected from the dyes into the zinc oxide conduction band. It was found convenient to study the process using the zinc oxide in aqueous solution (or alcoholic solution) with the dye dissolved in the solution. A substantial amount of information was determined regarding the electron transfer from the dye to the conduction band of the zinc oxide.

With this extensive background on processes involving the zinc oxide electrode in solutions containing dyes, it was considered to be useful to study the influence of surface damage (dislocations) on dye injection processes and dye reduction processes on zinc oxide to supplement our earlier work on the influence of damage on electron capture by ions at the surface of zinc oxide. It was anticipated that with excited dye molecules two effects may be observable: first, one might observe the anodic effect of the damage, where dye levels below the conduction band edge (by the Marcus–Gerischer model[3]) could still inject their electrons into the zinc oxide conduction band by having the electrons transported through dislocation levels. Second, in analogy to our earlier results, one might observe cathodic electron transport through the damage levels to the ground state of the dye, when the electron from the ground state is excited to the upper state of the dye. This could provide extra cathodic current and degrade the dye injection process, it being a mechanism for deexcitation of the dye.

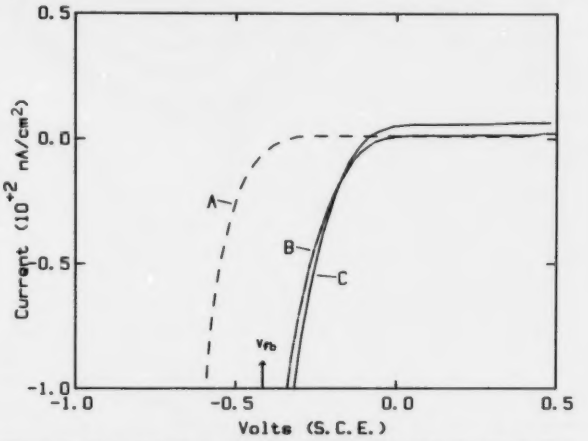


**Figure 3.** Current/voltage characteristics of etched ZnO with the dye rhodamine B. For code, See Figure 1 caption.

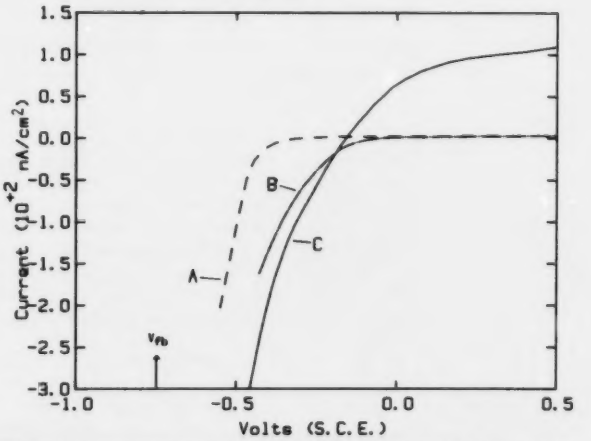


**Figure 4.** Current/voltage characteristics of damaged ZnO, ZnO with surface dislocation loops present. The dye is rhodamine B. For code, see Figure 1 caption.

## Experimental Section

Zinc oxide, purchased several years ago from 3M Corp., was etched on the (0001) face with 85% phosphoric acid for 1 h followed by a 10-s etch in nitric acid. For the measurements described below the sample area was 3 mm$^2$.

The surface was damaged when desired by rubbing the surface with alumina powder using a "Q-tip". The solvent was ethyl alcohol with 10% water added bubbled with nitrogen. The supporting electrolyte was 0.01 M KCl. The dye concentration was always $5 \times 10^{-4}$ M. The pH used was 7.4 with rose bengal and 5.8 with rhodamine B. The reference electrode, a commercial calomel electrode, was maintained in a separate compartment, separated by a frit from the working electrode and the counter electrode to avoid contamination by dyes. The current/voltage characteristics and the capacity/voltage characteristics of the zinc oxide electrode were monitored. Light was passed from a monochromator through the zinc oxide to intercept the dye at the zinc oxide electrolyte interface. Peaks in anodic current, at wavelengths corresponding to those observed in the literature, were observed for rose bengal and rhodamine B. In the studies reported, with rose bengal a wavelength of 563nm was used and with rhodamine B, 558nm.

## Results

Figures 1–4 show typical results with rose bengal (Figures 1 and 2) and rhodamine B (Figures 3 and 4). In each figure, curve A shows the results in the dark with no dye present, curve B shows

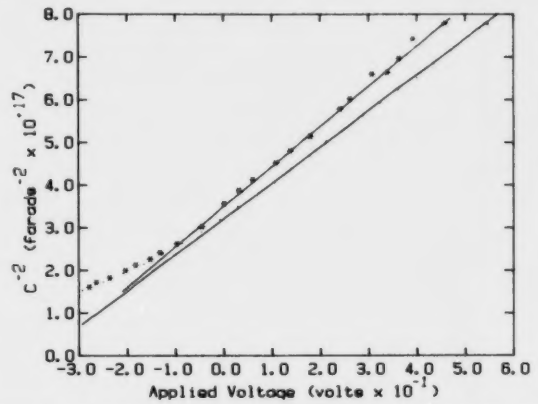


**Figure 5.** Mott–Schottky plot of dark (•) illuminated (·) etched ZnO with Rh B dye present. (λ = 558 nm). Computer fitting yields the following: dark, $V_{fb}$ = −0.39 V, $n_b$ = 1.5 × $10^{14}$ $cm^{-3}$; illuminated, $V_{fb}$ = −0.41 V, $n_b$ = 1.7 × $10^{14}$ $cm^{-3}$.

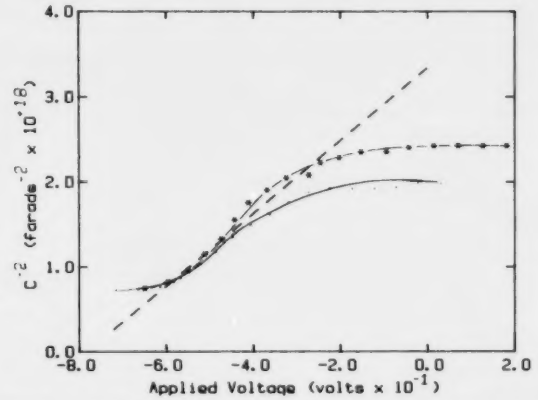


**Figure 6.** Mott–Schottky plot of dark (•) and illuminated (·) damaged ZnO with Ph 3 dye present. (λ = 558 nm). Computer fitting yields the following: dark, $V_{fb}$ = −0.77 V, $n_b$ = 2.8 × $10^{13}$ $cm^{-3}$; illuminated, $V_{fb}$ = −0.82 V, $n_b$ = 3.7 × $10^{13}$ $cm^{-3}$.

the results in the dark with dye present, and curve C shows the results in the light with dye present. Figures 1 and 3 show results with the ZnO etched; Figures 2 and 4 show results with the ZnO damaged. The measurements were made beginning at 0.5 V and the data were measured point-by-point through to the negative voltages. When cathodic current flowed, the current decayed with time, and the points indicate the values at about steady state. If the voltage is swept negative the cathodic current measured is higher. The reason for the decay was not determined.

It is observed that the presence of the dye, even in the dark, seems to lead to extra cathodic current, and the presence of the dye under illumination at the peak absorption of the dye leads to anodic photocurrent. There is some evidence even in these curves that there is also cathodic photocurrent.

Typical results for the Mott–Schottky curves for the more interesting system, the Rh B system, are shown in Figures 5 and 6. Figure 5 shows the results for an etched sample, Figure 6 results for a damaged sample. The influence of subbandgap illumination is observed to be negligible, but damage to the sample shows a strong effect, shifting $V_{fb}$ to a more negative value, increasing the slope at intermediate voltages, and inducing a low slope at high voltage. The slope increase at intermediate voltages has been interpreted as due to electron trapping at the dislocation[4] leading to an effectively low $n_b$. The lowering of the slope at high voltages has been interpreted as due to the deep trapping levels.[5]

(4) Morrision, S. R.; Freund, T. "Electrocatalysis on Non-metallic Surfaces"; *NBS. Spec. Publ. (U.S.)* **1976**, No. 455.
(5) Kennedy, J. H.; Frese, Jr., K. W. *J. Electrochem. Soc.* **1978**, *125*, 723.
(6) Gerischer, H.; Willig, F. *Top. Curr. Chem.* **1976**, *61*, 31.

**TABLE I: Flatband Potentials[a] As Determined by Mott–Schottky Plots**

| | etched | damaged |
|---|---|---|
| no dye | −0.75 | −0.9 |
| rose bengal | −0.54 | −0.84 |
| rhodamine B | −0.41 | −0.76 |

[a] The probable error is estimated to be ±0.1 V in all cases. The difference in $V_{fb}$ between rose bengal and rhodamine B is in the direction expected due to pH difference, but is more likely associated with differences in adsorption.

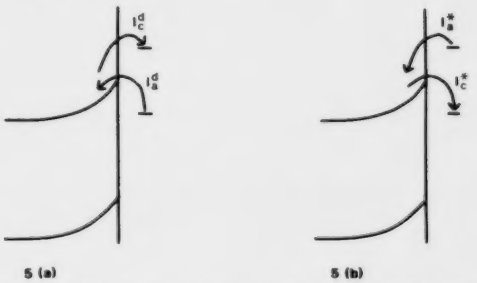


**Figure 7.** Cathodic and anodic electron exchange between the ZnO conduction band and the dyes. The part labeled 5a shows processes possible in the dark, a cathodic current $I^d$ to a high unoccupied level, and an anodic current $I^d$ from a low, occupied level. Under illumination these currents can occur plus in addition the processes of the part labeled 5b, namely a cathodic current $I^*$ to the unoccupied, ground state of the excited dye and an anodic current $I_a^*$ transferring the electron from the excited state to the ZnO.

## Model

The abscissas of Figures 1–4 must be corrected by the flatband potential, $V_{fb}$, in order to discuss the cathodic current more realistically. The current to the surface is expected to follow a first-order law such as

$$J_{cathodic} = \text{const} \times [Ox] n_b \exp(-qV_s/kT) \qquad (1)$$

where const represents some constant, [Ox] represents the density of oxidizing agent ions or molecules at the surface, and the last factor represents the density of electrons at the surface, $n_s$. The value of $n_s$ is the density of bulk electrons in the ZnO, $n_b$, times the Boltzmann factor associated with the surface barrier $V_s$. The surface barrier is given to a good approximation by

$$V_s = V_{app} - V_{fb}$$

Here $V_{app}$ is the applied voltage, $V_{fb}$ is the value of $V_{app}$ when the surface barrier is zero.

The flatband potential $V_{fb}$ is determined from a Mott–Schottky plot—the inverse square of a capacity plotted as a function of the applied voltage. The intercept of this line at $C^{-2} = 0$ is the flatband potential. The slope is proportional to $(n_b A^2)^{-2}$, where $A$ is the sample area. It is found that with an etched surface, the capacity/voltage characteristics are very well-behaved with negligible frequency dependence. Thus the flatband potentials are reliable. With a damaged surface, the capacity/voltage characteristics are not so well-behaved but the flatband potential is essentially independent of the frequency. Changes in the flatband potential reflect changes in the Helmholtz double layer in general. Thus for example the flatband potential at the $TiO_2/H_2O$ interface is much more positive than at the $TiO_2/(H_2O$ + methanol) interface studied here. The reason for the shift has not been investigated. When the dyes are added, the flatband potential becomes more positive again, presumably due to dye adsorption at the surface.

The cases of interest are given in Table I, all with 10% $H_2O$, 80% methanol as the solvent.

Using the flatband potential, we can plot the current against the more significant parameter, $V_s$. Below we describe how the currents to the various dye levels are calculated. These currents will be plotted as a function of the surface barrier $V_s$.

Insofar as the current is concerned, we are interested in the current to and from the dye. Possible current flows are indicated

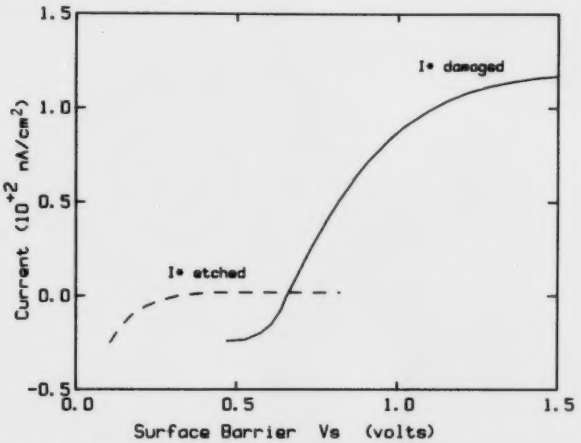


**Figure 8.** Current/surface barrier characteristics of etched vs. damaged ZnO with the excited dye rhodamine B. The current plotted is that calculated as cathodic electron capture on the ground state of the excited dye plus anodic electron injection from the dye excited state.

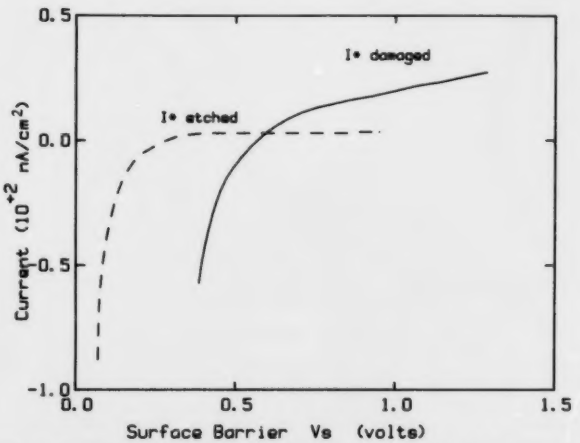


**Figure 9.** Current/surface barrier characteristics of etched vs. damaged ZnO with the excited dye rose bengal. The current plotted is that calculated as cathodic electron capture on the ground state of the dye plus anodic electron injection from the dye excited state.

in Figure 7. In addition to these current flows, there will be a small anodic leakage current of the ZnO Schottky barrier, plus a cathodic current, presumably mostly to reduce protons, and these currents will be observed when the solution is prepared without the dye present (curves A in Figure 1–4).

Thus to obtain the currents shown in Figure 5a, we, in principle, simply subtract the curve A from curve B of Figures 1–4, after replotting these figures as a function of $V_s$. This gives the current

$$I^d = I_a^d + I_c^d \tag{2}$$

To obtain the currents shown in Figure 5b, we simply subtract the current in the dark with the dye present (curve B of Figures 1–4) from the current in the light with the dye present (curves C of Figures 1–4), again after replotting the curves as a function of $V_s$. this gives the current

$$I^* = I_a^* + I_c^* \tag{3}$$

The currents of interest, $I^*$ to the excited dye, are shown in Figures 8 and 9, showing the current with both rose bengal and rhodamine B and comparing the damaged and etched surfaces.

## Discussion

The current to the dye in the dark, $I^d$, is negligible in the anodic direction, and shows a negligible increase compared to the competing cathodic process, presumably proton reduction, in the cathodic direction. This is observed most easily from Figures 1–4, keeping in mind the values of the flatband potential as given in Table I. The problem is that with the estimated probable error in the flatband potential, the analysis by eq 1 has an inherent probable error enough that we can only conclude that very large currents to or from the dye do not flow.

The current $I^*$, calculated from eq 3 and shown in Figures 8 and 9, is of more interest, primarily because the subbandgap light should have no effect on the flatband potential, and to our experimental accuracy, has none. Figure 6 shows the worst case, the damaged surface, and even here the region used to estimate $V_{fb}$ is changed negligibly by illumination. Because $V_{fb}$ does not change, we can first subtract the currents according to eq 3 without being concerned about the flatband potential. The value of $I^*$ is thus relatively reliable. Then we can plot $I^*$ either as a function of applied voltage, or, as shown in Figures 8 and 9, plot it as a function of $V_s$, where now the probable error in $V_s$ is of little concern.

In the anodic direction, highly anodic, it is found that the injection current is surprisingly high for the damaged surface. This is particularly true for the rhodamine B case, as illustrated in Figure 8, and to a certain degree is observed also in Figure 9 for rose bengal. If the energy level for the excited dye were well above the conduction band edge one would expect only minor difference in the electron injection (anodic) characteristics for etched and damaged surfaces. In fact, considering the possibility of the surface helping to deactivate the dye, one could expect a slightly smaller anodic current for damaged surfaces. It is observed, however, that the current is higher by a factor of about 7 in the case of rose bengal and a factor closer to 40 in the case of rhodamine B.

We can conclude that the extra electron injection at the damaged surface is not associated with subbandgap transitions within the zinc oxide. In such a model an electron from a dislocation level could be excited to the conduction band, and the "hole" in the dislocation level could move to the surface and oxidize a nonexcited dye molecule. This would give increased anodic $I^*$. However, in principle, the spectral distribution of the current should have no relation to the spectral response to the dye. However, it was found that the high current associated with damage showed exactly the same spectral characteristics as the rhodamine B dye, indicating that the light of interest is being absorbed not in the space charge region but by the dye itself. Another possible (although not probable) misinterpretation was considered to be that for some reason more illumination penetrated the damaged surface than the etched surface. This was tested by using a silicon photodiode to measure the light passing through the zinc oxide. To the accuracy of the measurment, the light was identical, independent of the small scratches introduced on the zinc oxide surface during abrasion. Finally, it could be suggested (and it is difficult to disprove) that the increased current with the damaged sample could be due to an increase in dye adsorption for some reason. However, such a mechanism involving reactant concentration would be expected simply to increase the current by a constant factor, while the observed increase varies in a strongly voltage-dependent fashion. This would imply that if an adsorption variation is the origin of the difference, then the adsorption must depend on voltage, and depend on voltage differently with dislocations present.

Our suggested model for the effect of dislocations on the anodic photocurrent is that most electrons from the excited dye are at too low an energy for direct injection into the conduction band but they can reach the conduction band via dislocation levels, and that electrons from the conduction band can reach the ground-state levels of the dye (allowing the reaction $e^- + D^* \rightarrow D^-$) via the dislocation levels. Such a model is qualitatively consistent with many of the observations. For example, the indication of a saturation of the cathodic current to the excited dye molecules in the case of rhodamine B (Figure 8) would be consistent with the density of unoccupied ground-state levels being limited. As another example we note the need for a high surface barrier before anodic dye injection currents $I_a^*$ are observed with a damaged

surface. This is due to the high cathodic currents $I_c^*$; $I_a^*$ must be greater than $I_c^*$ before the net current is anodic. The case can be compared with the etched case, where by the model no cathodic current to the ground state of the dye is observed and hence the anodic current begins near the flatband potential, $V_s = 0$.

If we accept the model that the dislocation levels transfer electrons reasonably freely through the Schottky barrier at the surface, the variation of the current with $V_s$ should be interpretable in terms of the density of states of the excited states of the dye. Such an analysis would depend on the cathodic current to the ground state of the dye being independent of bias in the bias range of interest and depend on the assumption that current flow through the dislocations is never rate-limiting in the region of interest. Until such assumptions are shown valid, such an exercise may be premature.

Another way of looking at the competition between the anodic $I_a^*$ and cathodic $I_c^*$ processes is to consider the process as deexcitation of the dye. In other words conceptually we can consider that the particular electron injected by the dye trickles down through the dislocation levels and is emitted cathodically into the ground state of the dye—the dislocations tend to restore the dye to its ground state. By this model dislocations in insulators may also deexcite dyes.

The observation of cathodic current $I_c^*$ to the excited dye is consistent with the observations in the eariler work[1] (where it was concluded that for energy levels deep in the bandgap the current with dislocations present is much higher than for a well-etched surface).

## Conclusions

In general it is observed that surface damage to the solid has a very strong effect on dye sensitization. There is no reason believe this is only true of ZnO; it could be valid for silver photography as well.

The surface damage appears to increase the rate of charge transfer to unoccupied, low energy, ground-state levels, as was suggested also in our recent studies of electron transfer to ions in solution.[1] In the case of rhodamine B on ZnO, damage also appears to increase the rate of electron injection from the excited state, and this observation is interpreted to mean that in the spectrum of excited-state levels, some large fractions are below the conduction band edge. Electrons in such levels can transfer to the conduction band, via the bandgap states due to damage, without surmounting the surface barrier.

**Registry No.** ZnO, 1314-13-2; Rhodamine B, 81-88-9; Rose Bengal, 11121-48-5.

APPENDIX D

# RHODAMINE B-SENSITIZED TIN (IV) OXIDE PHOTOELECTROCHEMICAL CELLS: EFFECTS OF DOPING, HYDROQUINONE, OXYGEN AND METHANOL

J. Hickman, S. Wessel, A. Mackintosh, K. Colbow*

Department of Physics
Simon Fraser University
Burnaby, B.C., Canada
V5A 1S6

*To whom correspondence should be addressed

## ABSTRACT

Rhodamine B-sensitized anodic photocurrents were measured in liquid junction $SnO_2$ semiconducting electrodes. The effects of pH, hydroquinone, oxygen and methanol in the supporting electrolyte solution on the sensitization currents and dark currents were analyzed and compared for doped and undoped $SnO_2$ electrodes. Photocurrents were generally smaller in the doped $SnO_2$ electrodes than in the undoped electrodes, due to a narrow depletion region and impurity states which may give rise to electron back tunnelling. However, the presence of the reducing agent hydroquinone caused photocurrents to be of similar magnitude in the two types of anodes, by preventing back tunnelling in the highly doped $SnO_2$. The presence of $O_2$, an oxidizing agent, suppressed the photocurrent in the undoped electrode, while causing an enhancement of the sensitized photocurrent in the doped electrode, particularly in the presence of 15-25% methanol.

## INTRODUCTION

Wide bandgap semiconductors utilize only a small portion of energy available from the solar spectrum. Thus, there has been much interest in developing solar cells using wide bandgap semiconductors in combination with a dye in aqueous electrolytic solutions, such that absorption of visible light causes electron transfer from the photoexcited dye to the semiconductor. It has been found [1] that the electron transfer between the semiconductor and the dye results from the dye molecules which are adsorbed onto the semiconductor surface, rather than from those in solution.

Some of the most extensive work in this field has been done by Memming et al. [2-5], who studied the photoeffects of dyes such as rhodamine B, eosin and methylene blue at semiconductor electrodes such as ZnO, GaP, SiC, and $SnO_2$, and at Pt and Au metal electrodes [2]. Anodic and cathodic currents were observed with n-type and p-type semiconductor materials, respectively, while the metal electrodes showed a photocurrent only with an additional reducing agent in the electrolytic solution. Memming and Tributsch studied the photoeffects of various dyes adsorbed at p-GaP photoelectrodes [3] and observed cathodic photocurrents, which could be enhanced by oxidizing agents such as $O_2$ and $H_2O_2$. Memming along with other researchers found that anodic currents due to $Ru(II)(bipy)_3^{2+}$ at n-$SnO_2$ and n-SiC

electrodes [4,5] were quenched, and they associated this observation with electron back tunnelling through the thin space charge region of the semiconductor to the solution. Pettinger et al. [6,7] observed this phenomenon with dye at ZnO, as did Nasielski et al. [8], with rhodamine B and hydroquinone at $SnO_2$ and Au electrodes. In addition, Watanabe, Miyasaka, and Honda et al. [9,10] have studied the photoeffects produced by layers of chlorophyll on n-$SnO_2$. They found that the photocurrent could be adjusted by pH, enhanced by reducing agents and suppressed by oxidizing agents.

In this paper, samples of n-$SnO_2$ with conductivities of 300 ohms/square and 30 ohms/square were sensitized in the visible region of the spectrum by rhodamine B. The two samples were compared in terms of photocurrent response, with emphasis on the effects of the additions of hydroquinone, methanol, oxygen, and $O_2$ saturated methanol.

Electrodes consisting of thin films of $SnO_2$ are of special interest, with the recent availability of large sheets coated on glass. These $SnO_2$ surfaces may be used to convert short chain hydrocarbons such as alcohols, alkanes, and alkenes to longer chain hydrocarbons, such as liquid fuels, using electrochemical methods [11,12].

## EXPERIMENTAL

Two different samples were used as anodes; each consisted of a 0.1 um thick film of $SnO_2$ on a 6.4 $cm^2$ sheet of quartz. The $SnO_2$ film was formed by spraying a solution $SnCl_2$ at 450°C, using a method developed in our laboratory (to be patented shortly). The undoped $SnO_2$ film had a sheet resistance of 300 ohms/square, and the fluorine-doped $SnO_2$ had a sheet resistance of 30 ohms/square. Ohmic contacts to the films were made with In-Ga eutectic and Cu wire covered with Electrodag; these metallic contacts were covered with Conap epoxy, to prevent them from coming into contact with the solution. Black wax was used to fasten the prepared samples to electrolyte-containing tubes, leaving exposed a 0.10-0.30 $cm^2$ $SnO_2$ working electrode. A Pt black counter electrode and a Ag/AgCl/saturated KCl reference electrode were used. The incident light was produced by a 75W PEK Xe lamp, and, where applicable, monochromatic light was obtained by using a Jarrell-Ash monochromator. Photocurrents were detected by a PAR lock-in amplifier using incident light chopped at 7 Hz. A Hewlett-Packard X-Y recorder recorded the responses, and a Keithley digital multimeter was used to measure the potentials applied. The method of cyclic voltammetry was used to measure the dark currents, using a PAR Universal Programmer in conjunction with a PAR potentiostat. The

supporting electrolyte in all solutions was aqueous 0.1N $Na_2SO_4$ and, where applicable, the electrolytic solution contained up to 50% reagent grade methanol. Solutions were bubbled with industrial grade $O_2$ or $N_2$, and the dye used was rhodamine B. A Fisher Scientific pH meter was used to monitor the pH. The irradiance of the monochromatic light, measured with a Tektronix digital photometer, was found to be 0.060 $mWcm^{-2}$ at 568 nm, where the rhodamine B photocurrent peak occurred, and 0.005 $mWcm^{-2}$ at 325 nm, which corresponds to the $SnO_2$ bandgap energy.

## RESULTS AND DISCUSSION

Fig. 1 shows the wavelength dependence of the anodic photocurents in $SnO_2$ electrodes, in the presence of rhodamine B. The peak in the ultraviolet region is due to bandgap absorption of $SnO_2$, and the long wavelength peak, caused by electron transfer from the excited dye molecules to the conduction band of $SnO_2$, closely resembles the absorption spectrum of the dye [2,13,14]. The shape of the dye peak is virtually independent of dye concentration, pH, the absence or presence of $O_2$ and methanol, and the sheet resistance of the $SnO_2$ films, but the height of the photocurrent peak depends on all of these parameters.

Fig.1 also shows the enhancement of the dye peak and the suppression of the $SnO_2$ peak by hydroquinone. The increase in sensitized photocurrent due to hydroquinone was found previously by Memming [2] and Gerischer et al. [13,14]. These authors suggested that hydroquinone donates an electron to the groundstate of the excited dye molecule, thereby increasing the probability of electron transfer to the conduction band of the semiconductor. The reduced photocurrent in the high energy photon region is caused by UV absorption of hydroquinone. In contrast, the presence of ferricyanide ions suppresses the photocurrent. Since ferricyanide is an oxidizing agent which

competes with the semiconductor for electrons donated by the excited dye, the photocurrent is thereby suppressed due to the decreased probability of electron transfer to the semiconductor.

Fig. 2 shows the enhancement of photocurrents in the doped and undoped samples of $SnO_2$ by various concentrations of hydroquinone. For both samples, an approximately linear increase in photocurrent with increasing hydroquinone was found for hydroquinone concentrations less than or approximately equal to the dye concentration. For greater hydroquinone concentrations, the photocurrent levels off. This suggests that one hydroquinone molecule is needed to reduce each dye molecule, thus the presence of any excess hydroquinone does not continue to appreciably increase the photocurrent [14].

Several studies on dye reactions at semiconductor electrodes show rapid photocurrent decay within a few seconds [2,5,6,8,13,15], since the dye molecules adsorbed on the semiconductor surface become oxidized and therefore no longer contribute to the photocurrent. One would expect, therefore, that this decay could be decreased by nitrogen bubbling and/or the addition of a reducing agent such as hydroquinone. This was found to be true when tested with the undoped sample, using a rhodamine B concentration of $1.5 \times 10^{-4}$ M. In addition, when the dye concentration was increased by a factor of ten, no time decay of the photocurrent was observed over an observation

period of 16 minutes. This is likely due to the fact that more dye molecules were available to be adsorbed onto the $SnO_2$ surface, resulting in a much slower depletion of reduced dye molecules.

The dependence of the photocurrent on pH is shown for the doped and undoped samples in Fig. 3. The pH was adjusted by dropwise additions of concentrated sulphuric acid or sodium hydroxide. As also reported by Miyasaka et al. [10], the photocurrent curve exhibits a maximum at around pH = 4 to 5, for both samples. At low pH, it is likely that the dye is protonated, since absorbance peaks were suppressed to the same extent as photocurrent peaks. The decrease of the photocurrent with increasing pH is to be expected, due to the adsorption of $OH^-$ ions onto the $SnO_2$ surface. This causes the flat-band potential to change with respect to the energy level of the excited dye, such that as the pH is increased, the excited state of the dye is shifted positively with respect to the semiconductor conduction band. Thus the probability of electron transfer to the semiconductor is decreased, leading to a suppressed photocurrent.

It can also be seen in Fig.3 that the 300 ohm sample shows a higher photoresponse than the 30 ohm sample. This behaviour may be attributed to the fact that in the 30 ohm sample the depletion region is very narrow, and/or contains a large concentration of interbandgap states. This allows a higher

probability of electron back tunnelling through the depletion region of the semiconductor to the solution than is possible in the 300 ohm sample, in which the depletion region is comparatively wide [6]. However, when hydroquinone is present (Fig.2), the photocurrents in the two samples are similar in magnitude. This could be due to the fact that hydroquinone is a strong reducing agent, which, by filling the ground state of the excited dye (as explained earlier), prevents back tunnelling of electrons in the 30 ohm sample, thus no reduction of photocurrent is observed.

A capacitance measurement of the 300 ohm $SnO_2$ electrode, without dye in 0.1 N $Na_2SO_4$, pH = 4.8, gave a flat-band potential of -0.85V vs Ag/AgCl, and a carrier concentration of $10^{19} cm^{-3}$. The same type of measurement was attempted on the 30 ohm sample, but unsuccessfully. It is likely that the Mott-Schottky equation does not hold for this sample, since the capacitance from the Helmholtz layer may not be neglected. Voltage dependent surface states may also interfere.

The IV characteristics of each sample were studied in the dark for integral pH values 1 to 11, varying parameters such as $N_2$ or $O_2$ bubbling, presence of methanol, and presence of dye (Fig.4). The effect of pH (not shown) revealed no change in current features other than a shift of 60 mV/pH unit in current onset, as predicted by the change in flat-band potential with pH. The dark currents in Fig.4 are shown for both samples with

and without $O_2$, dye and methanol for pH = 5 only. It can be seen that for the 300 ohm sample, in the presence of rhodamine B, the dark current does not vary substantially with the presence or absence of $O_2$ and/or $CH_3OH$. The anodic breakdown current occurring at about 2.0V with respect to Ag/AgCl results from $O_2$ production, while the cathodic current at about -0.25V indicates $H_2$ formation, as well as the formation of SnO by reduction. The shift in the anodic breakdown to about 1.2V in the presence of $O_2$ and methanol, without dye, is probably caused by the oxidation of methanol. The oxidation peak at approximately 0 V with respect to Ag/AgCl is likely due to the corrosion of SnO, the presence of which was confirmed by X-ray analysis, in both samples. The identification of this peak was verified by cyclic voltammetry, using a Pt working electrode in the presence of $Sn^{4+}$ ions. The presence of adsorbed rhodamine B or $O_2$ molecules on the $SnO_2$ surface inhibited the oxidation of $Sn^{2+}$ by acting as oxidizing agents, thereby suppressing the anodic current associated with the oxidation of $Sn^{2+}$, as indicated in Fig.4. In addition, the presence of $O_2$ may inhibit the corrosion of $Sn^{2+}$, as indicated by a further reduction in peak height. The negative shift of the corrosion peak without dye is likely due to a shift in flat-band potential.

The dark currents in the 30 ohm sample are also shown in Fig.4. In the presence of rhodamine B, the anodic breakdown current occurs at about 0.5V, which may indicate electron

tunnelling from the dye through the narrow space charge layer to the semiconductor. It is also possible that the adsorbed dye facilitates electron injection into the semiconductor via interbandgap states. Without dye, the breakdown occurs at about 1.5V, due to $O_2$ formation. In the presence of $O_2$ and methanol, however, the breakdown shifts to about 1.3V, due to the oxidation of methanol. This behaviour is similar to that observed in the 300 ohm sample. As expected, the dark current is in general larger in the 30 ohm sample than in the 300 ohm sample, due to its high doping level.

The photocurrent response of each sample due to the presence of rhodamine B was studied as a function of applied voltage, as shown in Fig.5. The samples were illuminated with light of wavelength corresponding to the rhodamine B photocurrent peak. The effects of $O_2$ and methanol on the photocurrents were found to be different for the two samples: while the presence of $O_2$ and methanol substantially reduced the photocurrent in the 300 ohm sample, the same conditions caused the photocurrent in the 30 ohm sample to be increased. In the 300 ohm sample, $O_2$ competes with the semiconductor for the photoexcited electron of the dye, thus reducing the photocurrent. In aqueous solution, oxygen undergoes a two-electron reaction [16]:

$$O_2 + 2e^- + H_2O \longrightarrow HO_2^- + OH^-$$

Thus two dye molecules are generally necessary for the oxygen reduction. The formed $OH^-$ causes the flat-band potential to shift, as can be seen in Fig. 5, also contributing to the lowered photocurrent.

The narrow depletion region and presence of interface states in the 30 ohm sample generally results in a strongly reduced photocurrent. In the presence of $O_2$ and $CH_3OH$, the increased photocurrent may be due to the shift in flatband potential, preventing electron back tunnelling from filling the ground state of the dye. Another factor may be a shift in surface states caused by the strong chemisorption of ions [17] such as the methoxy ion, formed by the reaction:

$$HO_2^- + CH_3OH \text{ ------} > H_2O_2 + CH_3O^-$$

The $CH_3O^-$ ions are extremely reactive, and thus may be strongly adsorbed onto the $SnO_2$ surface. A widely split surface state may result, lowering the probability of electron tunnelling through the $SnO_2$ space charge layer to the surface state. The net anodic photocurrent produced by the injection of electrons from the dye to the conduction band of highly doped $SnO_2$ is therefore not lowered by back tunnelling, but rather is enhanced by a shift in flat-band potential and/or a large shift in surface states.

The dependence of photocurrent on methanol concentration is shown in Fig.6. For the 300 ohm sample, photocurrents are

highest with methanol concentrations of less than 20%, and are suppressed in the presence of $O_2$. Larger concentrations of methanol suppress the photocurrent, since the dye solubility is increased, thereby decreasing its adsorption onto the $SnO_2$ surface. Oxygen alone also suppresses the photocurrent in this sample, due to its tendency to compete with the semiconductor for the electron from the excited dye. The presence of oxygen causes a small increase in photocurrent to be observed for the 30 ohm $SnO_2$, in the presence of rhodamine B and methanol concentrations of 0 to 50% by volume. The photocurrent in this sample seems almost independent of the $CH_3OH$ concentration. This is to be expected, since the effect of electron back tunnelling from the $SnO_2$ conduction band to the ground state of the dye via interbandgap states and surface states is greater than that of the desorption of dye molecules with larger methanol concentrations.

## CONCLUSION

It has been known for some time that greater sensitized anodic currents can be produced in n-type semiconducting electrodes which approach intrinsic purity, than in those which are highly doped. The effects of a reducing agent such as hydroquinone on the sensitized photocurrent have also been established, and it is now apparent from this work that the highly doped, wide bandgap n-type semiconductor $SnO_2$ can effectively be used as a rhodamine B-sensitized photoanode when electron back-tunnelling is prevented by hydroquinone. A similar but much smaller effect is achieved by shifting the flat-band potential in the presence of oxygen, and/or by shifting surface states with strongly adsorbed ions such as methoxy ions. Impurities are often difficult to avoid when films of $SnO_2$ are prepared, thus it is an advantage if such films can be used as photoanodes in the visible region of the spectrum as effectively as intrinsically pure samples.

ACKNOWLEDGEMENT

The authors wish to thank Dr. S.R. Morrison of Simon Fraser University for many valuable discussions.

This work was supported by a grant from the Department of Supply and Services, National Research Council, Ottawa, Ontario, Canada.

## REFERENCES


[1] M. Matsumura, Y. Nomura, H. Tsubomura Bull. Chem. Soc. Japan 50(10) 2533 (1977)

[2] R. Memming Photochem. Photobiol. 16 325 (1972)

[3] R. Memming, H. Tributsch J. Phys. Chem. 75(4) 562 (1971)

[4] R. Memming Surface Science 101 551 (1980)

[5] R. Memming, F. Schroppel, U. Bringmann J. Electroanal. Chem. 100 307 (1979)

[6] B. Pettinger, H.R. Schroppel, H. Gerischer Ber. Bunsenges. 77 960 (1973)

[7] B. Pettinger, H.R. Schroppel, H. Gerischer Ber. Bunsenges. 78(5) 450 (1974)

[8] J. Nasielski, A. Kirsh-De Mesmaeker, P. Leempoel Electrochim. Acta 23 605 (1978)

[9] T. Miyasaka, T. Watanabe, A. Fujishima, K. Honda Photochem. Photobiol. 32 217 (1980)

[10] T. Miyasaka, T. Watanabe, A. Fujishima, K. Honda J. Am Chem. Soc. 100(21) 6657 (1978)

[11] A.A. Adams, R.T. Foley J. Electrochem. Soc. 126(5) 775 (1979)

[12] A.A. Adams, H.J. Barger, Jr. J. Electrochem. Soc. 121(8) 987 (1974)

[13] H. Tributsch, H. Gerischer Ber. Bunsenges. 73(3) 251 (1969)

[14] H. Gerischer, H. Tributsch Ber. Bunsenges. 72(1) 437 (1968)

[15] R. Memming, G. Kursten Ber. Bunsenges. 1 4 (1972)

[16] F. Cotton, G. Wilkinson "Advanced Inorganic Chemistry: A Comprehensive Treatise" p. 410 (1972)

[17] A. Heller, B. Miller "Energy Storage: Transactions of the First International Assembly Held at Dubronic, Yugloslavia" J. Silverman (Ed.) p. 405 (1978)

CAPTIONS

FIG. 1

Quantum efficiency spectral response of the 300 ohm sample, with $1.5 \times 10^{-4}$ M rhodamine B (——); with $1.5 \times 10^{-4}$ M rhodamine B, and $1.5 \times 10^{-4}$ M hydroquinone (— - - —); and with $1.5 \times 10^{-4}$ rhodamine B and 1.5 x 10-4 M $K_3Fe(CN)_6$ (- - - - -). $V_{bias}$ = +0.3V.

FIG. 2

Dependence of quantum efficiency on hydroquinone concentration for the 300 ohm sample (ooo) and for the 30 ohm sample (•••), in the presence of $1.5 \times 10^{-3}$ M rhodamine B. $V_{bias}$ = +0.3V, $\lambda$= 568 nm.

FIG. 3

Dependence of quantum efficiency on pH for an undoped 200 ohm sample (ΔΔΔ), and a doped 30 ohm sample (ooo). [Rhodamine B] = $1.5 \times 10^{-3}$ M, $V_{bias}$ = +0.3V, $\lambda$= 568 nm.

FIG. 4

Dark current as a function of applied potential: (a) 300 ohm sample, no dye, $CH_3OH$ or $O_2$ (——); no dye, with 20% $CH_3OH$ and $O_2$ (- - -); with $1.5 \times 10^{-4}$ M rhodamine B, no $CH_3OH$ or $O_2$ (- - - - -); with $1.5 \times 10^{-4}$ M rhodamine B, 20% $CH_3OH$ and $O_2$ (——). Scan rate = 5 mV/sec, pH = 5.

(b) 30 ohm sample, no dye, $CH_3OH$ or $O_2$ (——); no dye, with 20% $CH_3OH$ and $O_2$ (– – –); with $1.5 \times 10^{-4}$ M rhodamine B, no $CH_3OH$ or $O_2$ (· · · · ·); and with $1.5 \times 10^{-4}$ M rhodamine B, 20% $CH_3OH$ and $O_2$ (– · – · –). Scan rate = 5 mV/sec, pH = 5.

FIG. 5

Dependence of quantum efficiency on applied potential for the 300 ohm sample, no $O_2$ or $CH_3OH$ (– · – · –), 20% $CH_3OH$ and $O_2$ bubbling (– –); and for the 30 ohm sample, no $O_2$ or $CH_3OH$ (——), and 20% $CH_3OH$ with $O_2$ bubbling (– – –). [Rhodamine B] = $1.5 \times 10^{-3}$ M. $V_{bias}$ = +0.3V, $\lambda$ = 568 nm.

FIG. 6

Quantum efficiency as a function of $CH_3OH$ concentration (% by volume) for the 300 ohm sample: $N_2$ bubbling (▲▲▲), $O_2$ bubbling (△△△); and for the 30 ohm sample: $N_2$ bubbling (○○○) and $O_2$ bubbling (●●●). [Rhodamine B] = $1.5 \times 10^{-3}$ M. $V_{bias}$ = +0.3V, $\lambda$ = 568 nm.

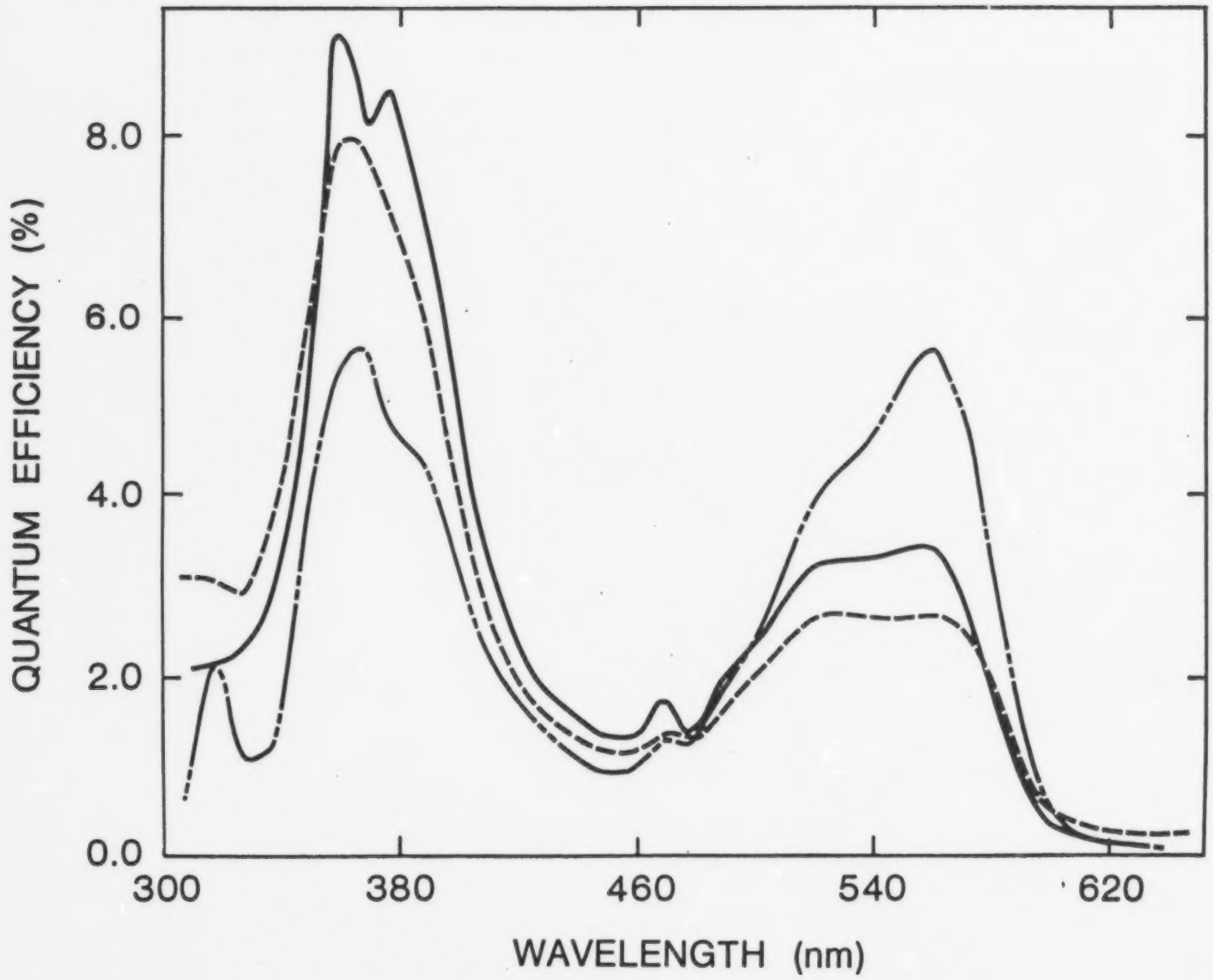
QUANTUM EFFICIENCY (%)
8.0
6.0
4.0
2.0
0.0
300
380
460
540
620
WAVELENGTH (nm)

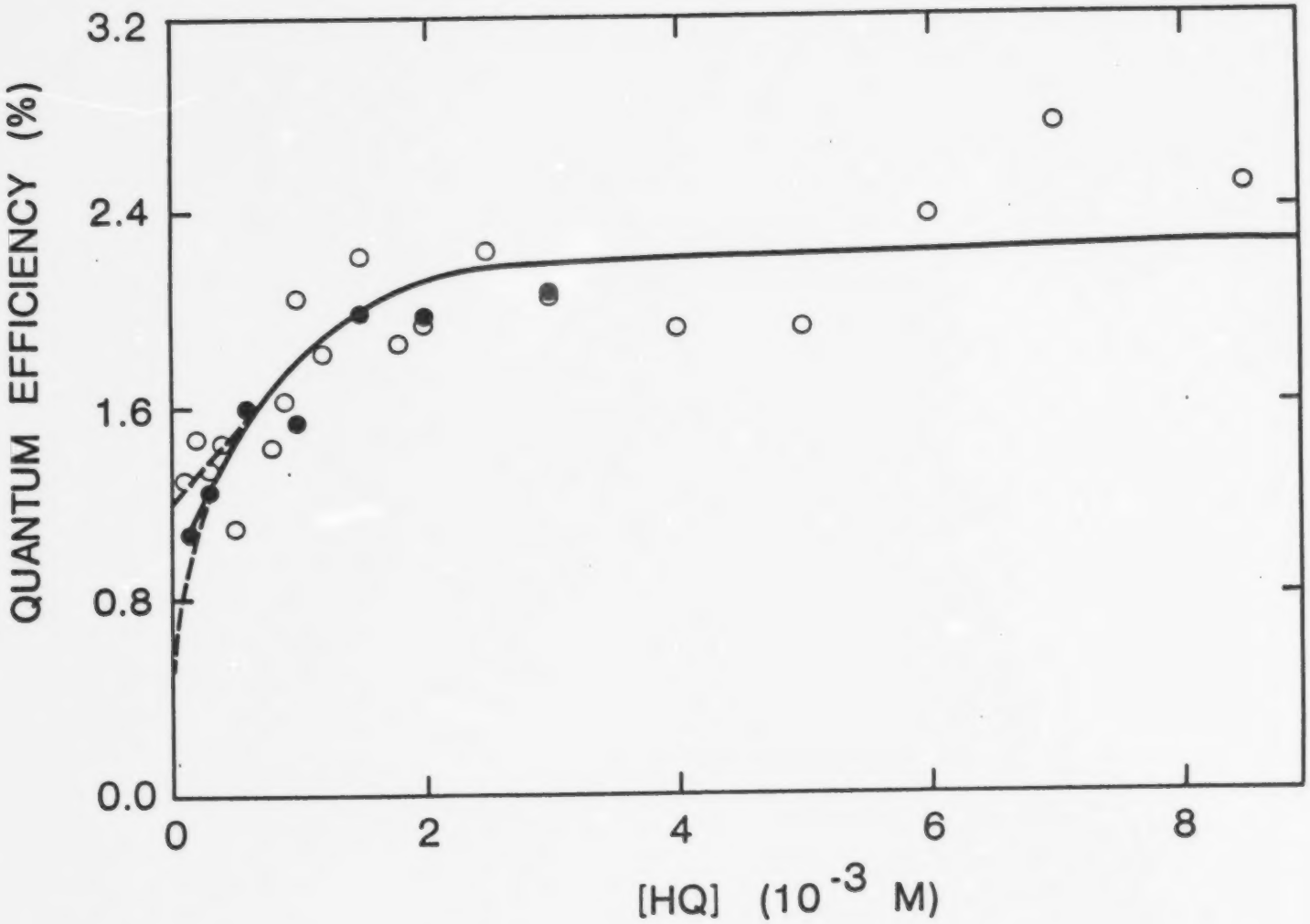
QUANTUM EFFICIENCY (%)
3.2
2.4
1.6
0.8
0.0
0
2
4
6
8
[HQ] (10 -3 M)

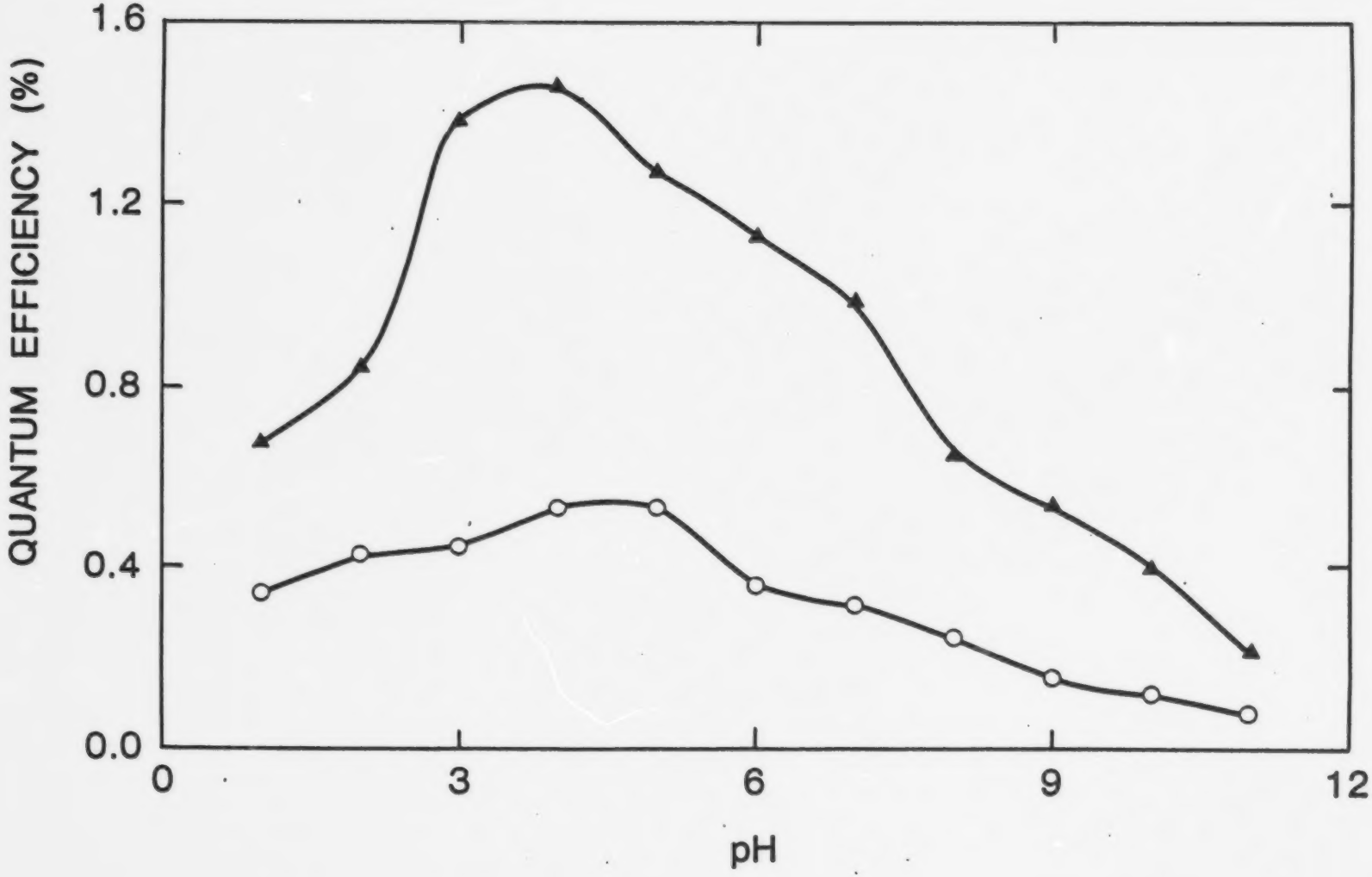
QUANTUM EFFICIENCY (%)
1.6
1.2
0.8
0.4
0.0
0
3
6
9
12
pH

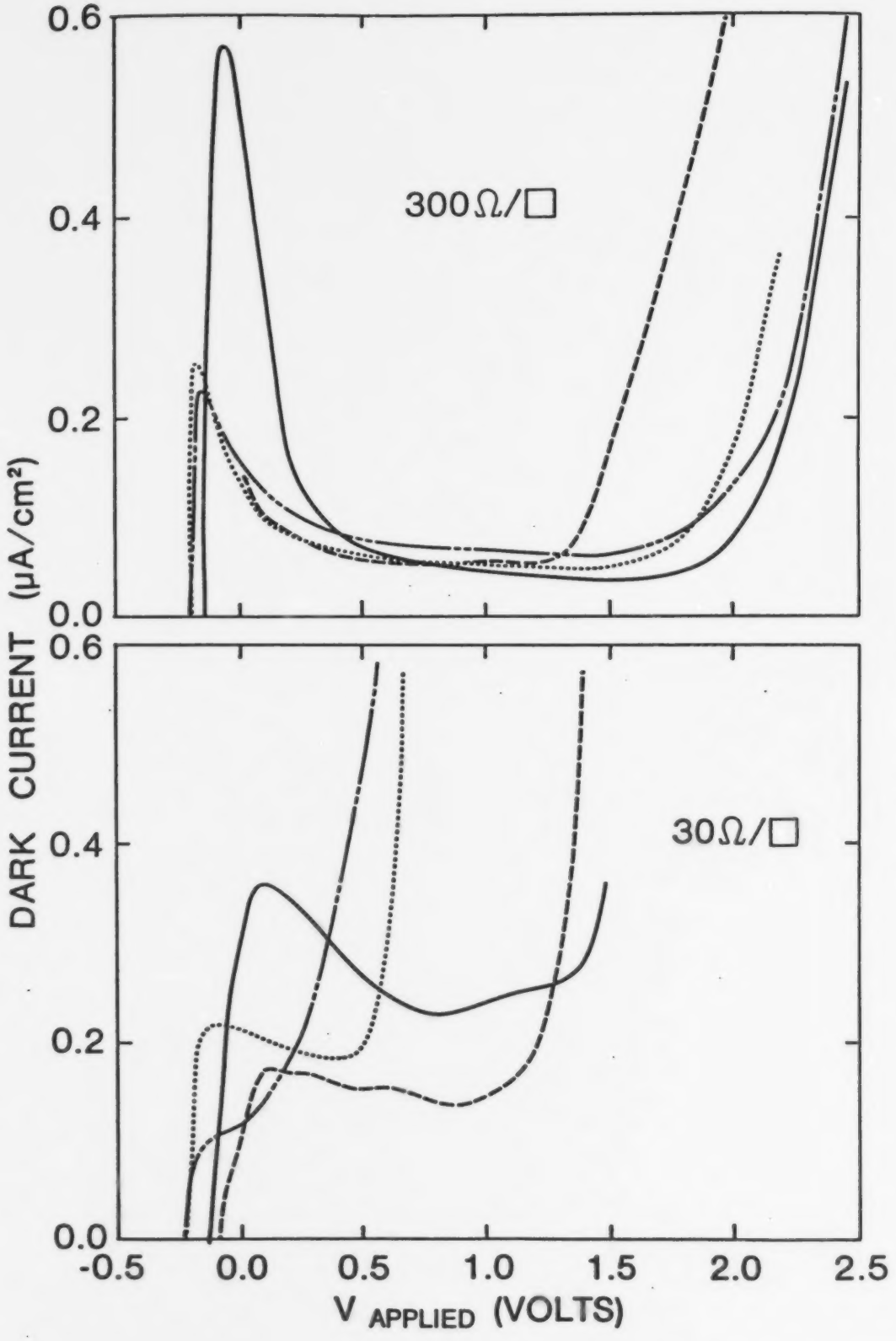
0.6
0.4
0.2
0.0
300Ω/□
0.6
0.4
0.2
0.0
30Ω/□
DARK CURRENT (μA/cm²)
-0.5
0.0
0.5
1.0
1.5
2.0
2.5
V APPLIED (VOLTS)

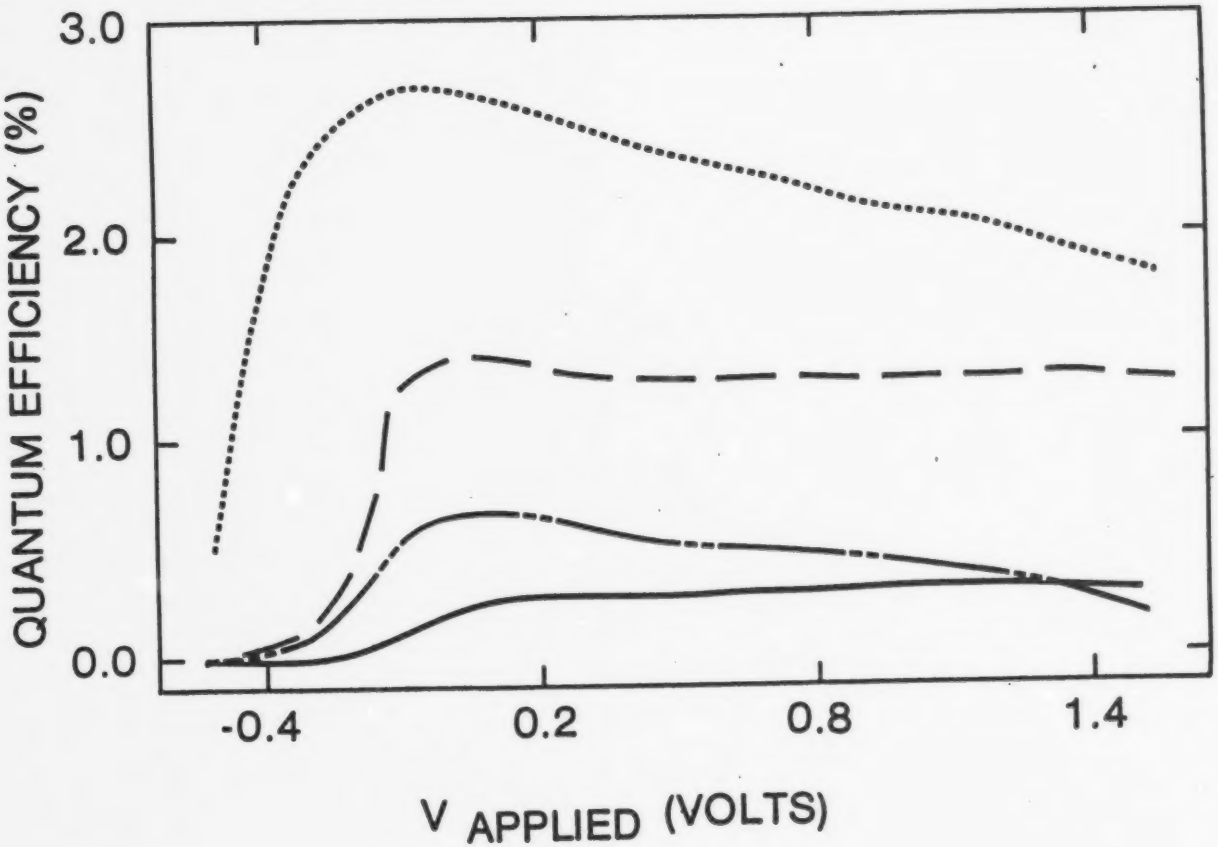
3.0
2.0
1.0
0.0
QUANTUM EFFICIENCY (%)
-0.4
0.2
0.8
1.4
V APPLIED (VOLTS)

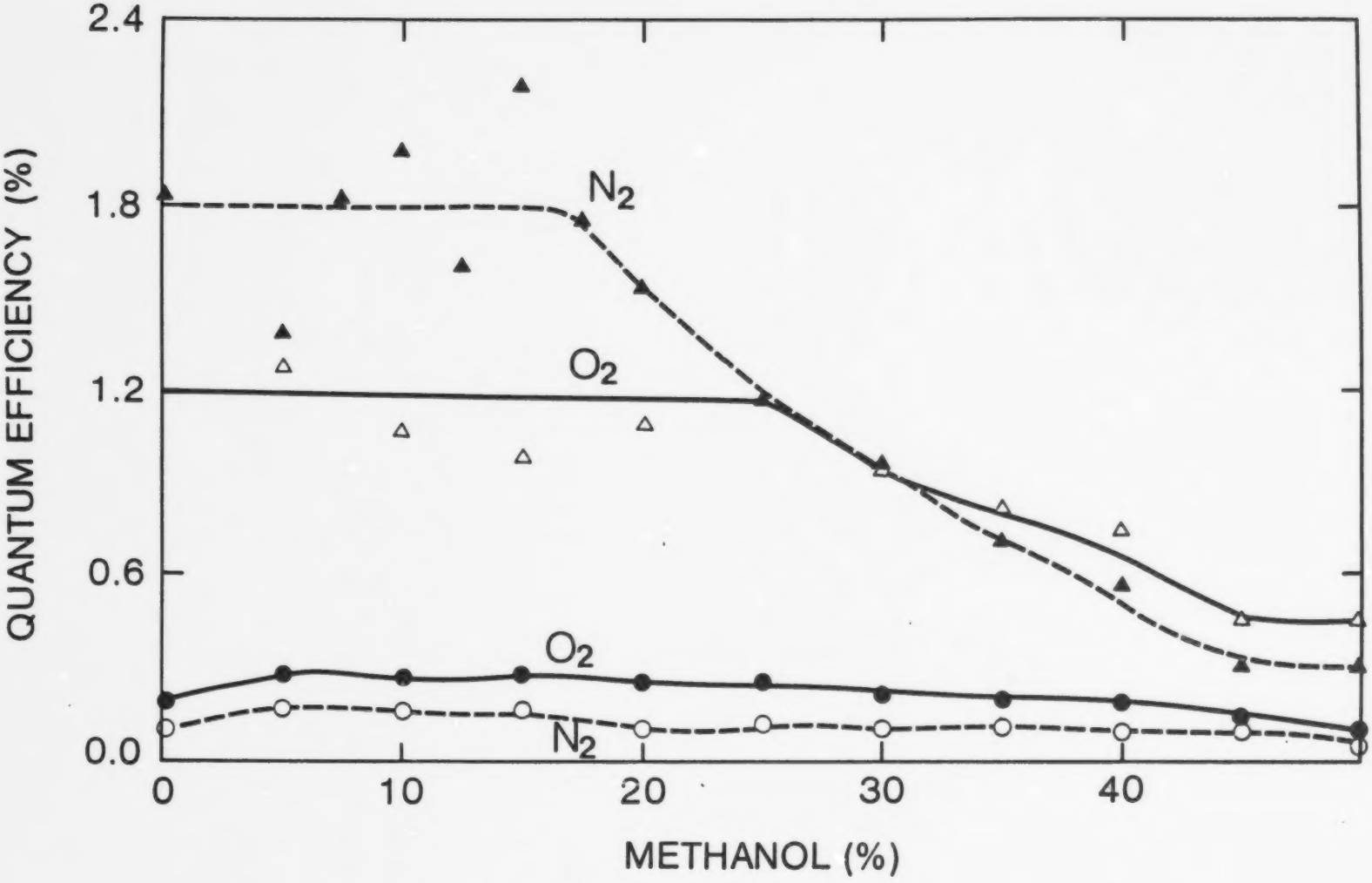
2.4
1.8
1.2
0.6
0.0
QUANTUM EFFICIENCY (%)
N2
O2
O2
N2
0
10
20
30
40
METHANOL (%)

sent to J. Phys. Chem.

APPENDIX E



# CURRENT DOUBLING REACTIONS ON TITANIUM DIOXIDE PHOTOANODES

Norma Hykaway, W.M. Sears, Hiroshi Morisaki*, and S. Roy Morrison

Energy Research Institute, Faculty of Science, Simon Fraser University, Burnaby, British Columbia, Canada V5A 1S6

* on leave from University of Electrocommunications, Tokyo, Japan

Abstract: A model to explain the current doubling mechanism on $TiO_2$ is advanced. This involves both the interaction of holes and cation radicals produced by the holes with the $TiO_2$ band levels, oxidizing agents, reducing agents, and the solvent. This model can be used to explain why current doubling is almost never twice the hole current. In individual experiments it was noted that the amount of current doubling is directly dependent on the degree of doping of the crystal which we relate to tunnelling effects at the conduction band edge. A large number of organic species were observed to produce current doubling on the $TiO_2$ electrode. In the case of methanol the concentration dependence of this current was used to calculate the relative competition for holes of the solvent as well as the ability

of the solvent to react with the cation radical. That is in preference to the radical injecting an electron into the conduction band. Relative capture cross sections of reducing agents (mostly cerous ion) with respect to the current doubling organic compounds were measured by titrating one against the other. In a similar manner the quenching effect of oxidizing agents was also examined although this was much harder to do. The acidity of the solvent was observed to have a big effect on the degree of current doubling which can be related to either increased stability of the cation radical or to hydroxyl surface layer effects. All these effects could easily be explained by the model. A number of synergistic effects which are harder to explain were observed as well. For example the increase in total current with the use of two current doublers bringing the ratio close to two. It was also noted that water added to the acetonitrile solvent usually used decreased the current doubling of methanol but also increased the quenching ability of dissolved oxygen.

# [1] INTRODUCTION AND MODEL

One reason for doing electrochemistry on semiconductor electrodes is the possibility of selective chemical reactions. As the carriers (holes and electrons) enter the solution at the energies of the band edges and not the Fermi level, reactions can occur which are not possible with a metal. One such reaction is the generation of relatively stable radicals that can be detected by current doubling. With n-type $TiO_2$ used as a photoanode highly energetic holes will oxidize species in solution and for some organic species this will produce a cation radical. A number of things can happen to a radical so formed. It can be oxidized by a second hole although the probability of this is low given the low density of photogenerated holes. This is the dominant step at a metal electrode. It can be reduced by a conduction band electron but under reverse bias conditions this is unlikely given the absence of majority carriers at the surface. The radical can and will often inject an electron into the conduction band and thus complete its oxidation. This is the current doubling process as it theoretically doubles the carrier generation from that produced by photon absorption. Finally the radical can react with other species (often oxidizing agents) in solution. The last process will depend on the nature of the solution and

the lifetime of the radical. If the radicals are sufficiently long lived they may have time to undergo all sorts of useful side reactions. A lifetime of up to 0.1 ms has been estimated. (1)

Of interest here is the fact that current doubling never is perfect (ie exactly 2). To understand this we will examine the reactions likely to occur upon hole capture:

$$h^+ + R \xrightarrow{k_1} R^+ \qquad (1)$$

$$R^+ \xrightarrow{k_2} R^{++} + e^- \qquad (2)$$

$$h^+ + X \xrightarrow{k_3} X^+ \qquad (3)$$

$$R^+ + Y \xrightarrow{k_4} Y^- + R^{++} \quad (\text{or } Y^+ + R) \qquad (4)$$

$$h^+ + S \xrightarrow{k_5} S^+ \qquad (5)$$

$$R^+ + S \xrightarrow{k_6} S^- + R^{++} \qquad (6)$$

Here R is an organic species which when oxidized by a hole

will produce an unstable radical, $R^{+}$, leading to current doubling (eq'ns 1 & 2), $R^{++}$ is the stable product(s) of the two-electron oxidation of R, X represents a one equivalent reducing agent ($X^{+}$ is stable) in competition for holes, Y similarly represents a one equivalent species which can react with the radical ($R^{+}$), and finally S represents a zeroth order competition for holes involving the solvent or electrolyte. We are ignoring any side reactions (such as $X^{+} + R \Rightarrow R^{+} + X$) as unimportant. One case of this reaction has been observed and will be reported below.

If we assume the reaction rates are first order in reactant concentration (no adsorption) with the exception of eq'ns 5 and 6 where we assume zeroth order in S, the above can be rewritten as currents in the form:

$$J_R^{\circ} = k_1 [h^{+}] [R] \qquad (7)$$

$$J_R^{e} = k_2 [R^{+}] \qquad (8)$$

$$J_X = k_3 [h^{+}] [X] \qquad (9)$$

$$J_R^{Y} = k_4 [R^{+}] [Y] \qquad (10)$$

$$J_S = k_5 [h^{+}] \qquad (11)$$

$$J_R^{B} = k_6 [R^{+}] \qquad (12)$$

where the total hole current is defined by:

$$J_h = J_R^{\circ} + J_x + J_B \qquad (13)$$

and the three possible paths of the radical give:

$$J_R^{\circ} = J_R^{e} + J_R^{Y} + J_R^{B} \qquad (14)$$

Combining eq'ns 7,9,11 and 13 we can obtain:

$$\frac{J_h}{J_R^{\circ}} = 1 + \frac{k_3\,[X]}{k_1\,[R]} + \frac{k_5}{k_1\,[R]} \qquad (15)$$

and combining eq'ns 8, 10, 12 and 14 we obtain:

$$\frac{J_R^{\circ}}{J_R^{e}} = 1 + \frac{k_4\,[Y]}{k_2} + \frac{k_6}{k_2} \qquad (16)$$

Finally combining eq'ns 15 and 16:

$$\frac{J_h}{J_R^{e}} = \left(1 + \frac{k_3\,[X]}{k_1\,[R]} + \frac{k_5}{k_1\,[R]}\right)\left(1 + \frac{k_4\,[Y]}{k_2} + \frac{k_6}{k_2}\right) \qquad (17)$$

where both $J_h$ and $J_R^{e}$ are easily measured quantities.

A number of points can be made concerning this equation. First we can calculate the maximum possible current doubling ratio by setting [X] = 0 and taking the

limit as [R] approaches infinity. This gives:

$$\text{Ratio} = \frac{J_n}{J_n} = \frac{2 + Z}{1 + Z} \qquad (18)$$

where $Z = \frac{k_4 [Y]}{k_2} + \frac{k_6}{k_2}$

This gives the lowering of the current doubling caused by an oxidizing agent, Y, in solution. It can also be used to explain why the current doubling ratio is never 2 if we consider eq'n 6 to be any process that prevents the radical from injecting an electron into the conduction band, for example, a reaction with the solvent or simply the desorption of the radical and its movement away from the electrode.

The effects of eq'n 17 involve four terms or ratios. The first ($1 + k_3 [X] / k_1 [R]$) gives the effect of adding a reducing agent to a current doubling solution. The effect has been examined in a number of publications (2-5) and is a method of measuring relative hole capture cross sections. The second term ($k_5 / k_1 [R]$) gives the effect of zeroth order oxidation when the concentration of R is relatively low but has no effect at saturation (of current doubling). (3) The third term ($1 + k_4 [Y] / k_2$) as mentioned gives the effect of an added oxidizing agent. The effect differs from that of the reducing agent only in being independent of the concentration of the current doubler. This is in contrast to

"gamma"

the empirical equation for "quenching" reported in reference 4 ($J_R^e / J_h = 1 - \gamma[Y]$). This discrepancy can be explained by replotting their data (in Figure 4 reference 4) as $J_h / J_R^e$. Doing this we notice that the first six data points follow the straight line expected from eq'n 17 whereas the remainder show a sharp deviation due perhaps to optical absorption or a chemical reaction. The final term ($k_4 / k_2$) represents all zeroth order effects on the radical which tend to limit the current doubling.

In the experiments to be reported here current doubling measurements were used to follow the reaction of the holes from $TiO_2$, to determine doping effects, to determine relative capture cross sections of various reducing agents, to determine the effect of the solvent on the reactivity of species in solution, and the effect of generated radicals on oxidizing agents in solution.

The ultimate objective of the program of which this is the first phase, is improved understanding and control of radical generation and radical reactions where the radicals are formed by holes from $TiO_2$.

## [2] EXPERIMENTAL

Samples of $TiO_2$ were cut directly from a single crystal boule which was aligned using X-rays (via Laue photographs). This allowed us to specify the crystallographic plane of the electrode used such as <100>, <110> and <001> to about 2 degrees.

Two different methods were used to dope the samples, involving Nb or $H_2$. For both cases the crystal slices were first mechanically polished using fine emery paper. Some were then coated with Nb metal using a vapor transport technique. An evacuated quartz tube containing the $TiO_2$ crystal and 0.1 g Nb powder was back filled with bromine to a pressure of 250 torr. With the Nb at 1000 $^{o}$C and the $TiO_2$ at 950 $^{o}$C the transport occured over a period of 2 days. The crystal was then removed and oxidized (pure oxygen flow or room air) at temperatures from 950 $^{o}$C to 1200 $^{o}$C for up to 3 hours. The sample was repolished (mechanically) and then chemically etched in molten NaOH at 400 $^{o}$C for 2 hours. Finally after rinsing in distilled water the crystal was hung in a concentrated nitric acid solution overnight which produced a shiny surface.

The rest were doped with hydrogen gas (5% and pure) from 600 to 700 $^{o}$C for one hour. In this case the chemical etch was done first.

Ohmic contact was made by annealing in indium metal and the electrode was finally masked with RTV self-leveling silicone. It was found that a final photoetching (6) was often necessary before current doubling measurements were done. This was accomplished under strong ultraviolet light in a solution of 2% $H_2SO_4$ plus 6% $CH_3COOH$ as will be discussed in more detail in the next section.

The $TiO_2$ electrode was mounted in a specially designed glass cell which contained a quartz widow to allow illumination of the sample with ultraviolet light (the bandgap of $TiO_2$ is about 3 eV). The pathlength of the light between window and electrode was kept less than 2 mm. A standard calomel electrode was used as reference and separated from the main chamber by a fine glass frit. Platinum was used as a counter electrode and provision was made for nitrogen and oxygen purging of the solution. A low pressure 5 W mercury lamp was used to provide the ultraviolet light for most of these experiments.

Standard electronics (interfaced to an IBM PC data acquisition system) was used to obtain the D.C. and A.C. characteristics of the anode. Specialized software has been developed at the institute to obtain real time Mott-Schottky and IV data.

Reagent grade chemicals were used in these experiments with the acetonitrile solvent normally used nominally containing from 0.01 to 0.03 % water impurity.

## [3] RESULTS

In the following experiments no consistent effect was observed due to the different crystal planes used despite the fact that in the <001> direction channeling of dopant atoms is expected to occur. (7)

Doping: The method used to dope the $TiO_2$ with Nb usually produced highly conductive crystals. However it was noticed that when the polished sample was reheated in oxygen that it became insulating again accompanied by a reversion to the original clear colour of undoped $TiO_2$ (doped samples are blue to black). This implies that the doping is not accomplished by the diffusion of Nb atoms as was originally hoped. Attempts to diffusion the Nb in at 1200$^{o}$C did seem to work but unfortunately also caused the crystal to become very brittle. We therefore conclude that the crystals used here (where about 1000$^{o}$C diffusion was attempted) where doped by oxygen vacancies caused by the surface layer of Nb metal. Reoxidation at this temperature allowed the oxygen vacancies to rapidly diffuse out again.

Figure 1 shows the effect of doping levels on the methanol current doubling ratio. The lower points represent hydrogen doping whereas the higher are Nb (Oxygen vacancy). This effect can be thought of in terms of eq'n 18 as a

competition for the current doubling radical's spare electron.

It was found in line with other publications (8-13) that surface preparation is an important factor in obtaining good current doubling results. It was found here that effects of added oxidizing agents on the current doubling ratio were even more sensitive to surface quality. Therefore in our measurements the $TiO_2$ electrodes were not only mechanically polished and chemically etched but were photoetched at current levels of about 0.5 mA/cm$^2$ (+3 V bias) for an hour.

Flatband Potential: Figure 2 shows the results of Mott-Schottky plots obtained with one of our samples. Because of the high capacitance we were limited to frequencies less than 2 kHz. Except for this loading of the electronics no appreciable dispersion was noticed. For the sulfuric acid solution a flatband potential of -0.33 V SCE and for the acetonitrile solution a value of -0.68 V SCE is obtained. If we assume the difference in pH between these solutions to be 6 this amounts to 58 mV/pH. This is in good agreement with literature values. (9,14-17) Assuming a dielectric constant of about 100 (9) the doping level of this crystal is about $1 \times 10^{19}$ cm$^{-3}$. From this we can then conclude that the conduction band of $TiO_2$ will lie at about -0.7 V and the valance band at about +2.3 V in a acetonitrile solution.

Although no shifts in the flatband potential were

noticed as a function of solvent except for these effects ascribed to pH we did observe sizable shifts for the onset of saturation photocurrent. Figure 3 shows these shifts for a few of the solutions used where the current (normalized to the value at saturation) is plotted against the voltage shift from flatband at the pH of the solution. This may be related to the ease with which the various solvents or reagents are oxidized. In the case of HCl presumably the chloride is oxidized and in the case of $H_2SO_4$ presumably the $TiO_2$ is corroded. Most of the organics dissolved in acetonitrile show the same photocurrent/voltage characteristics as methanol.

Current Doublers: Figure 4 shows the typical current doubling effect when methanol is added to the acetonitrile solvent under illumination. Similar curves are seen for a number of organics and solvents although absorption of the ultraviolet illumination often obscures the effect. (3,13,18,19) The figure also shows the effect of adding an oxidizing agent to the solution which can also represent the reduction caused by the addition of a reducing agent (see Sec I).

Current doubling has been observed with methanol, ethanol, 1-propanol, 2-propanol, 1-butanol, 2-butanol, iso-butyl alcohol, ethylene glycol, formic acid, ferrocene, ~~triethyl amine~~, dimethyl formamide, and glyoxal. It has not been seen with acetic acid, acetone, ethyl acetate, acrylamide, toluene, phenol, naphthalene, glycerol, quinones,

dichloromethane, 1-pentene, acetaldehyde, thianthrene, or triethylamine.

If we measure the added current, $J_R e$, as a function of methanol concentration we obtain the plot in Figure 5. This should follow eq'n 17 for [X] = 0. The intercept (1.41) gives us a current doubling ratio (eq'n 18) of 1.71. From the slope we can obtain the ratio ($k_5/k_1$) equal to $1.47 \times 10^{-2}$ M. This is the extent to which the zeroth order reaction competes for holes.

Capture Cross-Sections: If we were then to add a strong reducing agent, [X], to the solution we would obtain a curve as in Figure 6 where cerous ions (cerous nitrate) are titrated to a constant concentration of MeOH (0.246 M). A pool of amalgamated zinc was used at times to guarantee that the lowering of the current was not due to ceric ions. Eq'n 17 can again be used to describe this data assuming we can neglect the zeroth order term since [R] is large. As before the intercept gives the current doubling ratio (intercept = 1.51, ratio = 1.66). From the slope we can obtain the ratio $k_3/k_1$ which is the ratio of hole capture cross sections of the two reagents (assuming as always no adsorption). The value is here about 1500 although this ratio will vary about a factor of two from crystal to crystal and with time (aging of the crystal). The $k_5/k_1$ value was more stable although occasional aging effects were seen.

Titrations were also done using some of the other

current doubling organics with cerous or ferrous ions. The values obtained for ethanol, 1-propanol, 2-propanol, 1-butanol, 2-butanol, and iso-butyl alcohol were indistinguishable from those obtained for methanol. The value for ethylene glycol was difficult to obtain as it reacts with ceric ions (a mixture of ceric ammonium nitrate and ethylene glycol changes colour with time) but the ferrous titration gave a value consistent with that of methanol.

Another way that this titration can be done is by varying the amount of MeOH added to a fixed concentration of cerous ion and relating this to eq'n 17 as before. The zeroth order term will have a negligible contribution for the concentration of cerous ion ([X]) used. Figure 7 shows this plot where the intercept (1.70) gives a current doubling ratio of 1.59 and the slope gives a $k_3/k_1$ value of 540 for a cerous concentration of $3.92 \times 10^{-3}$ M. This value for the ratio seems to be consistently lower than for the case of cerous variation.

Other Observations: Synergistic effects were observed when other species were added to MeOH in acetonitrile solution. In general three types of behavior resulted; the additive had no effect, it lowered the current, or raised it. No effect (and no independent current doubling) would mean no interaction with holes from the $TiO_2$ or with radical species formed with the holes. If the current is lowered by a non-current doubler than we assume competition for holes. The

third effect must involve complicated cross reactions. Acetaldehyde, acetic acid, acetone, and dichloromethane when added to the solution were inactive. Dimethylformamide, triethylamine, and most strong reducing and oxidizing agents showed competitive effects. Finally 2-butanol, formic acid, and ethylene glycol showed a cooperative effect with methanol by increasing the current doubling ratio close to 2.

Because cation radicals are normally more stable in more acid organic solvents, a series of solvents was examined and both the current doubling and the relative capture cross-sections ($k_3/k_1$) were tested as a function of solvent characteristics. The Table shows the results of these measurements. The second column shows the donor number of some of the solvents (20), the third shows the amount of current doubling observed with MeOH, and the remaining columns show the capture cross-sections for various species relative to MeOH. The list of solvents increases in acidity travelling up the table. Both the current doubling ratio and the cerous cross section increases with the acidity of the solvent.

Radical Reactions: In Figure 4 we saw the effect of an oxidizing agent (dissolved $O_2$) on current doubling, presumably occurring through a radical reaction (eq'n 4). In applying eq'n 17 to this observation we can rewrite it as:

$$F = 1 + \frac{k_4 [Y]}{k_2} + \frac{k_5}{k_2} \qquad (19)$$

where $F = J_h/J_R^e$ and $k_4/k_2$ is the unknown factor limiting the current doubling even when [Y] is zero. We are, as before, also assuming that [X] is zero and [R] is large. Values of $k_4/k_2$ for typical current doubling ratios are 0.05 for 1.95, 1.00 for 1.5, and 9.00 for 1.10.

The difference in F values for $O_2$ purging and $N_2$ purging gives $k_4$ [Y] / $k_2$ = 0.73 for a crystal where this effect was large and 0.25 for a crystal where it was not.

For added p-benzoquinone ($6.7 \times 10^{-4}$ M) we get $k_4$ [Y] / $k_2$ = 1.0 after correcting for absorption of the ultraviolet light. This also gives $k_4 / k_2 = 1.5 \times 10^3$ $M^{-1}$ which is the relative competition of quinone and the conduction band to oxidize the radical.

When we attempted to use ceric ion (ceric ammonium nitrate) as an oxidizing agent we found that it underwent a photochemical reaction (possibly with the solvent) under ultraviolet illumination. The solution originally yellow became clear.

The competition for the radical's electron we found was very sensitive to the quality of the crystal surface (re. polishing and photoetching) and the above experiments were very difficult to reproduce.

It was found that adding water to the solvent (acetonitrile) reduced the amount of current doubling in methanol. From an initial value of 1.82 ($k_4/k_2$ = 0.22) in a

solvent with very little water, we observed a value of 1.70 ($k_4/k_2$ = 0.42) in 0.56 M water and 1.31 ($k_4/k_2$ = 2.19) in 2.2 M water. The water may simply compete for holes or the effect may be much more complex involving competition for the radical. The addition of water also had an influence on the ability of dissolved oxygen to react with the current doubling electron. Comparing $k_4$ [Y] / $k_2$ values we have 0.27 for the solvent with very little water (similar to above), 1.1 for 0.56 M water, and 1.6 for 2.2 M water. These synergistic effects are much more complicated than can be deduced from eq'ns 17 or 19.

## [4] DISCUSSION

The increase in current doubling with doping displayed in Figure 1 is most likely due to tunnelling effects. At high doping levels the space charge region is very narrow and the resultant band bending makes it possible to inject electrons below the conduction band edge. This would improve the $TiO_2$ crystal's ability to compete for electrons from the radical.

To understand Figure 3 which shows various onset potentials for different solutions we must realize that in $TiO_2$ the holes do not necessarily enter the solution directly from the band edge. Imperfection sites near the surface of the electrode will allow them to enter with a less positive energy. As the bias is increased (made more positive) the states will fill up with photogenerated carriers making the surface positively charged (if the species in solution are difficult to oxidize) leading to a modification of the Helmholtz layer that raises the energy level of species in solution relative to the energy level of the surface states. Thus the energy of the holes being injected into the solution will effectively increase. Given that various solvents and oxidizable species in solution will have different reducing powers (determined by their energy levels in the solution) we are led to the voltage dependence seen in Figure 3.

Figures 5 to 7 show the applicability of eq'n 17 in describing the underlying mechanism for current doubling on $TiO_2$. However the synergistic effects with water, oxygen, the other solvents mentioned, and possably the low slope of Figure 7 show that it is not the whole story and that complex cross reaction may also be going on.

We also noticed that current doubling depends on the acidity of the solvent, the lower the donor number (more acidic) the higher the current doubling ratio. There are two possible reasons for this effect. One is based on the stability of cation radicals, which are increasingly stable the more acid the solvent. The other is based on the removal of the hydroxyl layer from the $TiO_2$ surface with acid solvents. Consider first the effect of acid solvents on the stability of cation radicals. Hole capture presumable leads to cation radicals, in general, and if we assume they are the injecting species then the longer lived radicals have a greater probability of injecting the unpaired electron before reacting with the solvent. The reaction of the cation with the solvent may be the ultimate limitation on current doubling in a given solvent, and such a reaction may be the reason why "perfect current doubling" is seldom seen. Other limitations could be provided by reactions with impurities, corrosion of the crystal, or at low bias hole-electron recombination.

In the case involving the hydroxyl layer occupying basic sites on the $TiO_2$ surface we might write

$$h^+ + Ti^+OH^- \Rightarrow Ti^+ + OH \qquad (20)$$

$$OH + CH_3OH \Rightarrow H_2O + CH_3O \qquad (21)$$

and then either

$$CH_3O \Rightarrow CH_2O + H^+ + e^- \qquad (22)$$

or the neutral radical reacts with the solution. With fewer basic hydroxyl ions on the surface the reaction would likely be direct.

$$h^+ + CH_3OH \Rightarrow (CH_3OH)^+ \qquad (23)$$

If the cation radical in eq'n 23 is more likely to inject electrons, and also more stable in acid solution, than the neutral radical in eq'n 21 we will observe improved current doubling in increasingly acid solutions.

The increase of relative capture cross section for cerous ions (see the Table) may also be understood if eq'n 20 represents a more vigorous reaction than eq'n 23.

In conclusion, the measurement of current doubling is a first simple step toward the understanding of reactions of holes from semiconductors with organic molecules in solution. We have shown that the stability of the radicals produced and the hole reactivity of the molecules in solution depends

strongly on such factors as the acidity of the solvent, the doping level of the electrode, and synergistic effects when in complex solutions. We have also presented a model for the current doubling mechanism which explains why perfect current doubling is seldom observed, based on cation radicals as the injecting species.

Acknowledgements: We would like to thank Yutaka Harima for valuable discussions on the current doubling process. The financial help of a CANMET grant from Energy Mines and Resources, Canada is acknowledged.

## REFERENCES

(1) Von J. Lilie, G. Beck and A. Henglein, Berichte der Bunsen-Gesellshaft 75, 458 (1971).

(2) E.C. Dutoit, F. Cardon, and W.P. Gomes, Berichte der Bunsen-Gesellschaft 80, 475 (1976).

(3) E.C. Dutoit, F. Cardon, and W.P. Gomes, Berichte der Bunsen-Gesellschaft 80, 1285 (1976).

(4) W.P. Gomes, T. Freund, and S.R. Morrison, J. Electrochem. Soc. 115, 818 (1968).

(5) W.M. Sears and S. Roy Morrison, J. Phys. Chem., 88, 976 (1984).

(6) A. Praet, F. Vanden Kerchove, W.P. Gomes, and F. Cardon, Solar Energy Materials 7, 481 (1983).

(7) J.B. Bates, J.C. Wang, and R.A. Perkins, Phys. Rev. B 19, 4130 (1979).

(8) M.A. Malati and W.K. Wong, Surface Tech. 22, 305 (1984).

(9) H.D. Finklea, J. Electrochem. Soc. 129, 2003 (1982).

(10) L.A. Harris and R.H. Wilson, J. Electrochem. Soc. 123,1010 (1976).

(11) Fu-Tai Liou, C.Y. Yang, and S.N. Levine, J. Electrochem. Soc. 130, 893 (1983).

(12) H.S. Jarrett, Phys. Rev. Lett. 54, 217 (1985).

(13) Y. Nosaka, H. Sasaki, K. Norimatsu, and H. Miyama, Chem. Phys. Lett. 105, 456 (1984).

(14) M. Abe, H. Morisaki, and K. Yazawa, Jpn. J. Appl. Phys. 19, 1421 (1980).

(15) K. Kinoshita and M.J. Madou, J. Electrochem. Soc. 131, 1089 (1984).

(16) G. Nogami, J. Electrochem. Soc. 132, 76 (1985).

(17) J.R. Wilson and Su-Moon Park, J. Electrochem. Soc. 128, 2369 (1981).

(18) H. Yoneyama, Y. Toyoguchi, and H. Tamura, J. Phys. Chem. 76, 3460 (1972).

(19) Y. Maeda, A. Fujishima, and K. Honda, J. Electrochem. Soc., 128, 1731 (1981).

(20) "Experimental Electrochemistry for Chemists", Donald T. Sawyer and Julian L. Roberts, Jr., John Wiley & Sons, New York, 1974, pp 172-175.

## FIGURE CAPTIONS

FIGURE 1

Current doubling ratio of 1 M methanol in a 0.1 M tetra-n-butylammonium perchlorate (TBAP) / acetonitrile (AN) solution versus doping concentration of n-type $TiO_2$

FIGURE 2

Mott-Schottky curves for a $TiO_2$ electrode

(A) 0.1 M TBAP in AN at 500 Hz

(B) 0.5 M $H_2SO_4$ at 500 Hz

(C) 0.5 M $H_2SO_4$ at 1000 Hz

(D) 0.5 M $H_2SO_4$ at 2000 Hz

FIGURE 3

Normalized photocurrents of a number of solutions versus voltage shift from flatband

(A) 0.3 M HCl

(B) 0.5 M $H_2SO_4$

(C) 1 M MeOH (0.1 M TBAP in AN)

(D) 0.1 M TBAP in AN

FIGURE 4

Current doubling on a $TiO_2$ electrode

(A) 0.1 M TBAP in AN (dark)

(B) under Hg lamp illumination

(C) plus 0.5 M MeOH and nitrogen purging

(D) plus 0.5 M MeOH and oxygen purging

FIGURE 5

Effect of MeOH concentration, [R], on $TiO_2$ current doubling in a 0.1 M TBAP / AN solution (slope = $2.07 \times 10^{-2}$ M, intercept = 1.41)

FIGURE 6

Effect of cerous nitrate concentration, [X], on $TiO_2$ current doubling in a 0.1 M TBAP / AN solution with MeOH, [R], held constant at 0.246 M (slope = $2.21 \times 10^{3}$, intercept = 1.51)

FIGURE 7

Effect of MeOH concentration, [R], on $TiO_2$ current doubling in a 0.1 M TBAP / AN solution with cerous nitrate, [X], held constant at $3.92 \times 10^{-3}$ M (slope = $9.14 \times 10^{2}$, intercept = 1.70)

TABLE 1 Effect of solvent on current doubling with $TiO_2$ electrodes

| Solvent | Donor # | C.D. | $k_3$ (Ce) | $k_3$ (Fe) | $k_3$ (Th) |
|---|---|---|---|---|---|
| Dichloromethane | ---- | 1.9 | 14000 | | |
| Acetonitrile | 14.1 | 1.75 | 1460 | 3.6 | 88 |
| Acetone | 17.0 | 1.4 | 600 | | |
| Water | 18.0 | 1.5 | | | |
| Dimethylformamide | 26.6 | 1.0 | | | |

note: the C.D. values are for MeOH, $k_1$ (MeOH) is set equal to 1, Th = Thianthrene, Fe = Ferrous, Ce = Cerous, a lower donor number implies a more acid solvent, and the electrolyte used was tetra-n-butylammonium perchlorate for all solvents

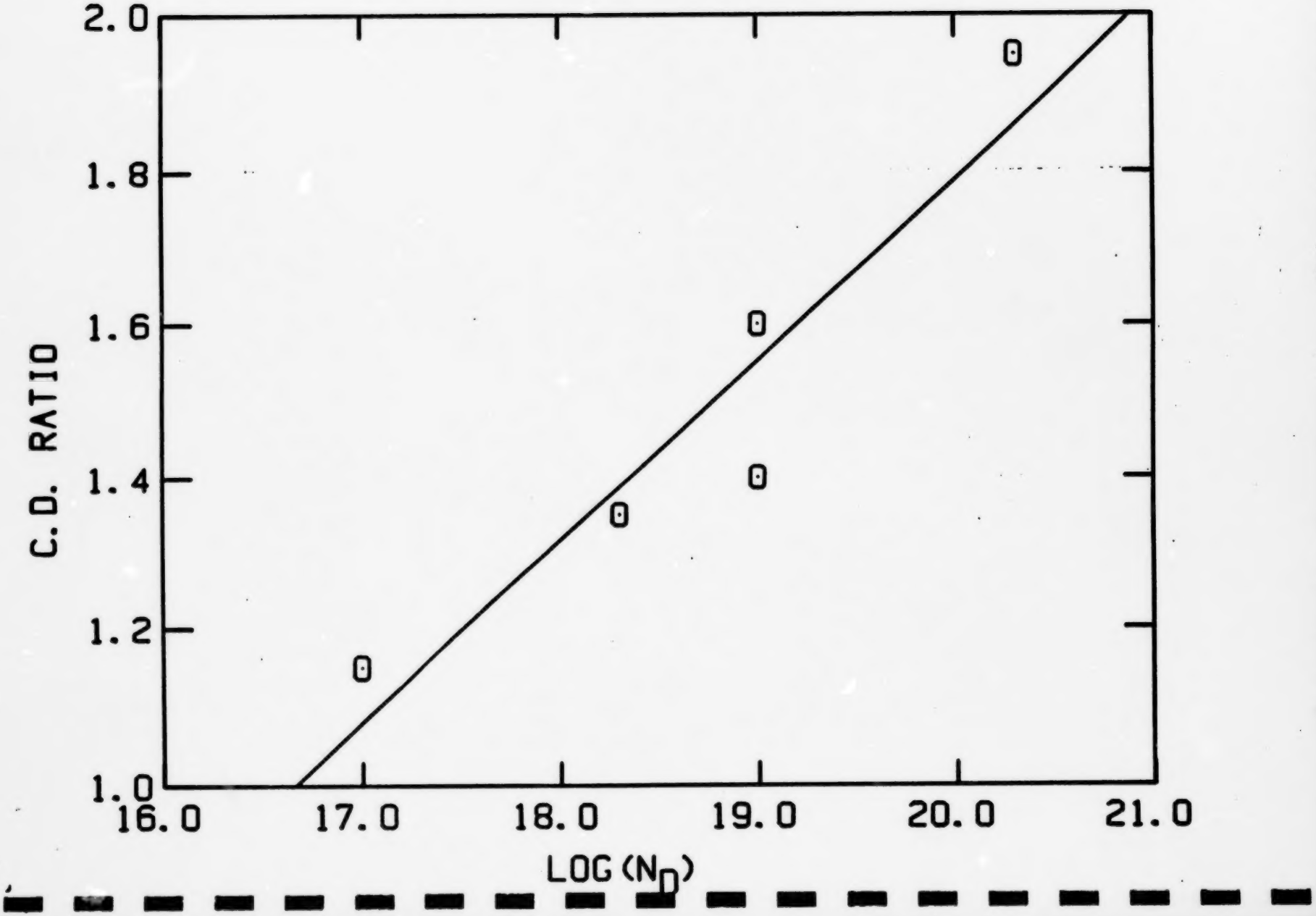
2.0
1.8
1.6
1.4
1.2
1.0
C.D. RATIO
16.0
17.0
18.0
19.0
20.0
21.0
LOG (N_D)

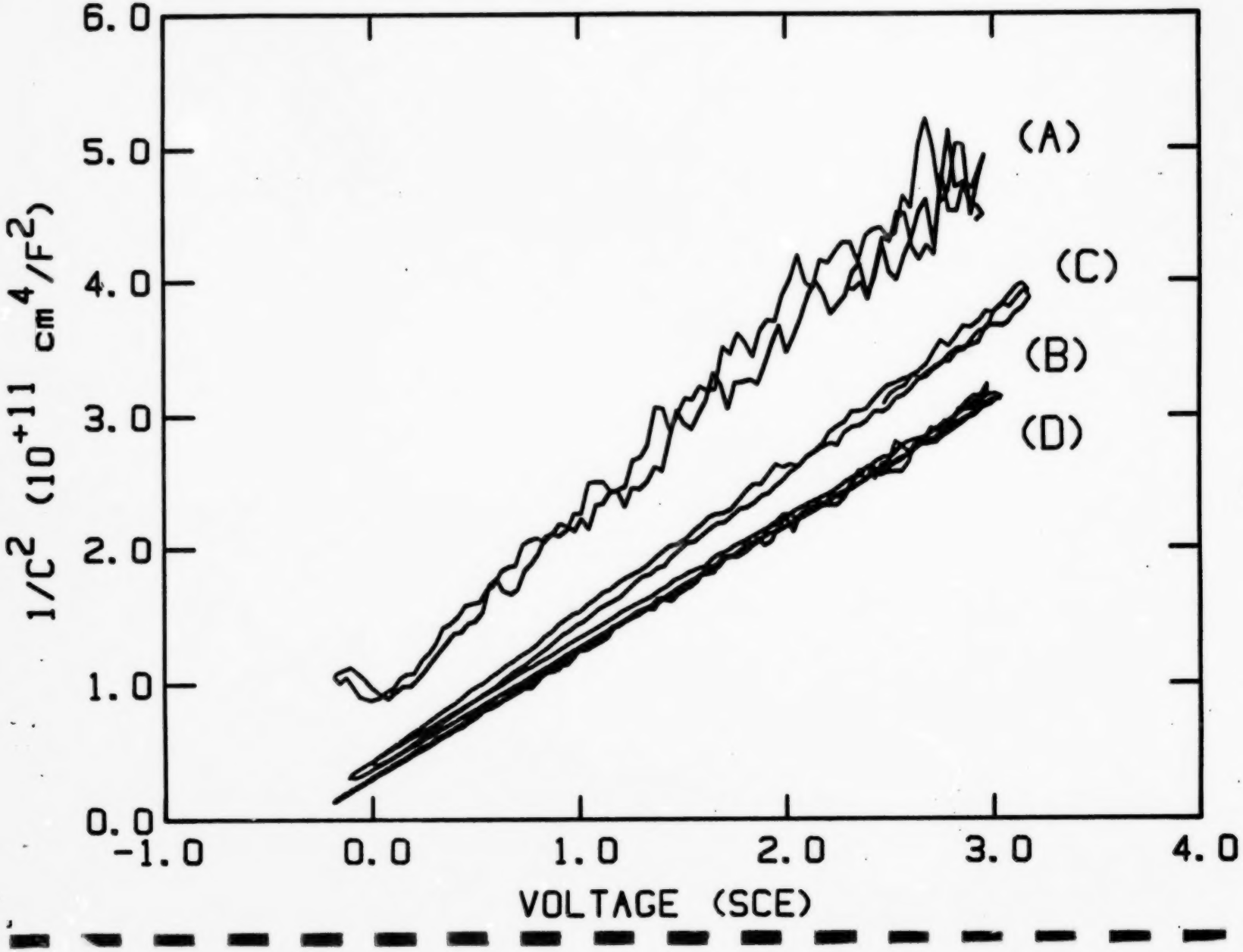
6.0
5.0
4.0
3.0
2.0
1.0
0.0
-1.0
0.0
1.0
2.0
3.0
4.0
$1/C^2$ ($10^{+11}$ $cm^4/F^2$)
VOLTAGE (SCE)
(A)
(C)
(B)
(D)

(3)

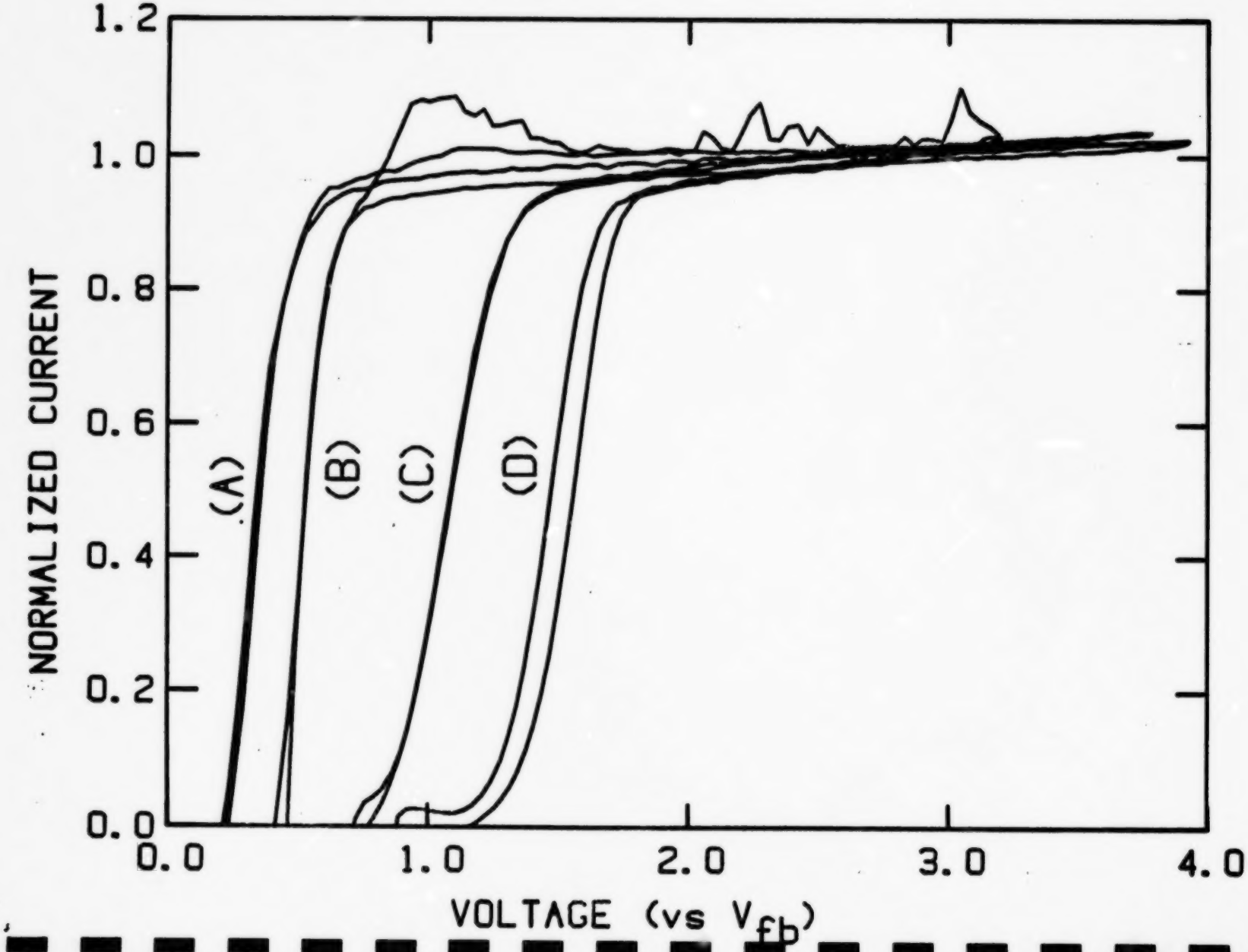
1.2
1.0
0.8
0.6
0.4
0.2
0.0
NORMALIZED CURRENT
(A)
(B)
(C)
(D)
0.0
1.0
2.0
3.0
4.0
VOLTAGE (vs $V_{fb}$)

(4)

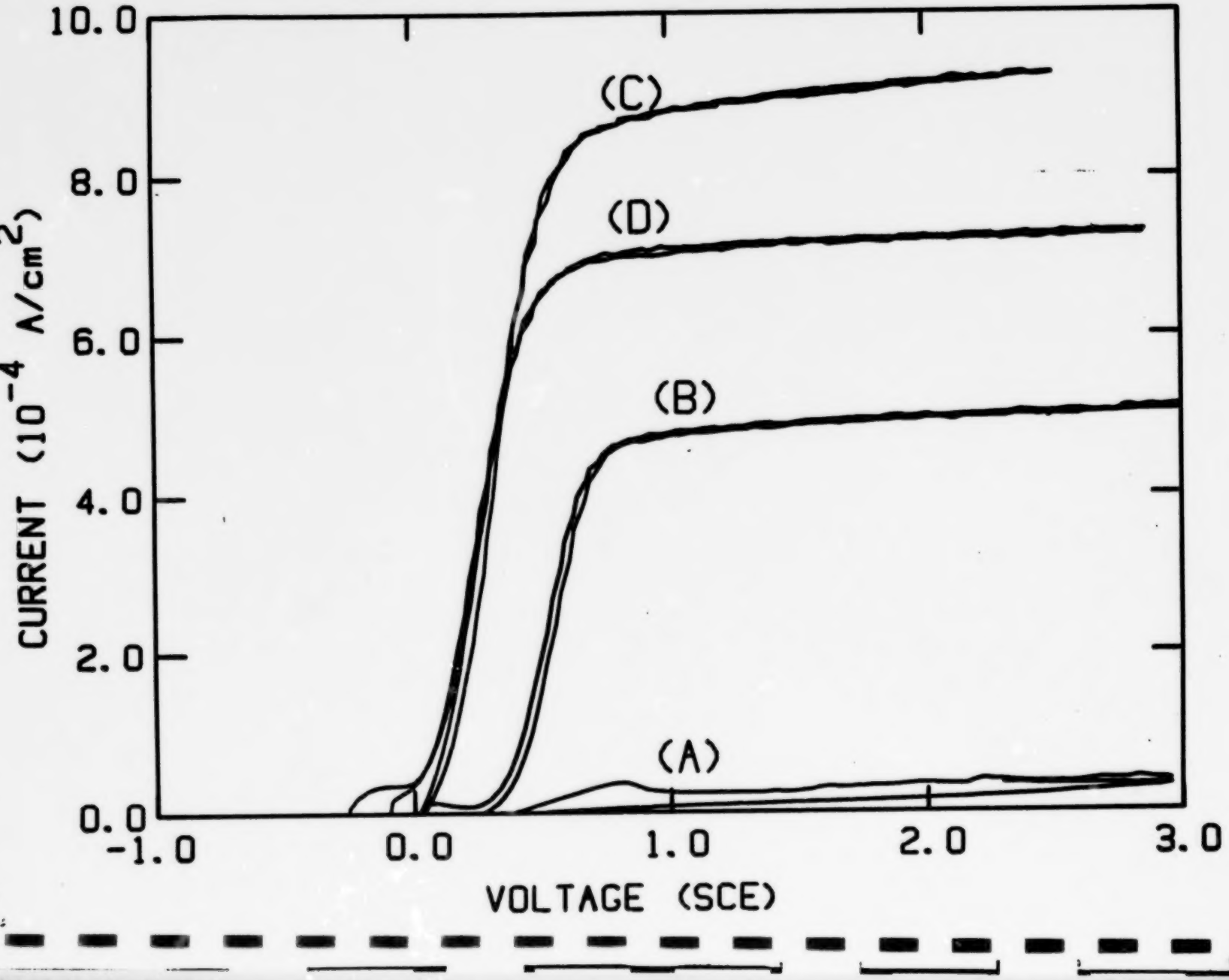
10.0
8.0
6.0
4.0
2.0
0.0
CURRENT ($10^{-4}$ A/cm$^2$)
(C)
(D)
(B)
(A)
-1.0
0.0
1.0
2.0
3.0
VOLTAGE (SCE)

(5)

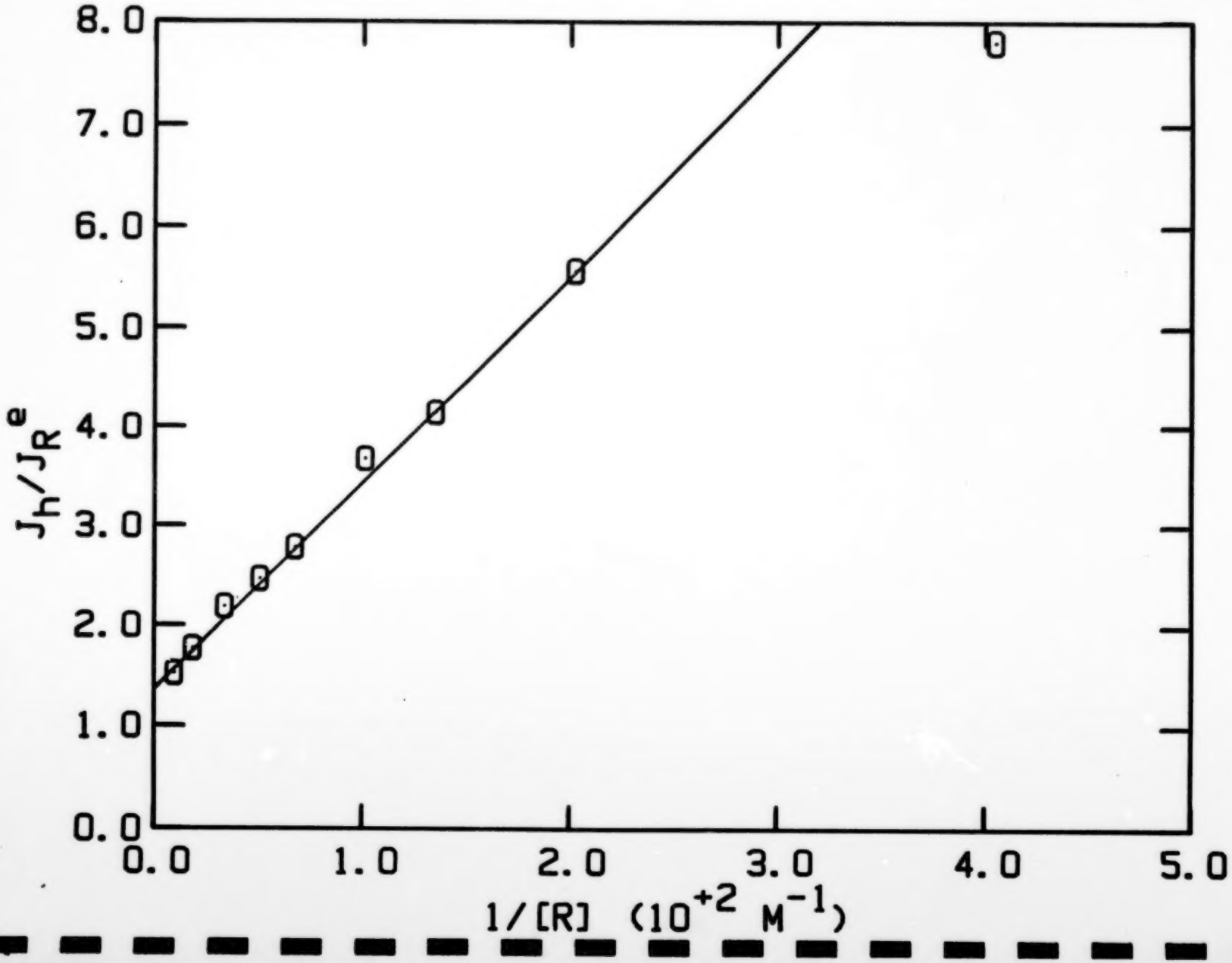

(b)

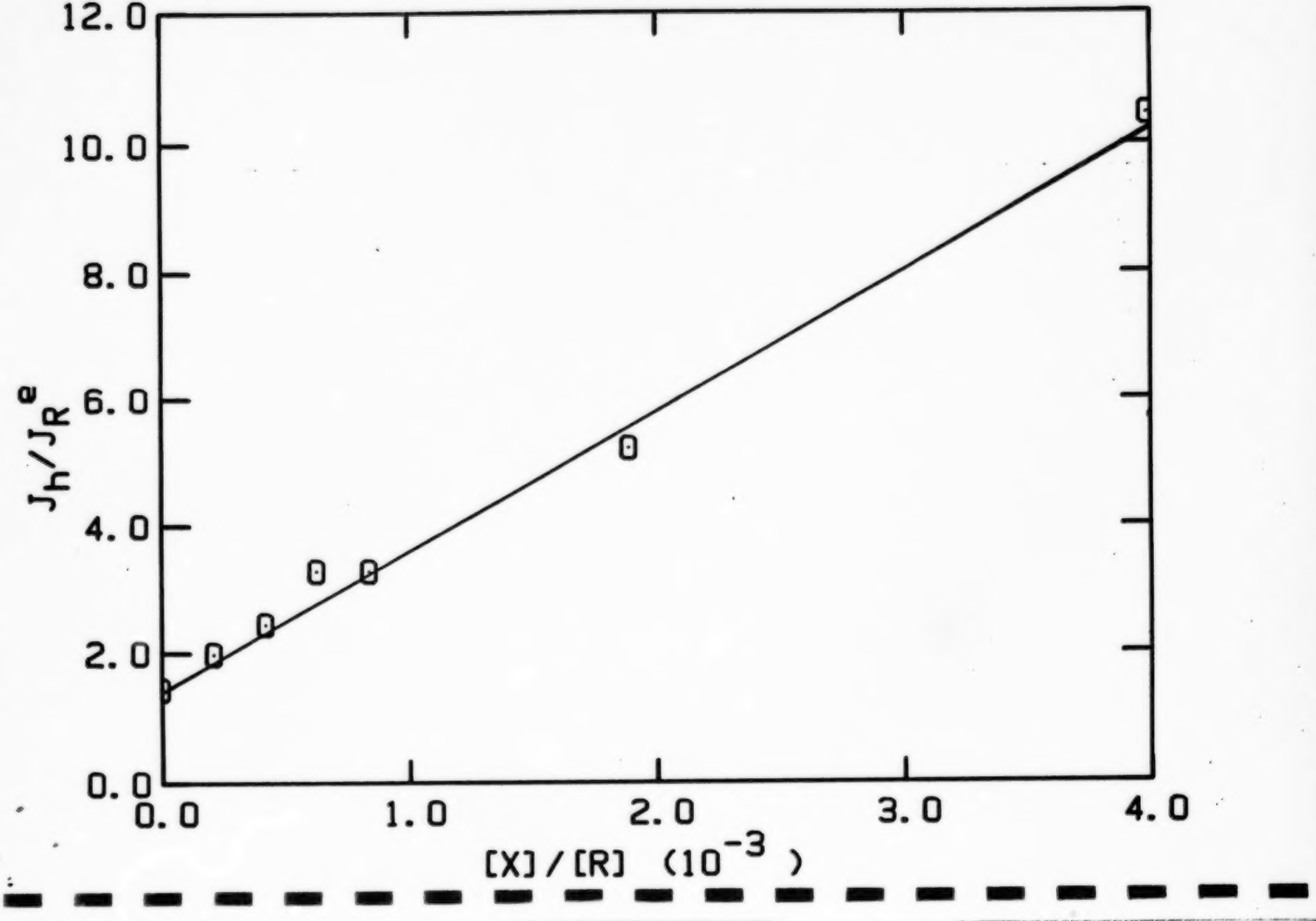

(7)